博 士 学 位 論 文

Studies on the mechanisms underlying rupture of abdominal aortic aneurysm and the preventive methods by functional food factors

近畿大学大学院

農学研究科 応用生命化学専攻

久後 裕菜

博 士 学 位 論 文

Studies on the mechanisms underlying rupture of abdominal aortic aneurysm and the preventive methods by functional food factors

2019 年 3 月

近畿大学大学院

農学研究科 応用生命化学専攻

久後 裕菜

(英文題目)

Studies on the mechanisms underlying rupture of abdominal aortic aneurysm and the preventive methods by functional food factors

Hirona Kugo

March 2019

Department of Applied Biological Chemistry,
Graduate School of Agriculture, Kindai University
Laboratory of Applied Cell Biology

(和文題目)

腹部大動脈瘤の破裂機構と機能性食品成分による予防法に関する研究

近畿大学大学院
農学研究科 応用生命化学専攻
久後 裕菜

－ －

Submitted to the Graduate School, Kindai University, to fulfill the requirement for the Doctorate Degree.

CONTENTS

Chapter 1 - General Introduction

1.1 Abdominal aortic aneurysm (AAA)

Abdominal aortic aneurysm (AAA) is a lethal disease characterized by the irreversible dilation of the abdominal aorta (**Fig. 1**), and high mortality rate caused by vascular rupture with a sudden death. Vascular rupture is defined by the breakdown of the aortic structure and the retroperitoneal hemorrhage. The risk factors of AAA include advanced age, male sex, smoking, family history and hypertension.[1)] The detailed molecular mechanisms underlying vascular expansion and rupture are not completely clear. AAA is a silent disease with almost no subjective symptoms. Therefore, we cannot predict the AAA rupture, and this disease is often coincidentally found at hospitals. Preventing rupture is most important in AAA treatment, because almost patients die due to hemorrhaging when AAAs rupture. A major problem with AAA treatment is that no drug to prevent rupture or inhibit expansion has been developed. Patients with increased rupture risk have no choice but to undergo surgical treatment by means of either open repair with prosthetic graft replacement or endovascular stent graft placement.[2)] Surgical operations involve taking various risks. Therefore, it is desirable to establish preventive methods with drugs or diet to prevent AAA rupture.

1.2 Pathophysiology of AAA

Pathophysiology of AAA is characterized by the degradation of vascular structure due to chronic inflammation, and aortic dilation.[3)] These pathological events are caused by immune cells, such as neutrophils, monocytes and macrophages, and inflammatory cytokines, including monocyte chemoattractant protein (MCP)-1, tumor necrosis factor (TNF)-α, and interleukin (IL)-6, which are increased in AAA lesion. Subsequently, increased matrix metalloproteinase (MMP) proteins derived from vascular smooth muscle cells (SMCs) and immune cells disrupt the elastin and collagen fibers those are the major structural components of the arterial extracellular matrix (ECM) and play an important role in maintaining the integrity and elasticity of the vascular wall.[2, 4, 5)] Indeed, pathological analyses of human AAA wall have reported an increase in chronic inflammation characterized by MMPs expressions, and the activation of MMP-2 and MMP-9 is especially associated with aneurysm formation.[6, 7)]

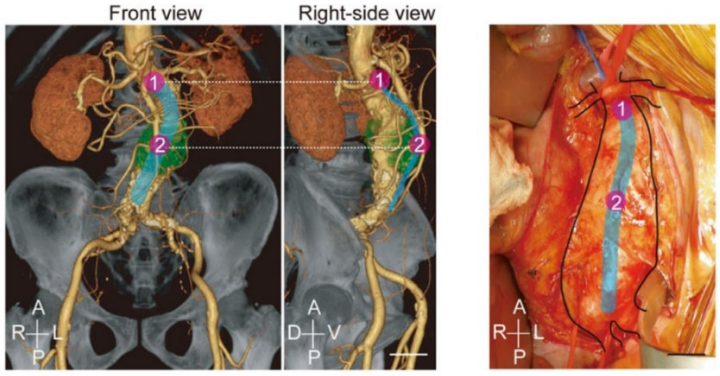

Figure 1 Images of abdominal aortic aneurysm (AAA). 1: Normal region (infrarenal aortic neck). 2: Aneurysmal region (aortic aneurysm sac). Reproduced from a figure previously published in *PLoS One*.[8)]

1.3 Hypoperfusion-induced AAA animal model

Aortic wall consists of the three layers: the intima, media and adventitia, and the adventitial wall has a blood supply system called vasa vasorum (VV) (**Fig. 2a**). Vascular wall is constituted by various cells such as fibroblast, SMC and endothelial cell, and these cells exert their respective functions. It is necessary to sufficiently supply oxygen and nutrients to these cells. This role is played by direct perfusion from the aortic blood flow, and perfusion via small blood vessels in the adventitial VV.[9)]

Previous studies obtained the finding that Heme B, a blood marker, was observed abundantly in the normal region (neck), but was hardly detected in the dilated region (sac) by analysis of the vascular wall in human AAA tissue by matrix-assisted laser desorption/ionization mass spectrometry imaging (MALDI-MSI) (**Fig. 2b, c**).[8)] The luminal area of the VV in the sac wall was significantly smaller than that in the neck wall (**Fig. 2d-f**).[8)] Here, experimental AAA was formed by the induction of artificial vascular hypoperfusion in the abdominal aortic wall of rat.[10)] Based on these findings, the obstruction of VV and thereby the hypoperfusion of aortic wall could cause AAA formation. Formed AAAs in hypoperfusion-induced animal model have similar morphological and pathological characteristics to human AAA. Fortunately, this AAA model shows not only aortic dilation but also spontaneous rupture, and this model can be used to evaluate the effects on AAA rupture. Hypoperfusion-induced AAA model can be expected as a novel model capable of analyzing the mechanisms that is a black box in the findings on AAA.

Induction of hypoperfusion could cause lack of oxygen and nutrients. It has been reported that the response to hypoxia is closely associated with inflammatory response,[11)] and the expression of hypoxia-inducible factor (HIF) -1α affects various

inflammatory mediators.[12] The production of MMP-2 and MMP-9 is increased by the activation of HIF-1α.[13, 14] HIF-1α strongly may associate with differentially expressed genes in AAA wall.[15] Vascular hypoxia due to hypoperfusion may be one of the cause of AAA progression.

1.4 Objective of this study

Since AAA rupture is lethal, the preventing aortic rupture is most important in treatment of this disease. In this research, the mechanisms underlying AAA rupture which is not currently clarified were studied. In Chapter 2, pathological analyses of ruptured abdominal aortic walls in hypoperfusion-induced AAA model were performed to investigate the cause of AAA rupture. In Chapter 3, pathological evaluation of human thoracic aortic aneurysm (TAA) tissue was performed to obtain the findings on the difference between the type of other aortic aneurysm and the mechanism of AAA progression.

Here, as a functional food factor expected to be effective in suppressing the AAA dilation and/or rupture, the effects of fish oil on hypoperfusion-induced AAA were studied in Chapter 4. N-3 polyunsaturated fatty acids (n-3PUFAs) are fatty acids, such as eicosapentaenoic acid (EPA) and docosahexaenoic acid (DHA), which is rich in fish oil. N-3 PUFAs are already widely used as a supplement or medicine because of anti-inflammatory and anti-oxidative effects.

Among the risk factors of AAA, it has been reported that cigarette smoking is particularly associated.[1, 16] In addition, nicotine which is main component of cigarette smoke may increase not only AAA progression but also AAA rupture.[17] Previous study has revealed that nicotine could weaken the vascular wall through the degradation of fibers.[18] In Chapter 5, the effects of functional food factors on the vascular wall injury due to nicotine were evaluated.

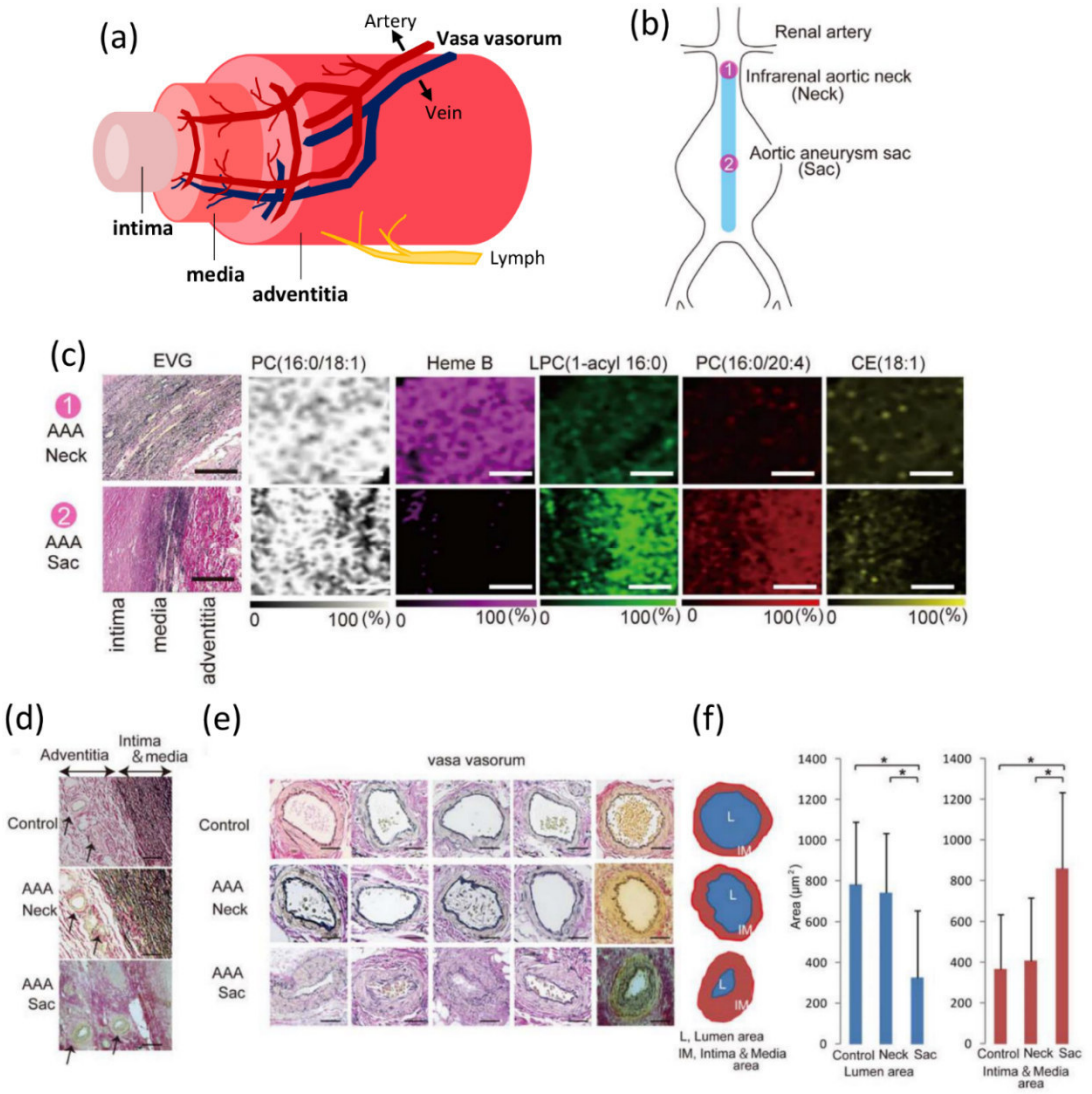

Figure 2 Structure of aortic wall, and the stenosis of adventitial vasa vasorum (VV) in AAA wall. (**a**) Schema of the structure of aortic wall, and (**b**) the AAA (1: Normal region (infrarenal aortic neck). 2: Aneurysmal region (aortic aneurysm sac)). (**c**) Comparison of the distribution of Heme B, phosphatidylcholine (PC) (16:0/18:1), lyso-PC (LPC) (1-acyl 16:0), PC (16:0/20:4), and cholesteryl ester (CE) (18:1) as analyzed by MALDI-IMS. Scale bar = 100 mm. (**d**) Representative adventitial VV. Scale bar = 200 mm. (**e**) Comparison of the luminal and intima–medial areas among the control, neck, and sac adventitial VV. Scale bar = 100 mm (**f**) Comparison of the luminal and intima & medial areas among the control, neck, and sac adventitial VV. Reproduced from a figure previously published in *PLoS One* with slight modification.[8)]

Chapter 2 - The mechanisms underlying abdominal aortic aneurysm rupture

2.1 Introduction

Because AAA rupture is lethal, the prevention of vascular rupture is most important for AAA treatment. It has been reported that the AAA rupture risk increases as the aneurysm diameter increases and/or the expansion rate increases. Currently, the mechanisms underlying AAA progression and rupture has not been elucidated, and there is no effective medical treatment for preventing rupture of AAA. In hypoperfusion-induced AAA animal model, spontaneous vascular rupture was observed.[10] Histological analyses of ruptured walls in hypoperfusion-induced model are suitable for studies on the elucidation of the mechanisms underlying AAA rupture.[10] However, the rupture rate in this animal model was too low (around 10%) to obtain enough samples for pathological analysis of the ruptured walls. Here, the administration of triolein, a triglyceride (TG) species, increased rupture risk in this model. In this research, pathological change between the non-ruptured and ruptured AAA tissues in triolein-administered rats was compared to elucidate the mechanisms underlying AAA rupture.

2.2 Materials and Methods

Materials and methods in this chapter were previously described in *Sci. Rep.* with slight modifications.[19]

2.2.1 Animals

All animal experiments were approved by the Kindai University Animal Care and Use Committee and performed according to the Kindai University Animal Experimentation Regulations (Approval number; KAAG-25-001). Six-week-old male Sprague-Dawley rats (SHIMIZU Laboratory Supplies Co., Ltd, Kyoto, Japan) were provided with food (**Table 1**) and water *ad libitum*, in a humidity-controlled room, with a 12-hour light and 12-hour dark cycle. The room temperature was maintained at 25 ± 1 °C. After acclimatization for a week, the induction of hypoperfusion in abdominal aortic wall was performed in all rats to induce AAA. Rats were then orally administrated either water (control group) (n=16), or triolein (n=24) (1145 mg/kg body weight/day) for 4 weeks. Aortic diameters were then measured, and the rats sacrificed. When a rat died by AAA rupture, the aortic diameter was measured and the abdominal aorta immediately isolated. All surgery was performed under anesthesia, and all efforts were made to minimize suffering.

Table 1 Diet composition

Diet composition	(%)
choline chloride	0.25
cystine	0.3
AIN-93 vitamin mix	1
AIN-93G mineral mix	3.5
cellulose	5
sucrose	10
casein	20
cornstarch	55.75
coconut oil	4.2
	100

2.2.2 Induction of hypoperfusion in abdominal aortic wall (Fig. 3)

Induction of hypoperfusion in abdominal aortic wall in rats was performed as previously described.[20] First, the infrarenal aorta was exfoliated from the perivascular tissue. Next, the vessels branching from the abdominal aorta were ligated with a 5-0 silk string (Akiyama Seisakusyo Co., Tokyo, Japan) to block blood supply at a point away from the aorta that does not narrow the aortic lumen. The abdominal aorta was ligated with a 5-0 silk string just below the renal artery and just above the bifurcation of the aorta to block aortic blood flow. A plastic catheter (Medikit, Tokyo, Japan), shortened to 9 mm in length, was inserted via a small incision adjacent to the renal artery branches, and the incision was then repaired with a 6-0 monofilament string (Alfresa Pharma, Osaka, Japan). The abdominal aorta was ligated with a 5-0 silk string together with the plastic catheter. Finally, the 5-0 silk string that blocked the blood in the aorta was untied and blood flow was initiated again. Using this treatment, hypoperfusion is induced in the aortic wall only while blood flow is maintained in the vascular lumen.

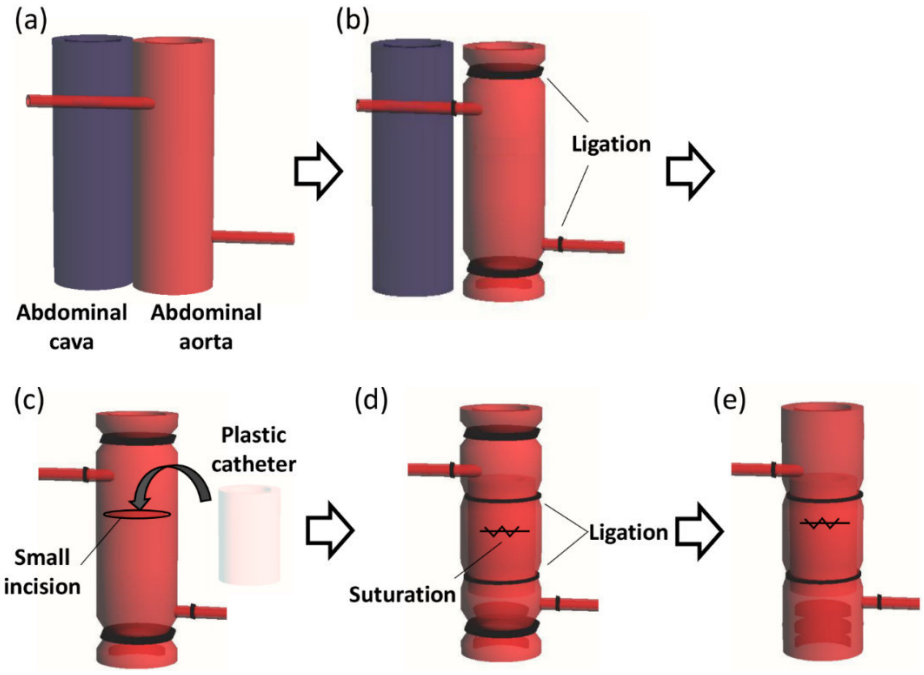

Figure 3 Induction of abdominal aortic wall hypoperfusion. (**a**) The infrarenal aorta is exfoliated from the perivascular tissue. (**b**) Vessels branching from the abdominal aorta are ligated with a 5-0 silk string to block the blood supply, and the abdominal aorta is ligated with a 5-0 silk string just below the renal artery and just above the bifurcation of the aorta to block the aortic blood flow. (**c**) A plastic catheter shortened to 8–10 mm long is inserted via a small incision adjacent to the renal artery branches. (**d**) The incision is then repaired with a 6-0 monofilament string and the abdominal aorta is ligated with a 5-0 silk string together with the plastic catheter. (**e**) The 5-0 silk string blocking the blood flow in the aorta is untied.

2.2.3 Sample collection

The diameter of abdominal aorta was measured using digital calipers (A&D, Tokyo, Japan). The dilation ratio was calculated according to the following formula: dilation ratio (sac/neck) = maximal aneurysm diameter / non-dilated aortic diameter. Aneurysm formation was considered to be formed when the dilation ratio was greater than two. Isolated tissues were fixed in 4% paraformaldehyde (PFA) (Nacalai Tesque, Kyoto, Japan), soaked in sucrose (10%, 15% and 20%), and then embedded in O.C.T. Compound (Sakura Finetek Japan Co., Ltd.). These were stored at −80 °C until required.

2.2.4 Histological analysis

Abdominal aortae were cut with a cryostat (CM1850; Leica Microsystems, Wetzlar, Germany) into 10-μm-thick sections, and mounted on glass slides. Tissue

sections were subjected to Hematoxylin-Eosin (HE) staining, Elastica van Gieson (EVG) staining, Picrosirius red (PSR) staining, Oil Red O staining and immunohistochemical staining. Quantitative analysis of histological staining was performed using ImageJ software (National Institutes of Health, Bethesda, Maryland, USA). Areas within 100 μm of an adipocyte were defined as 'around adipocyte'.

2.2.5 Hematoxylin-Eosin (HE) staining

PFA-fixed tissue sections were placed in hematoxylin for nuclear staining for 10 minutes, and then decolorized in acid alcohol (1% hydrochloric acid (HCl) in 70% ethanol). After rinsing in tap water, the sections were stained with eosin for 5 minutes, and then dehydrated in ethanol (80%, 90%, and 100%). Thereafter, the sections were cleared in xylene and covered with a lipid-soluble mounting medium, Entellan® New (Merck KGaA, Germany), and glass cover slips. Quantitative analysis of the thickness of the aortic wall was performed.

2.2.6 Elastica van Gieson (EVG) staining

PFA-fixed tissue sections were stained in resorcin-fuchsin solution for 30 minutes. After rinsing in tap water, the tissue sections were stained for 10 minutes in a 1:1 mixture of Weigert's iron hematoxylin solution I (1% hematoxylin in ethanol) and solution II (2% ferric chloride in 0.25% HCl). After rinsing with tap water, the sections were stained with 1% fuchsin solution, diluted 3:20 in van Gieson P solution, for 3 minutes. The tissue sections were dehydrated in ethanol (70%, 90%, and 100%), cleared in xylene, and covered with a lipid-soluble mounting medium and glass cover slips. Elastic lamina was categorized into 4 grades: intact elastic lamina was designated grade 1; deletion of wave form or/and dilution of elastic lamina was designated grade 2; partial disappearance of elastic lamina was designated grade 3; and disappearance of elastic lamina was designated as grade 4, with this being the worst state (**Fig. 4**). EVG stained-sections were then used for the measurement of medial wall thickness.

2.2.7 Picrosirius red (PSR) staining

PFA-fixed tissue sections were stained in Weigert's iron hematoxylin solution for 10 minutes. The tissue sections were then decolorized in acid alcohol (1% HCl in 70% ethanol). After rinsing in tap water, the tissue sections were stained in 1% Sirius Red (Waldeck) solution, diluted 1:20 in van Gieson P solution, for 10 minutes. The tissue sections were dehydrated in 100% ethanol and covered with a lipid-soluble mounting medium. Quantitative analysis of collagen-positive areas was performed.

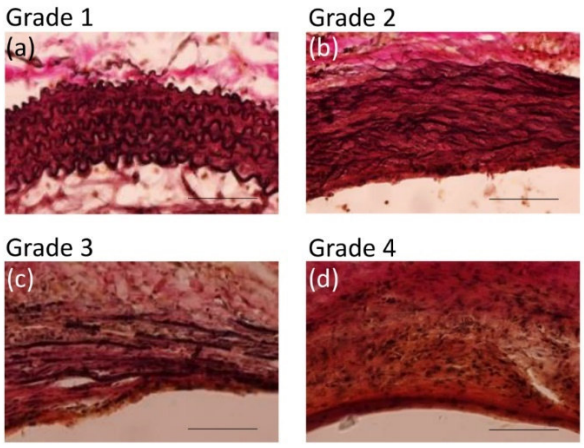

Figure 4 Elastin grade. (**a**) Intact elastic lamina (grade 1), (**b**) deletion of wave form or/and dilution of elastic lamina (grade 2), (c) partial disappearance of elastic lamina (grade 3), and (**d**) disappearance of elastic lamina (grade 4). Scale bar = 100μm.

2.2.8 Oil Red O staining

PFA-fixed tissue sections were rinsed in 60% isopropanol for 1 minute. The tissue sections were then incubated in Oil Red O solution for 10 minutes. After rinsing in 60% isopropanol for 1 minute, the tissue sections were placed in hematoxylin for nuclear staining for 5 minutes. After rinsing in tap water, slides were covered with an aqueous mounting medium (Nichirei Biosciences, Tokyo, Japan) and glass cover slips.

2.2.9 Immunohistochemical staining

PFA-fixed tissue sections were rinsed in phosphate-buffered saline (PBS) with 1% Triton-X100 and then incubated in 10% oxalic acid for 1 hour. For antigen activation, 0.1% trypsin in PBS was added to the tissue sections. Endogenous horseradish peroxidase (HRP) in the tissue sections was blocked using 3% aqueous hydrogen peroxide in methanol for 8 minutes. After washing in PBS, the tissue sections were blocked with Blocking One Histo. The sections were incubated with the appropriate primary antibody overnight at 4 °C. The histological results from the aortic wall were assessed after staining using the following antibodies: rabbit anti-matrix metalloproteinase (MMP) 2 (1:100; Thermo Scientific), goat anti-MMP9 (1:100; Santa Cruz Biotechnology, Inc.), rabbit anti-MCP-1 (1:50; Novus Biologicals), mouse anti-monocytes/macrophages (MAC387) (1:50; Bio-Rad Laboratories), mouse anti-α-smooth muscle actin (1:400; Santa Cruz Biotechnology, Inc.), rabbit anti-CD163 (1:100; Bioss Antibodies). On the following day, the sections were rinsed in PBS, and incubated with the appropriate secondary antibody conjugated to HRP. Slides were developed with DAB (Vector Laboratories,

Burlingame, CA, USA), dehydrated in ethanol (80%, 90%, and 100%), cleared in xylene, and covered with a lipid-soluble mounting medium and glass cover slips.

2.2.10 Serum analysis

Blood samples were collected from rats after 4 weeks of the AAA induction. Serum TG concentration and total cholesterol concentrations were measured, respectively, with triglyceride kit and total cholesterol kit (Wako Pure Chemical industries, Osaka, Japan).

2.2.11 Human study

The study protocol was reviewed and approved by the Hamamatsu University School of Medicine Ethics Committee of Clinical Research (The Ethic Committee's approval number is 20372012). All procedures used in this study were carried out in accordance with the Clinical Research Ethics Committee of Hamamatsu University School of Medicine. Aortic tissues were collected from patients who underwent elective open surgery for the repair of infra-renal AAA. Aortic diameters were measured pre-operatively by three-dimensional multi-detector computed tomography imaging of the AAA. During surgery, longitudinal tissue strips were collected from the aorta, from the nearby distal portion of the bifurcation of the renal artery to the region of maximal dilation of the aneurysm. The patients were all male, 58 to 89 years old (mean age 69.8 ± 12.0 years). Tissue samples were preserved in rapid freeze storage until required for analysis with biochemical quantitation. Total lipids were extracted from homogenized tissue.

2.2.12 Statistical analysis

Values were expressed as mean ± S.E.M. For between-group comparisons, the Chi-square test or Fisher's exact test (for situations with small frequencies) was used for categorical variables. Student's t test for continuous data with Tukey-Kramer test and Mann-Whitney test for scoring data were used. Kaplan–Meier method was used for analysis of survival analysis, and intergroup differences were evaluated by the log-rank test with Holm adjustment for multiple comparisons. A P value < 0.05 was considered to indicate a statistically significant difference. Statistical analyses were performed using StatView 5.0 software (SAS Institute, Cary, USA) and R 3.2.0 with the EZR package.[21)]

2.3 Results

2.3.1 Increase in AAA rupture risk by triolein administration

The triolein administered group significantly increased AAA rupture risk compared with the control group (**Fig. 5a**). The triolein group was divided into a non-ruptured group and a ruptured group. Aneurysm formation was observed in both groups, and area with a non-dilated diameter (neck) was observed in both groups (**Fig. 5b**). The diameter of the dilated aorta (sac) and the dilation ratio (sac/neck) in the ruptured group were significantly increased compared with those in the non-ruptured group (**Fig. 5c, d**). The initial body weight (g) was not significantly different between the non-ruptured group (239.5 ± 24.0 (g)) and the ruptured group (250.7.5 ± 22.5 (g)). The gain in body weight (g) were not significantly different between the non-ruptured group (4.01 ± 1.1 (g)) and the ruptured group (4.47 ± 1.0 (g)). Serum TG levels were not significantly different between the non-ruptured group (150.0 ± 20.2 (mg/dL)) and the ruptured group (163.2 ± 15.8 (mg/dL)). Total cholesterol levels were not significantly different between the non-ruptured group (61.8 ± 8.2 (mg/dL)) and the ruptured group (67.1 ± 6.4 (mg/dL)).

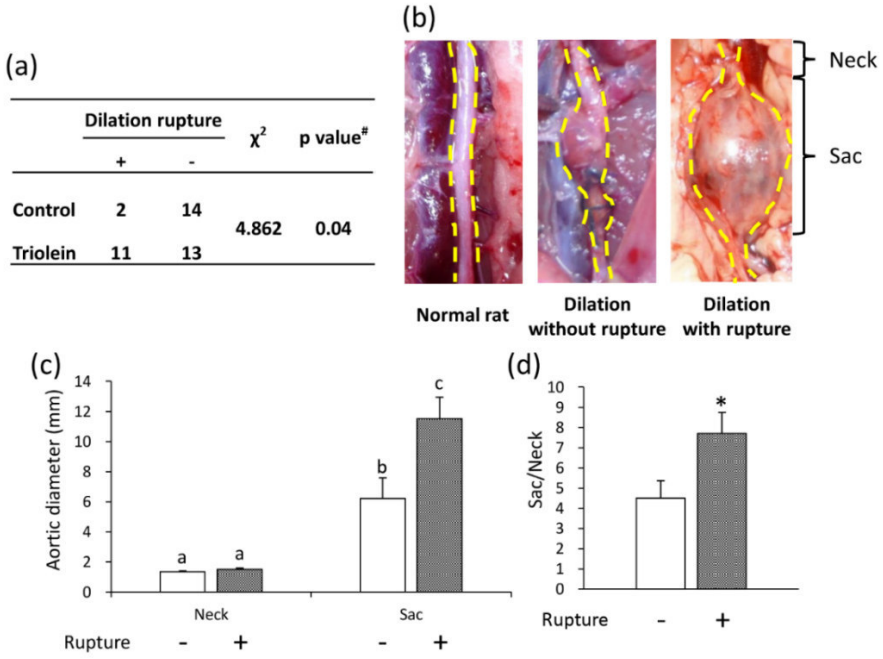

Figure 5 Effects of triolein administration on AAA rupture and aortic diameter. (**a**) Effect of triolein administration on AAA rupture ratio. Data are presented as number of rats. #*P* value of Fisher's exact test. (**b**) Representative images of the abdominal aorta from a normal rat and from rats in the triolein administered group. (**c**) Aortic diameter. (**d**) Dilation ratio (sac/neck). Data are the mean ± S.E.M. Non-ruptured (n = 13), ruptured (n = 11). Values with different letters are significantly different ($P < 0.05$). *$P < 0.01$ versus non-ruptured group. Reproduced from a figure previously published in *Sci. Rep.*[19]

The vascular wall thickness was significantly increased in the AAA sac wall in both ruptured and non-ruptured groups compared with the neck wall (**Fig. 6a-d, m**). The t vascular wall thickness in the AAA sac wall of the ruptured group was significantly increased compared with that of the non-ruptured group (**Fig. 6m**). Elastin fibers were observed by EVG staining (**Fig. 6e-h**). Elastin degradation score was not significantly different between groups (**Fig. 6n**). Areas positive for SMCs and the thickness of medial wall in the AAA sac wall were significantly decreased compared with those in the neck wall (**Fig. 6i-l, o, p**). However, there was no difference between the thickness of the medial wall between groups (**Fig. 6p**).

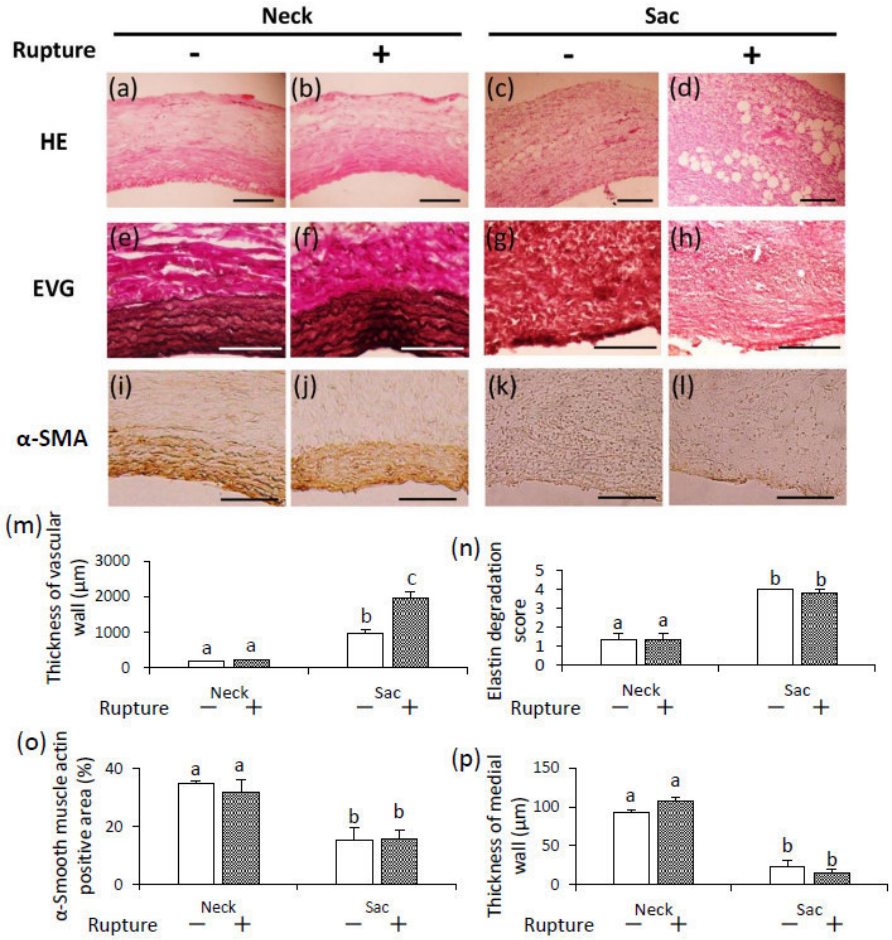

Figure 6 Thickness of vascular wall, elastin degradation score, and thickness of medial wall. (**a-d**) Representative images of HE staining (scale bar = 200 μm), (**e-h**) EVG staining (scale bar = 100 μm), and (**i-l**) immunostaining for α-smooth muscle actin (scale bar = 100 μm). (**m**) Quantification of vascular wall thickness, (**n**) elastin degradation scores, (**o**) α-smooth muscle actin-positive areas, and (**p**) medial wall thickness. Data are the mean ± S.E.M. Non-ruptured (n = 5), ruptured (n = 5). Values with different letters are significantly different ($P < 0.05$). Reproduced from a figure previously published in *Sci. Rep.* with slight modification.[19)]

2.3.2 Adipocytes accumulation in ruptured vascular wall

Adipocyte-like cells were observed in the adventitial sac wall in both groups, but not in the neck wall (**Fig. 7a-f**).

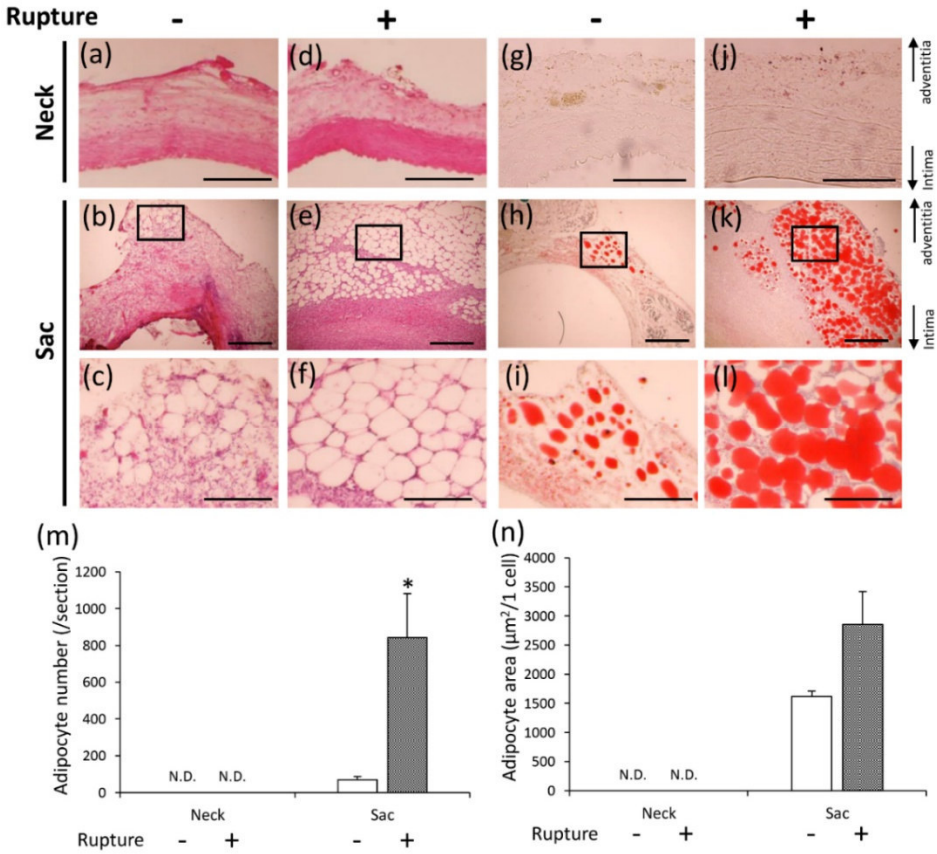

Figure 7 Adipocyte accumulation in non-ruptured and ruptured groups. (**a-f**) Representative images of HE staining (a, c, d, f: scale bar = 200 μm; b, e: scale bar = 500 μm), and (**g-l**) Oil Red O staining (g, j: scale bar = 100 μm; h, k: scale bar = 500 μm; i, l: scale bar = 200 μm). The square area in the middle panels is magnified in the bottom panels. (**m**) Quantification of adipocyte number, and (**n**) adipocyte area in the non-ruptured and ruptured groups. Data are the mean ± S.E.M. Non-ruptured (n = 7), ruptured (n = 8). *$P < 0.01$ versus non-ruptured group. N.D. = not detected. Reproduced from a figure previously published in *Sci. Rep.*[19]

These adipocyte-like cells possessed the characteristic morphology of adipocytes as shown in Electron microscopy (**Fig. 8b**). Peroxisome proliferator-activated receptor γ (PPARγ) was detected in the nucleus of these cells (**Fig. 8f**), and adipocyte-like cells in the AAA sac wall stained positively with Oil Red O staining (**Fig. 7g-l**). Therefore, adipocyte-like cells were determined to be adipocytes.

The number of adipocytes (/section) in the vascular wall of the AAA sac in the ruptured group was significantly increased compared with the non-raptured group (**Fig. 7m**). The size of adipocytes (μm²/cell) tended to increase in the ruptured group (**Fig. 7n**).

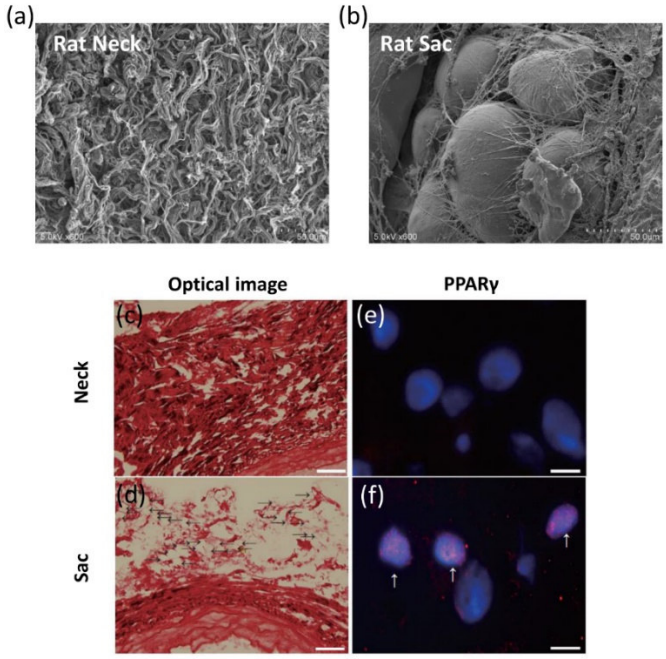

Figure 8 Observation of adipocyte and PPARγ staining. Representative electron microscopic image of the vascular wall of the AAA neck (**a**) and sac (**b**) from a model rat. Representative optical images of the neck (**c**) and sac (**d**) (Scale bar = 200 μm). Representative images of PPARγ staining of neck (**e**) and sac (**f**) (Scale bar = 10 μm). Red: PPARγ. Blue: nucleus. Reproduced from a figure previously published in *Sci. Rep.*[19)]

2.3.3 Pathology of area with adipocytes in vascular wall

In order to elucidate the pathological significance of ectopic vascular adipocytes, the regions surrounding adipocytes in the vascular wall were analyzed. The ruptured tissues were divided into two groups: area with adipocytes and area without adipocytes. Collagen fibers in the vascular wall were observed by PSR staining (**Fig. 9a-e**). Collagen-positive areas were significantly decreased in the AAA sac wall compared with the AAA neck wall (**Fig. 9p**). Collagen-positive areas were significantly decreased in the ruptured group compared with the non-ruptured group (**Fig. 9p**). In addition, collagen-positive areas were significantly decreased in the areas with adipocytes compared with the areas without adipocytes (**Fig. 9p**).

Because collagen fibers degradation was enhanced in the areas with adipocytes, immunohistochemical examination for MMP-2 (**Fig. 9f-j**) and MMP-9 (**Fig. 9k-o**) was performed. Areas positive for MMP-2 and MMP-9 were significantly increased in the AAA sac wall compared with the AAA neck wall (**Fig. 9q, r**). Areas positive for MMP-2 and MMP-9 in the AAA sac wall between the non-ruptured and the ruptured groups were not significantly different (**Fig. 9q, r**). On the contrary, areas positive for MMP-2 and MMP-9 in areas with adipocytes were significantly greater compared with areas without adipocytes in the AAA sac wall (**Fig. 9q, r**).

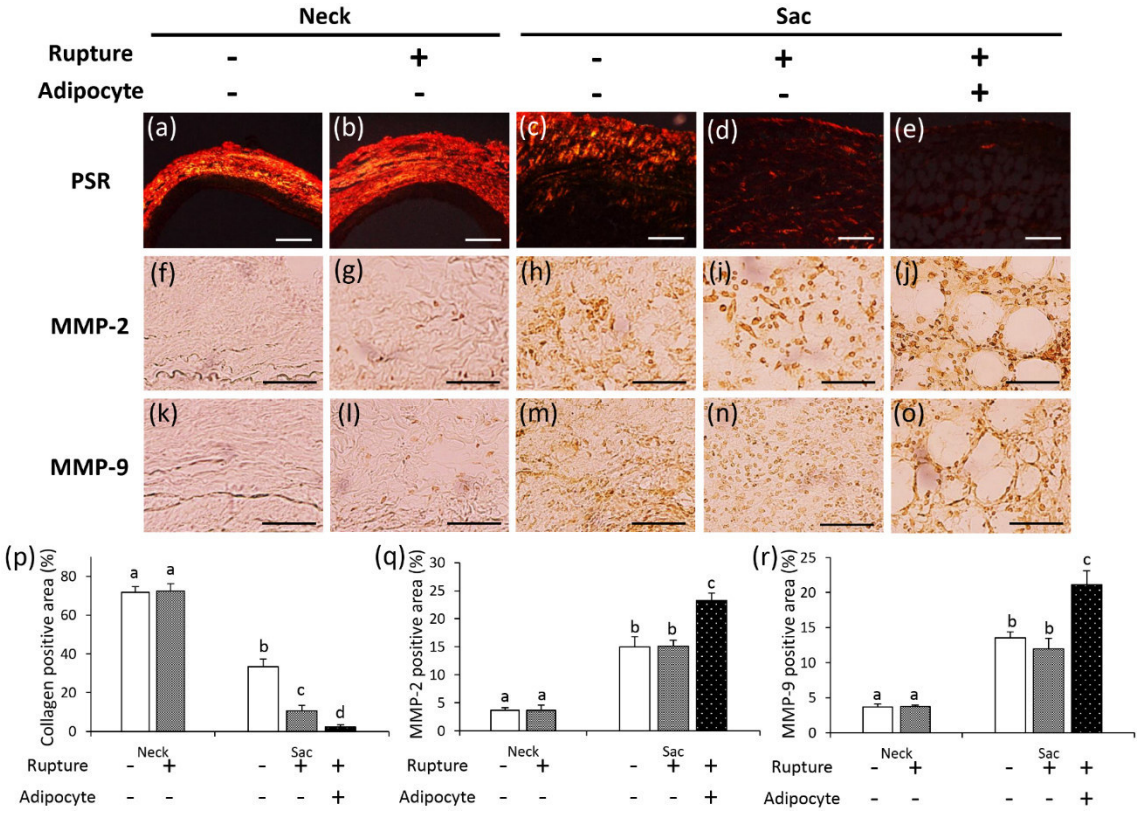

Figure 9 Observation of collagen fibers, and immunohistochemical staining for MMP-2 and MMP-9. (**a-e**) Representative images of PSR staining (scale bar = 200 μm), and (**f-j**) immunostaining for MMP-2 (scale bar = 50 μm) and (**k-o**) MMP-9 (scale bar = 50 μm). (**p**) Quantification of the collagen-positive area, (**q**) MMP-2 positive areas, and (**r**) MMP-9 positive areas of the vascular wall. Data are the mean ± S.E.M. Values with different letters are significantly different ($P < 0.05$). Reproduced from a figure previously published in *Sci. Rep.*[19)]

To clarify the mechanisms underlying the increased areas positive for MMP-2 and MMP-9 and the decreased collagen in the areas with adipocytes, immunohistochemical examination for MCP-1 (**Fig. 10a-e**), Mac387^{+} monocytes/macrophages (potentially M1-like macrophages) (**Fig. 10f-j**), and CD163^{+} macrophages (consistent with M2-like macrophages) (**Fig. 10k-o**) was performed. Areas positive for MCP-1, Mac387, and CD163 were significantly increased in the AAA sac wall compared with the AAA neck wall (**Fig. 10p-r**). Areas positive for MCP-1, Mac387, and CD163 in the AAA sac wall between the non-ruptured and the ruptured groups were not significantly different (**Fig. 10p-r**). On the contrary, areas positive for MCP-1, Mac387, and CD163 in areas with adipocytes were significantly greater compared with areas without adipocytes in the AAA sac wall (**Fig. 10p-r**).

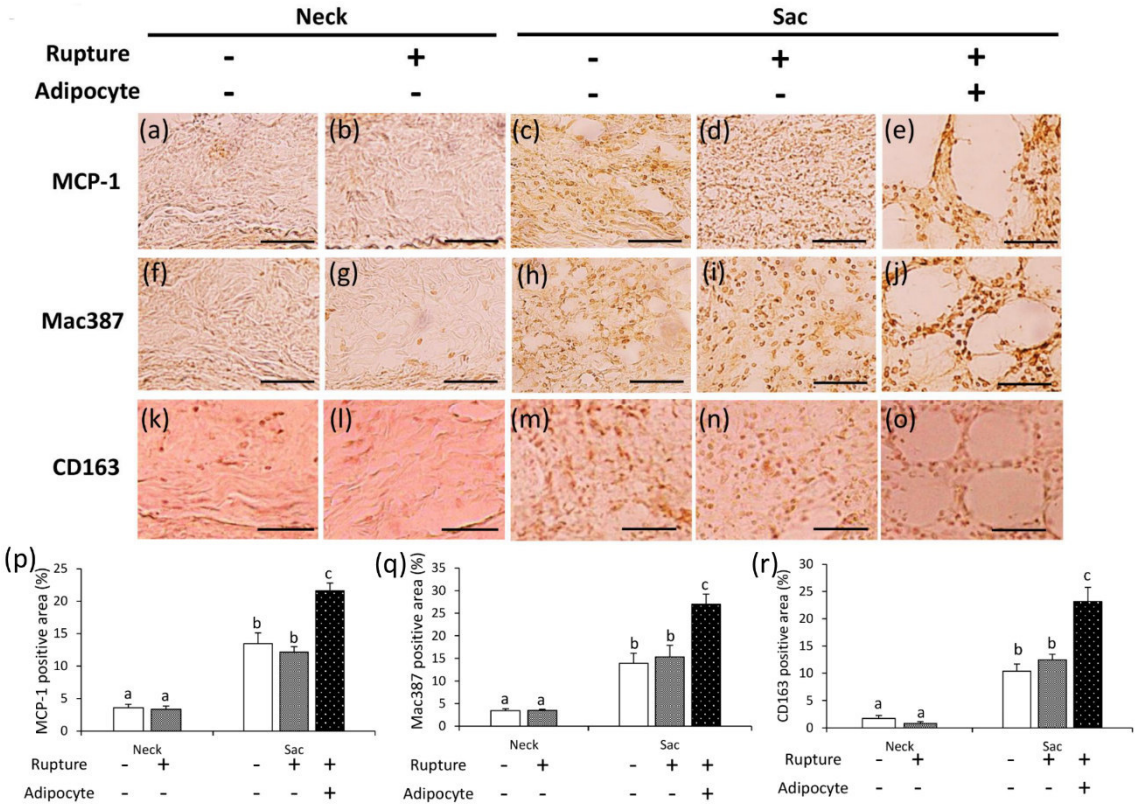

Figure 10 Immunohistochemical staining for MCP-1, Mac387 and CD163. (**a-e**) Representative images of immunostaining for MCP-1 (scale bar = 50 μm), (**f-j**) Mac387^{+} monocytes/macrophages (scale bar = 50 μm), and (**k-o**) CD163 (scale bar = 50 μm). (**p**) Quantification of the MCP-1-positive area, (**q**) Mac387^{+} monocyte/macrophage-positive areas, and (**r**) CD163-positive areas of the vascular wall. Data are the mean ± S.E.M. Values with different letters are significantly different ($P < 0.05$). Reproduced from a figure previously published in *Sci. Rep.* with slight modification.[19)]

2.3.4 Histological analyses of the ruptured area in hypoperfusion-induced model rat

The ruptured area was successfully identified in hypoperfusion-induced model. The intraperitoneal abundance of blood clot was observed (**Fig. 11a**). Following careful removal of the blood clot, the ruptured area in the vascular wall was identified **(Fig. 11b and c)**.

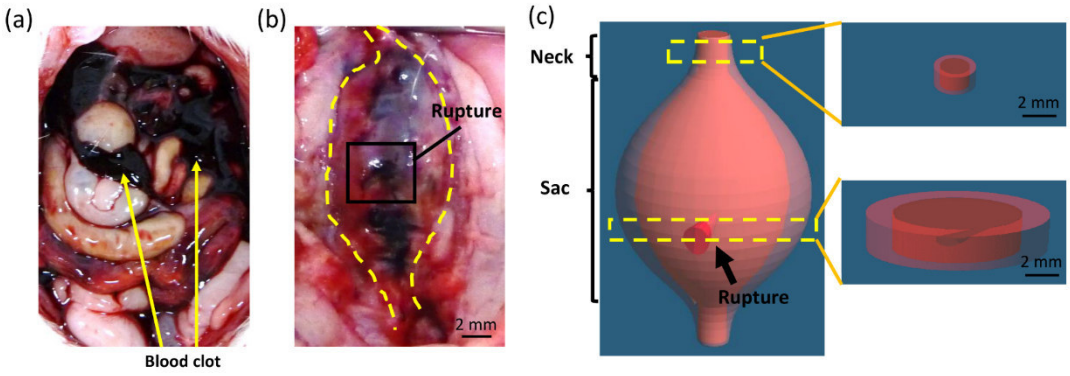

Figure 11 Images of the ruptured AAA. Ruptured AAA pictured before washing away blood (**a**) and after washing away blood (**b**). Schema of the ruptured AAA (**c**). Reproduced from a figure previously published in *J. Oleo Sci.*[22)]

Pathological analyses were performed in the ruptured area. **Figure 12a** showed the neck wall, and **Figure 12b** and **c** showed the cross-section around the ruptured area. The blood clot and adipocytes were observed along the tear in the aortic wall (**Fig. 12b, c**). Next, the aortic wall were divided into the four groups as shown in **Figure 12d**: neck area, designated as region 1; sac area without adipocytes, designated as region 2; sac area with adipocytes away from the tear in the aortic wall, designated as region 3; and sac area with adipocytes along the tear in the aortic wall, designated as region 4 (**Fig. 12a, b, d-h**).

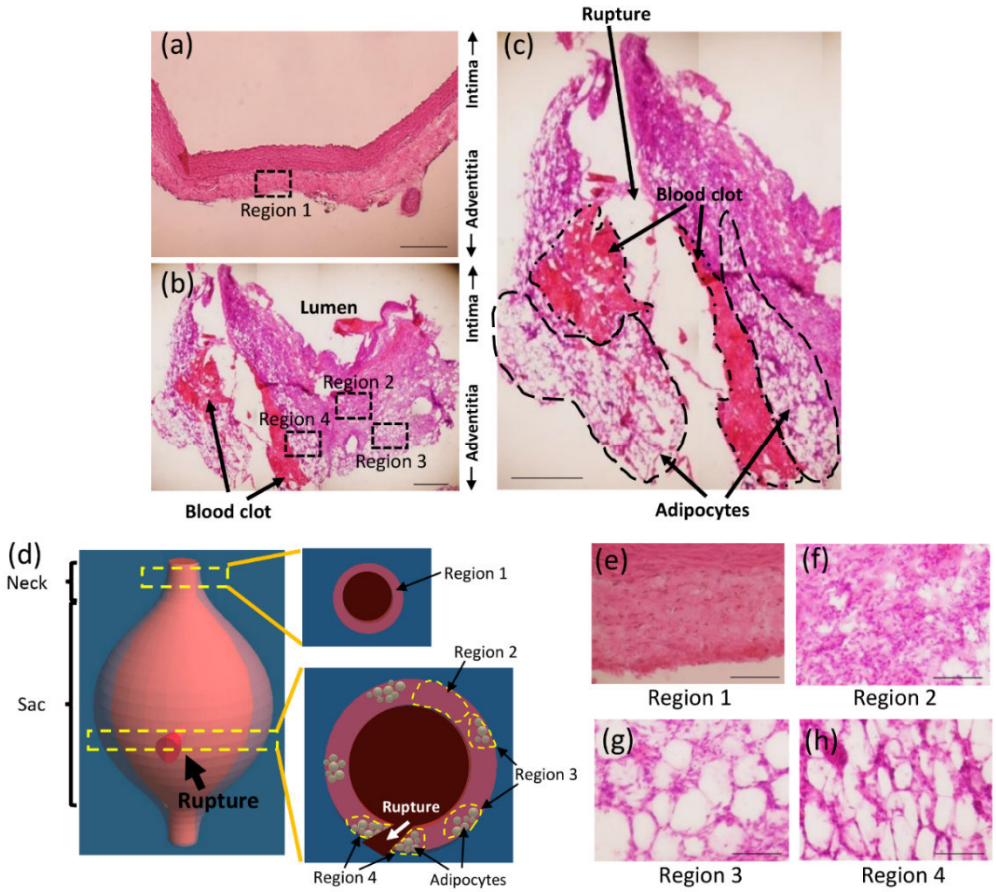

Figure 12 Histological analyses of the ruptured AAA wall. Representative images of AAA neck wall (**a**) and sac wall (**b**). AAA ruptured area is magnified in the panel (**c**). (a: scale bar = 200 μm; b, c: scale bar = 500 μm). (**d**) Aortic wall areas were divided into four groups. Region 1: neck wall (**e**), region 2: sac wall without adipocytes (**f**), region 3: sac wall with adipocytes away from the tear in the aortic wall (**g**) and region 4: sac wall with adipocytes along the tear in the aortic wall (**h**). (e-h: scale bar = 100 μm). Reproduced from a figure previously published in *J. Oleo Sci.*[22]

Collagen positive areas were significantly decreased in the regions 2, 3, and 4 compared with those in the region 1 (**Fig. 13a-d, q**). In addition, collagen positive areas were significantly decreased in the regions 3 and 4 compared with those in the region 2 (**Fig. 13a-d, q**). Collagen positive areas were not significantly different between the regions 3 and 4 (**Fig. 13a-d, q**). Areas positive for MMP-2, MMP-9, and Mac387$^+$ monocytes/macrophages in each group were evaluated by immunohistochemical staining (**Fig. 13e-p**). Areas positive for MMP-2, MMP-9, and Mac 387$^+$ monocytes/macrophages were significantly increased in the regions 2 to 4 compared with those in region 1 (**Fig. 13r-t**). In addition, areas positive for MMP-2, MMP-9, and Mac 387$^+$

monocytes/macrophages were significantly increased in the regions 3 and 4 compared with those in the region 2 (**Fig. 13r-t**). Areas positive for MMP-2, MMP-9, and Mac387$^+$ monocytes/macrophages were not significantly different between the regions 3 and 4 (**Fig. 13r-t**).

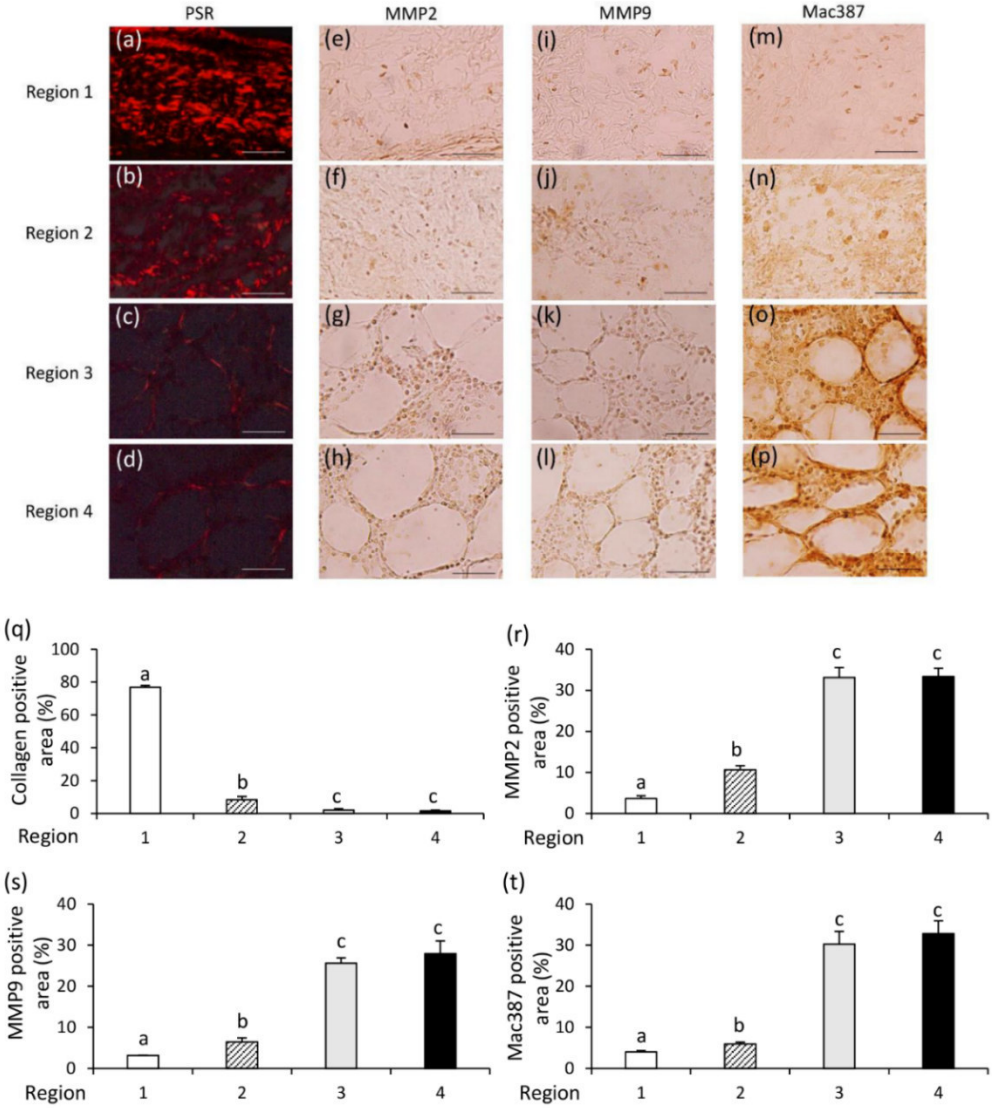

Figure 13 PSR staining and immunohistochemical staining for MMP2, MMP9 and MAC387$^+$ monocytes/macrophages. (**a-d**) Representative images of PSR staining, and (**e-h**) immunostaining for MMP-2, (**i-l**) MMP-9, and (**m-p**) Mac387$^+$ monocytes/macrophages. Scale bar = 50 μm. (**q**) Quantification of the collagen-positive area, (**r**) MMP-2 positive area, (**s**) MMP-9 positive area, and (**t**) Mac387$^+$ monocyte/macrophage positive area. Data are the mean ± S.E.M. Values with different letters are significantly different ($P < 0.05$). Reproduced from a figure previously published in *J. Oleo Sci.* with slight modification.[22)]

2.3.5 Correlation between the number of adipocytes in vascular wall and AAA diameter in hypoperfusion-induced AAA model

Histological analyses suggested that the ectopic appearance of adipocytes in the aortic wall could be closely associated with AAA rupture. Next, the relationship between vascular adipocytes and AAA diameter was investigated in hypoperfusion-induced model. The dilation ratio was correlated with the number of adipocytes in the aortic wall in hypoperfusion-induced model (**Fig. 14a**). The dilation ratio was not correlated with the size of adipocytes in the aortic wall in hypoperfusion-induced model (**Fig. 14b**). In addition, the number and size of adipocytes was not correlated with the body weight in hypoperfusion-induced model (**Fig. 14c, d**). Next, the relationship among the serum lipids, AAA diameter, and the number of adipocytes. Serum TG and total cholesterol levels were not correlated with the dilation ratio (**Fig. 14e, f**). In addition, serum TG and total cholesterol levels were not correlated with the number of adipocytes in the aortic wall (**Fig. 14g, h**).

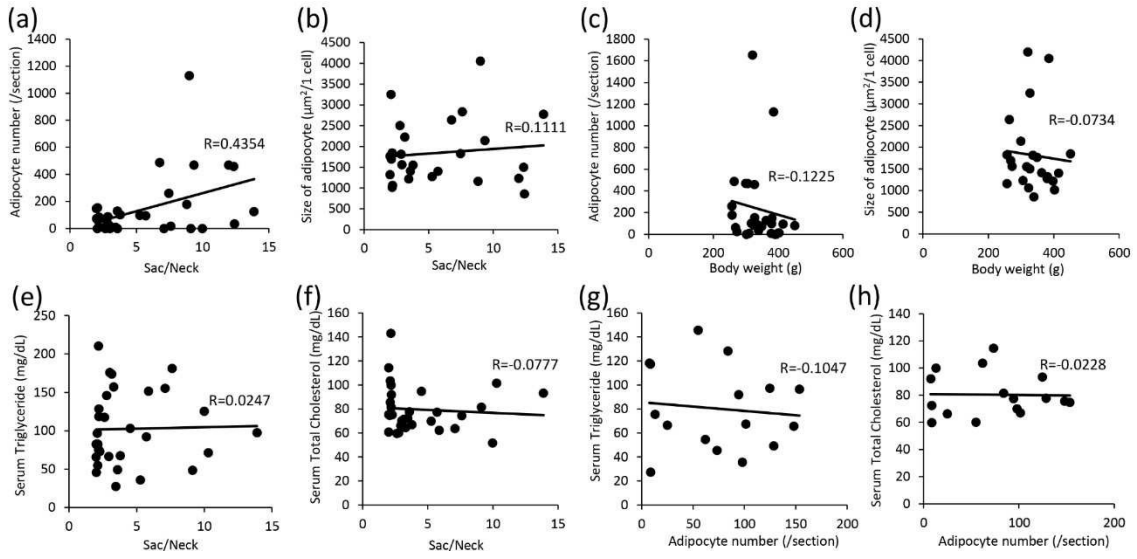

Figure 14 Relationships between adipocytes in the vascular wall, the dilation ratio (sac/neck), and body weight. The dilation ratio versus the number of adipocytes (**a**), and the size of adipocytes in aortic wall (**b**). Body weight versus the number of adipocytes (**c**), and the size of adipocytes in aortic wall (**d**). The dilation ratio versus serum triglyceride levels (**e**), and serum total cholesterol levels (**f**). The number of adipocytes in aortic wall versus serum triglyceride levels (**g**), and serum total cholesterol levels (**h**). Reproduced from a figure previously published in *J. Oleo Sci.* with slight modification.[22)]

2.3.6 Correlation between the amount of TG in human AAA wall and AAA diameter

The relationship between the TG content in human AAA tissue and AAA diameter was studied. The abnormal appearance of adipocytes was mainly observed in the adventitial region in both human and animal model (**Fig. 15a-c**). The human AAA vascular wall was divided into two groups: 1) the intima and media, and 2) the adventitia. The amount of TG in the adventitia was correlated with AAA diameter, but not in the in the intima and media (**Fig. 15d**). The amount of total cholesterol in the aortic tissue was not correlated with AAA diameter (**Fig. 5e**).

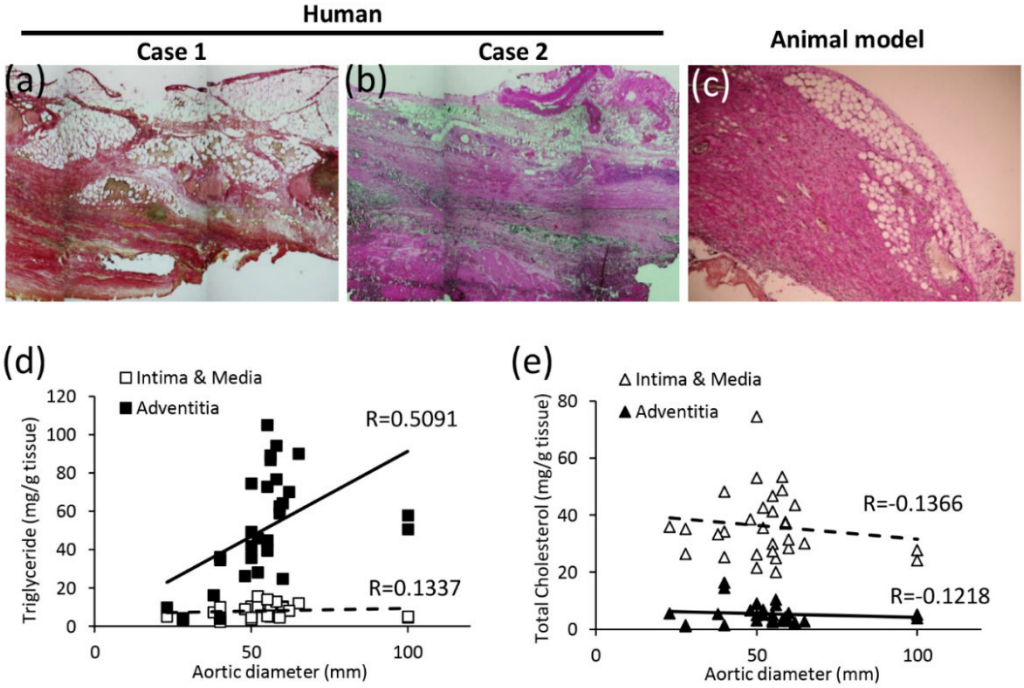

Figure 15 Correlation between lipids in the aortic wall and the aortic diameter in human AAA samples. Appearance of adipocytes in human AAA tissues (**a, b**), and in hypoperfusion-induced animal model (**c**). The abnormal appearance of adipocytes in human AAA vascular wall has been previously reported.[23] (**d**) The amount of triglyceride in aortic wall versus the aortic diameter (mm). (**e**) The amount of total cholesterol in aortic wall versus the aortic diameter (mm). Reproduced from a figure previously published in *Sci. Rep.*[19]

The amount of TG in the aortic tissue was not correlated with serum TG levels (**Fig. 16a**), serum total cholesterol levels (**Fig. 16b**), or body mass index (BMI) (**Fig. 16c**). The amount of total cholesterol in the aortic tissue was not correlated with serum TG levels (**Fig. 16d**), serum total cholesterol levels (**Fig. 16e**), or BMI (**Fig. 16f**). The AAA diameter was also not correlated with serum TG levels (**Fig. 16g**), serum total cholesterol levels (**Fig. 16h**), or BMI (**Fig. 16i**).

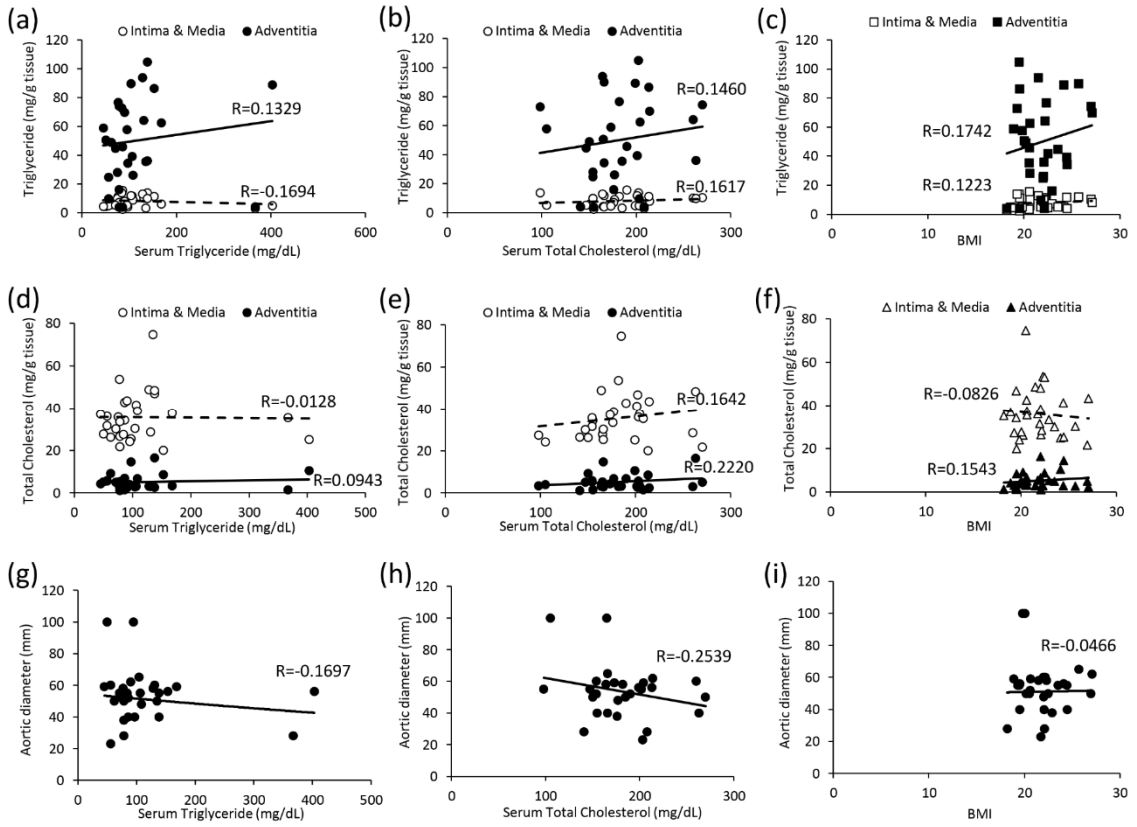

Figure 16 Relationships between serum lipids (triglyceride (TG) and total cholesterol), BMI and aortic diameter in human AAA samples. The amount of TG in aortic wall versus serum TG levels (**a**), serum total cholesterol levels (**b**), and body mass index (BMI) (**c**). The amount of total cholesterol in aortic wall versus serum TG levels (**d**), serum total cholesterol levels (**e**), and BMI (**f**). Aortic diameter versus serum TG levels (**g**), serum total cholesterol levels (**h**) and BMI (**i**). Aortas were divided into two groups: 1) intima and media, and 2) adventitia. Reproduced from a figure previously published in *Sci. Rep.*[19)]

2.4 Discussion

Vascular dilation was significantly promoted in the ruptured group (**Fig. 5, 6**). Histological analyses showed that adipocytes were observed in the sac wall, but not in the neck wall (**Fig. 7**). This ectopic appearance of adipocytes has been previously reported in human tissues,[24] and the pathology in hypoperfusion-induced model was consistent with the pathology in human AAA. The number of adipocytes in the AAA sac wall in ruptured group was significantly increased (**Fig. 7**). In the areas with adipocytes, the destruction of collagen fibers and the increase of MMP-2 and MMP-9 expressions were observed (**Fig. 9**). In addition, the increase of positive areas for MCP-1 and macrophages was observed in the areas with adipocytes (**Fig. 10**). Therefore, it was suggested that adipocytes accumulated in the vascular wall can induce the chronic inflammation around adipocytes in the aortic wall. It has been reported that hypertrophic adipocytes due to lipid accumulation could cause chronic inflammation in tissues[25, 26], and adipocytes themselves secrete MMP-2 and MMP-9.[27] It is speculated that hypertrophic adipocytes can promote the production of MCP-1, induce the infiltration of macrophages into the areas surrounding adipocytes, and increase the MMP-2 and MMP-9 expressions. The collagen fibers degradation around adipocytes could be enhanced, and thereby the aortic wall weakness and aortic rupture could be accelerated.

Pathological analyses along the tear in the ruptured wall showed many adipocytes in the adventitial wall (**Fig. 12**). Collagen-positive areas significantly decreased and the protein levels of MMPs and positive areas of monocytes/macrophages significantly increased in this region with adipocytes (**Fig. 13**). These findings strongly suggest the hypothesis that the abnormal appearance of adipocytes in the vascular wall can be closely involved in AAA rupture.

The amount of TGs in the adventitia was correlated with AAA diameter in human AAA (**Fig. 15**). In human AAA wall, ectopic adipocytes were observed in the adventitia (**Fig. 15**). Therefore, the increase of the amount of TGs in the adventitia imply the increase and hypertrophy of adipocytes in the adventitia. In addition, the number of adipocytes was correlated with the aortic dilation ratio in hypoperfusion-induced AAA model (**Fig. 14**). In human clinical studies, the risk of death from AAA rupture has been reported to correlate with serum TG levels.[28, 29] Increased serum TG levels might induce adipocytes hypertrophy in human AAA wall. However, this study reported that aortic diameter was not correlated with serum TG levels in AAA patients and hypoperfusion-induced model. Further studies are needed to validate the correlation between serum TG levels and AAA.

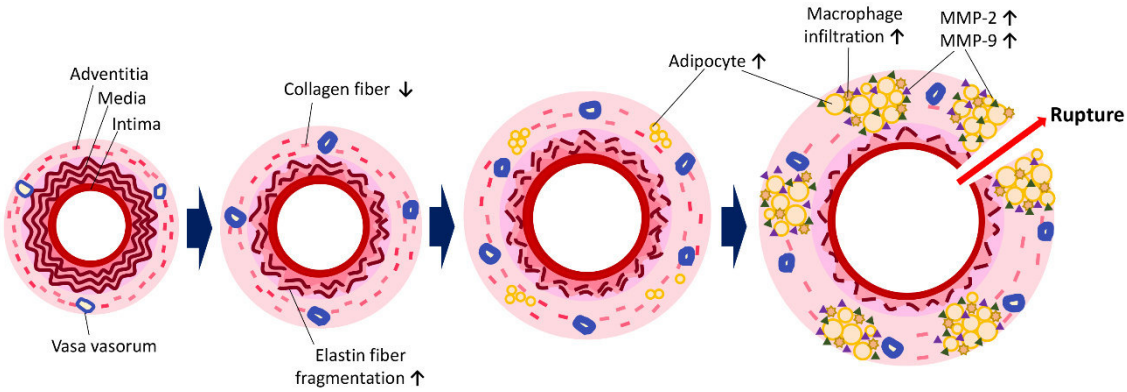

Figure 17 Proposed mechanisms underlying AAA rupture. Vascular hypoperfusion due to the stenosis of adventitial vasa vasorum (VV) may cause the degradation of collagen and elastin fibers and the abnormal appearance of adipocytes in the vascular wall. Hypertrophic adipocytes may induce the recruitment of macrophages around adipocytes. These immune cells may increase matrix metalloproteinase (MMP) -2 and MMP-9 expressions and degrade collagen fibers around adipocytes. The weak vascular wall around adipocytes can tend toward AAA rupture. Reproduced from a figure previously published in *J. Oleo Sci.* with slight modification.[22)]

Figure 17 shows the hypothesis of mechanisms underlying uninvited vascular adipocytes-related AAA rupture. Stenosis of the VV occurs in the aortic wall and triggers the degradation of vascular fibers with chronic inflammation and abnormal adipocytes appearance. Adipocytokines secreted from adipocytes may be involved in one of the causes of AAA progression and rupture due to abnormal appearance of adipocytes in the aortic wall. Immune cells such as macrophages accumulate in tissues surrounding adipocytes by secretion of MMPs due to hypertrophic adipocytes. It is speculated that vulnerable areas are developed in the aneurysm wall by the increased number of adipocytes. Doderer et al. also reported the adventitial adipogenic degeneration of the vascular wall in human AAA.[30)] Krueger et al. reported an increase in inflammation related factors around adipocytes in the adventitial region of human aneurysm tissue.[31)] The mechanisms underlying the appearance of adipocytes and the pathological significance of adipocytes in AAA remain unknown, and further studies are necessary. The appropriate control of vascular adipocytes may treat or prevent AAA rupture.

Chapter 3 - Appearance of adipocytes in thoracic aortic aneurysmal wall

3.1 Introduction

Thoracic aortic aneurysm (TAA) is a vascular disease characterized by the gradual and irreversible pathological dilation of the thoracic aortic aorta. The mortality rate due to TAA rupture is very high, and risk factors for TAA include age, sex, hypertension, hyperlipidemia, smoking, and family history.[32] The underlying molecular mechanisms in TAA progression and rupture are still largely unknown. Here, AAA is the most common aneurysm type. It was described in Chapter 2 that the abnormal appearance of adipocytes in aortic wall was strongly associated with AAA rupture risk. However, it was recently reported that adipocytes accumulation was not observed in the vascular wall of popliteal artery aneurysm (PAA), in which rupture is rare.[30] Therefore, the appearance of adipocytes in the vascular wall may be not common pathology among aneurysms formed in different aortae. Whether adipocytes abnormally appear in the TAA wall remains unknown. This study aimed to investigate the relation between adipocytes in the vascular wall and TAA by the pathological analysis of the human TAA walls.

3.2 Materials and Methods

Materials and methods in this chapter were previously described in *J. Oleo Sci.* with slight modifications.[33]

3.2.1 Human study

This study was approved by the Ethical Review Committee of the National Cerebral and Cardiovascular Center and Kindai University. Aortic tissue was collected from patient with TAA undergoing operation by artificial vessel replacement. Control thoracic aortic tissue was collected from surgical specimen. The specimens of the thoracic aortic wall were cut out for analyses, immediately frozen, and stored at -80° C. Availability of specimen size was at least 20×5 mm.

Characteristic of patients are presented in **Table 2**. The study subjects were patients with ascending aortic aneurysm or descending aortic aneurysm. The present study comprised controls (n=5) and patients with TAA (n=7) with a mean are of 57.6 ± 18.1 years and 69.1 ± 9.4, respectively.

Table 2 Characteristic of patients

Subject No.	Gender	Site	Age	BMI	TG (mg/dL)	Cho (mg/dL)	HbA1C (%)	CRP (mg/dL)
Control 1	F	Arch and Descending	60	17.9	126	213	5.2	0.01
Control 2	F	Ascending and Arch	59	15.9	85	264	5.1	25.72
Control 3	F	Ascending and Arch	72	27.5	127	187	5.5	0.50
Control 4	M	Sinus of Valsalva	27	20.0	166	201	5.1	0.11
Control 5	F	Ascending	70	19.5	110	225	5.0	0.13
TAA 1	F	Descending	71	24.7	N.D.	214	6.0	1.35
TAA 2	M	Ascending	77	27.0	72	202	5.1	0.09
TAA 3	F	Ascending	69	20.2	62	276	N.D.	0.06
TAA 4	M	Ascending	72	23.9	193	201	5.7	0.05
TAA 5	M	Ascending	70	23.9	229	206	5.6	0.06
TAA 6	F	Ascending and Arch	76	25.9	83	176	5.7	0.02
TAA 7	F	Ascending	49	26.8	47	208	5.2	0.02
Average								
Control			57.6 ± 18.1	20.2 ± 4.4	122.8 ± 29.3	218.0 ± 29.3	5.2 ± 0.2	5.29 ± 11.42
TAA			69.1 ± 9.4	24.6 ± 2.3*	114.3 ± 76.7	211.9 ± 30.7	5.6 ± 0.3	0.24 ± 0.49
*P value			0.1675	0.0882	0.3613	0.7453	0.0552	0.2232

Characteristic of control and TAA samples. Body mass index; BMI, triglyceride; TG, cholesterol; Cho, Hemoglobin A1c; HbA1c, C-reactive protein; CRP. Data are the mean ± S.D. Statistical differences were determined by the Mann-Whitney U-test. N.D. = not determined.

Reproduced from a figure previously published in *J. Oleo Sci.*[33)]

3.2.2 Histological analysis

Aortic tissue cross-sections (10-μm-thick) were prepared using a cryostat (CM1850; Leica Microsystems, Wetzlar, Germany), and aortic walls were used for pathological examinations. Immunohistochemical staining was performed as described in Chapter 2. The patency rate of VV (%) was calculated by dividing the lumen area by the entire area of VV and lumen.

3.3.3 Statistical analysis

Values were expressed as mean ± S.D. Statistical differences were determined by the Mann-Whitney U-test and the Scheffe test. The P-value <0.05 was considered to indicate a statistically significant difference. Statistical analyses were performed using StatView 5.0 software (SAS Institute, Cary, USA).

3.3 Results

3.3.1 The appearance of adipocytes in human TAA tissue

The appearance of adipocytes was mainly observed in the adventitia in both human control and TAA walls (**Fig. 18A-C**), and these adipocytes stained positively with Oil Red O staining (**Fig. 18D-F**). Adipocytes areas in the vascular wall were significantly increased in the TAA wall compared to the control wall (3.6 ± 4.4 % in the control group, 20.7 ± 11.7 % in the TAA group) (**Table 3**).

Table 3 Adipocyte area

Subject No.	Adipocyte area (%)	
Control 1	0.0	
Control 2	9.1	
Control 3	1.4	
Control 4	0.0	
Control 5	7.6	
TAA 1	0.0	
TAA 2	27.9	
TAA 3	17.2	
TAA 4	23.0	
TAA 5	16.7	
TAA 6	22.0	
TAA 7	38.3	
	Average	*P value
Control	3.6 ± 4.4	0.0284
TAA	20.7 ± 11.7*	

Data are the mean ± S.D. Statistical differences were determined by the Mann-Whitney U-test.

Reproduced from a figure previously published in *J. Oleo Sci.*[33)]

Collagen positive areas were significantly decreased in the TAA wall compared with the control wall (**Fig. 18G-J**). In addition, collagen positive areas were significantly decreased in the region with adipocytes compared with the region without adipocytes in the TAA wall (**Fig. 18G-J**).

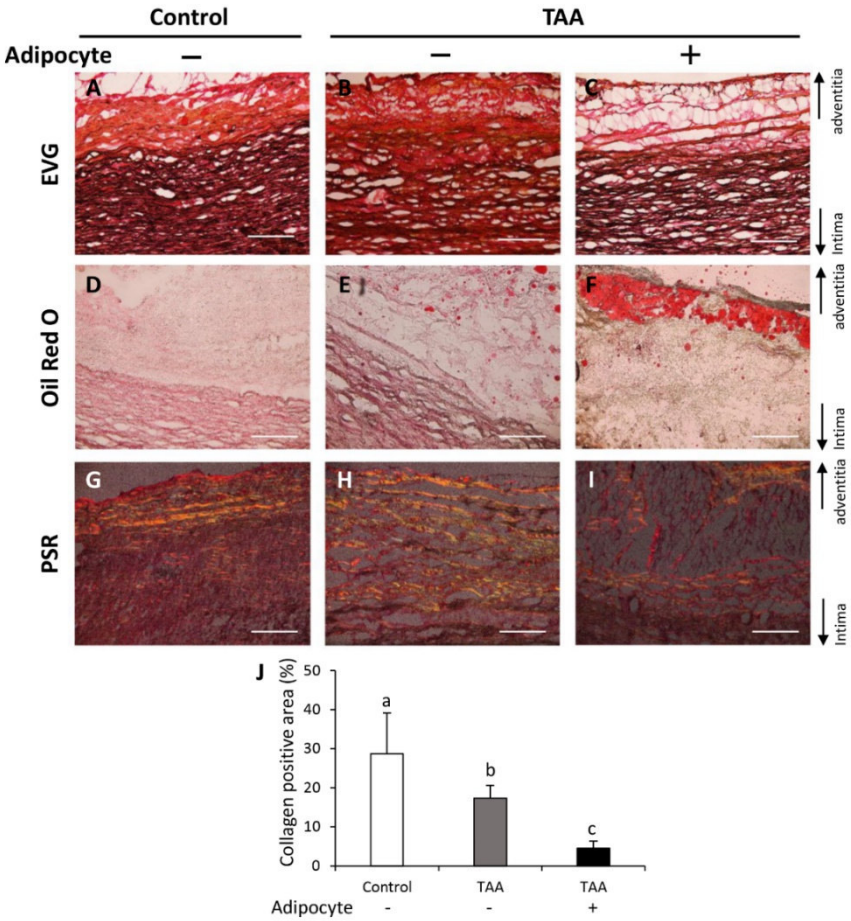

Figure 18 Observation of the adipocytes and collagen fibers in TAA wall. (**A-C**) Representative images of EVG staining (scale bar = 400 μm), (**D-F**) Oil Red O staining (scale bar = 400 μm), and (**G-I**) PSR staining (scale bar = 400 μm). (**J**) Quantification of collagen-positive area in the vascular wall. Data are the mean ± S.D. Values with different letters are significantly different (P<0.05) by analysis of variance followed by Scheffe test. Control (n = 5), TAA (n = 7). Reproduced from a figure previously published in *J. Oleo Sci.*[33]

3.3.2 Histological pathology of areas around adipocytes in TAA wall

Immunohistochemical analyses for MMP-2 (**Fig. 19A-C**), MMP-9 (**Fig. 19D-F**), and Mac387$^+$ monocytes/macrophages (**Fig. 19G-I**) were performed. Areas positive for MMP-2, MMP-9 and Mac387$^+$ monocytes/macrophages were significantly increased in the TAA wall compared with the control wall (**Fig. 19J-L**). In addition, areas positive for MMP-2, MMP-9 and Mac387$^+$ monocytes/macrophages were significantly increased in the region with adipocytes compared with the region without adipocytes in the TAA wall (**Fig. 19J-L**). VVs in TAA walls were observed (**Fig. 20A-H**). However, VV stenosis was not observed in this experimental group (**Fig. 20I**).

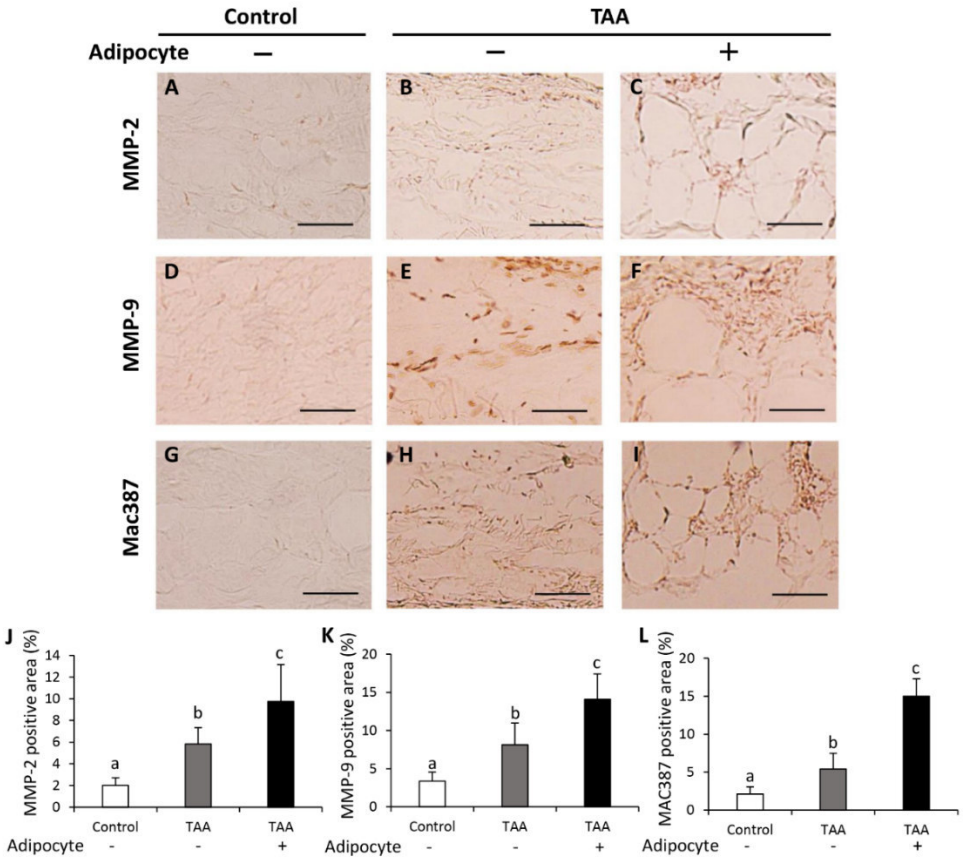

Figure 19 Immunohistochemical staining for MMP-2, MMP-9, and Mac387$^+$ monocyte/macrophage. (**A-C**) Representative images of immunostaining for MMP-2 (scale bar = 50 μm), (**D-F**) MMP-9 (scale bar = 50 μm), and (**G-I**) Mac387 (scale bar = 50 μm). (**J**) Quantification of MMP-2 positive area, (**K**) MMP-9 positive area, and (**L**) Mac387 positive area in the vascular wall. Data are the mean ± S.D. Values with different letters are significantly different (P<0.05) by analysis of variance followed by Scheffe test. Control (n = 5), TAA (n = 7). Reproduced from a figure previously published in *J. Oleo Sci.*[33]

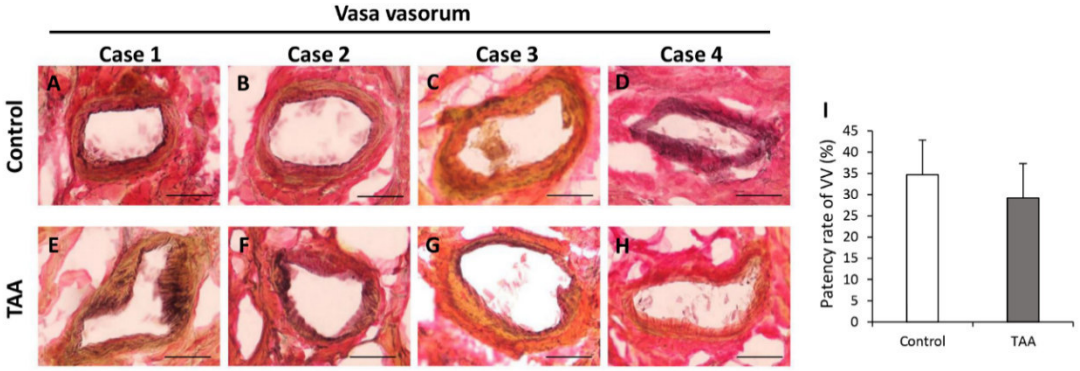

Figure 20 Observation of adventitial vasa vasorum (VV). Representative images of VV in the control wall (**A-D**), and in the TAA wall (**E-H**) (scale bar = 50 μm). (**I**) Quantification of patency rate of VV in control and TAA walls. Statistical differences were determined by the Mann-Whitney U-test. Data are the mean ± S.D. Control (n = 5), TAA (n = 7). Reproduced from a figure previously published in *J. Oleo Sci.*[33]

3.4 Discussion

The appearance of adipocytes, and the destruction of collagen fibers and increase of MMP-2 and MMP-9 expressions surrounding adipocytes were observed in human TAA tissue (**Fig. 18, 19**). The weakening of the vascular wall due to ectopic adipocytes may be related to not only AAA but also TAA.

TAA is divided into 3 types: aneurysm of ascending aorta, aortic arch aorta, and descending aorta. The mechanisms underlying TAA progression may be dependent on the part of aorta. Perivascular adipose tissue (PVAT) may be associated with the vascular function, inflammation, and diseases,[34] and the increased epicardial adipose tissue may lead to the ascending aortic dilation.[35] In this study, the effect of adipocyte accumulation depending on the site of aneurysm remains unknown and further studies are needed.

Hypoperfusion in "abdominal aortae" due to stenosis of VVs can be associated with the abnormal appearance of adipocytes, and the AAA progression and rupture.[10, 19] However, stenosis of VVs in "thoracic aortae" were not observed in this study (**Fig. 20**). The appearance of adipocytes in the TAA wall may be mediated by factors other than the stenosis of VVs.

This study reported that vascular adipocytes accumulation was observed in not only the AAA wall but also the TAA wall. The abnormal appearance of adipocytes may be associated with the TAA wall weakness. Whether the increase in adipocytes directly lead to the development or the rupture of TAA, and the pathological significance of adipocytes in the TAA wall remain unknown. Further studies are needed.

Chapter 4 - Suppressive effects of fish oil on development of abdominal aortic aneurysm

4.1 Introduction

Hypoperfusion in the aortic wall due to the obstruction of VV could cause the vascular inflammation and AAA formation. However, the preventive methods for hypoperfusion-induced AAA remain unknown. AAA has been histologically characterized by chronic inflammation of the vascular wall. The inflammation in the aortic wall may be important target for suppressing AAA development. Here, this study focused on fish oil. Fish oil contains rich n-3 polyunsaturated fatty acid (n-3PUFA), such as eicosapentaenoic acid (EPA) and docosahexaenoic acid (DHA), which have anti-inflammatory and anti-oxidative effects. The anti-inflammatory effect of n-3PUFA has multiple underlying mechanisms. For example, anti-inflammatory metabolites produced by EPA and DHA, such as resolvin and protectin.[36] In addition, fish oil has an inhibitory effect on the growth of adipocytes.[37] The suppressive effects of n-3PUFAs on the AAA development were previously reported in various AAA animal models.[38-42] In clinical research, low serum EPA levels were associated with the size and growth of AAA.[43] However, the effects of n-3PUFAs on hypoperfusion-induced AAA development remain unknown.

In this study, to evaluate the effects of fish oil on the development and rupture of AAA, EPA-rich fish oil was orally administrated to hypoperfusion-induced AAA model rats, and the suppressive effects of fish oil were studied.

4.2 Materials and Methods

Materials and methods in this chapter were previously described in *Biosci. Biotechnol. Biochem.* and *Sci. Rep.* with slight modifications.[19, 44]

4.2.1 Animals

All animal experiments were approved by the Kindai University Animal Care and Use Committee and performed according to the Kindai University Animal Experimentation Regulations (Approval number; KAAG-25-001). Six-week-old male Sprague-Dawley rats (SHIMIZU Laboratory Supplies Co., Ltd, Kyoto, Japan) were provided with food (**Table 1**) and water *ad libitum*, in a humidity-controlled room, with a 12-hour light and 12-hour dark cycle and at 25 ± 1 °C.

4.2.2 Fish oil administration from before the induction of hypoperfusion in vascular wall

After acclimatization for a week, rats were then orally administrated either triolein (1145 mg/kg body weight/day) (n=5) (control group), or fish oil (1145mg/kg body weight/day; purified TG extracted from sardines; Nippon Suisan Kaisha Ltd. Tokyo, Japan) (n=9) (fish oil group) respectively, for a week. Hypoperfusion was induced in abdominal aortic wall in all rats to induce AAA. After administration for 4 weeks, aortic diameters were then measured, and the rats sacrificed. The fatty acid composition of the fish oil is shown in **Table 4**.

Table 4 Fatty acid composition

Fatty acid	coconut oil (%)	fish oil (%)
8 : 0	7.1	-
10 : 0	7.6	-
12 : 0	27.6	-
14 : 0	19.8	5.2
16 : 0	14.9	6.6
16 : 1	-	9.3
16 : 2	-	1.7
16 : 3	-	2.8
16 : 4	-	4.8
18 : 0	6.6	0.5
18 : 1	13.3	9.6
18 : 2 n-6	3.1	1.4
18 : 3 n-3	-	0.9
18 : 4 n-3	-	5.1
20 : 4 n-6	-	1.3
20 : 4 n-3	-	1.1
20 : 5 n-3	-	30.8
22 : 5 n-6	-	0.3
22 : 5 n-3	-	2.9
22 : 6 n-3	-	15.7

4.2.3 Fish oil administration from after the induction of hypoperfusion in vascular wall

After acclimatization for a week, hypoperfusion was induced in abdominal aortic wall in all rats to induce AAA. Rats were then orally administrated either water (control group) (n=16), triolein (1145 mg/kg body weight/day) (n=24) (triolein group), or fish oil (1145mg/kg body weight/day) (n=19) (fish oil group) for 4 weeks. Aortic diameters were then measured, and the rats sacrificed. The fatty acid composition of the fish oil is shown in **Table 4**. When a rat died by AAA rupture, the aortic diameter was measured and the abdominal aorta immediately isolated.

4.2.4 Sample collection

The diameter of abdominal aorta was measured using digital calipers (A&D, Tokyo, Japan). Aneurysm was considered to be formed when the dilation ratio was greater than two. Isolated tissues were fixed in 4% PFA (Nacalai Tesque, Kyoto, Japan), soaked in sucrose (10%, 15% and 20%), and then embedded in O.C.T. Compound (Sakura Finetek Japan Co., Ltd.). These were stored at −80 °C until required.

4.2.5 Histological analysis

Abdominal aortae were cut with (CM1850; Leica Microsystems, Wetzlar, Germany) into 10-μm-thick sections, and mounted on glass slides. Tissue sections were subjected to histological stainings. The elastin degradation score was evaluated as shown in **Figure 4**. Quantitative analysis of histological staining was performed using ImageJ software (National Institutes of Health, Bethesda, Maryland, USA). Areas within 100 μm of an adipocyte were defined as 'around adipocyte'.

4.2.6 Statistical analysis

Values were expressed as mean ± S.E.M. For between-group comparisons, the Chi-square test or Fisher's exact test (for situations with small frequencies) was used for categorical variables. Student's t test for continuous data with Tukey-Kramer test and Mann-Whitney test for scoring data were used. Kaplan–Meier method was used for analysis of survival analysis, and intergroup differences were evaluated by the log-rank test with Holm adjustment for multiple comparisons. A P-value < 0.05 was considered to indicate a statistically significant difference. Statistical analyses were performed using StatView 5.0 software (SAS Institute, Cary, USA) and R 3.2.0 with the EZR package.[21)]

4.3 Results

4.3.1 Suppressive effect of fish oil administration before the induction of hypoperfusion on the aortic dilation

The average final body weight (g) did not differ significantly between the groups (364.3 ± 17.5 g in the control group (administration of triolein), 368.4 ± 42.8 g in the fish oil group (administration of EPA-rich fish oil)). Serum TG levels (mg/dL) were significantly decreased in the fish oil group compared to the control group (57.8 ± 21.1 mg/dL in the control group, 29.5 ± 16.5 mg/dL in the fish oil group). Four weeks after the induction of hypoperfusion, aneurysm formation was observed in both groups (**Fig. 20a**). Aortic diameter in the AAA sac wall and the dilation ratio were significantly suppressed in the fish oil group compared to the control group (**Fig. 20b, c**).

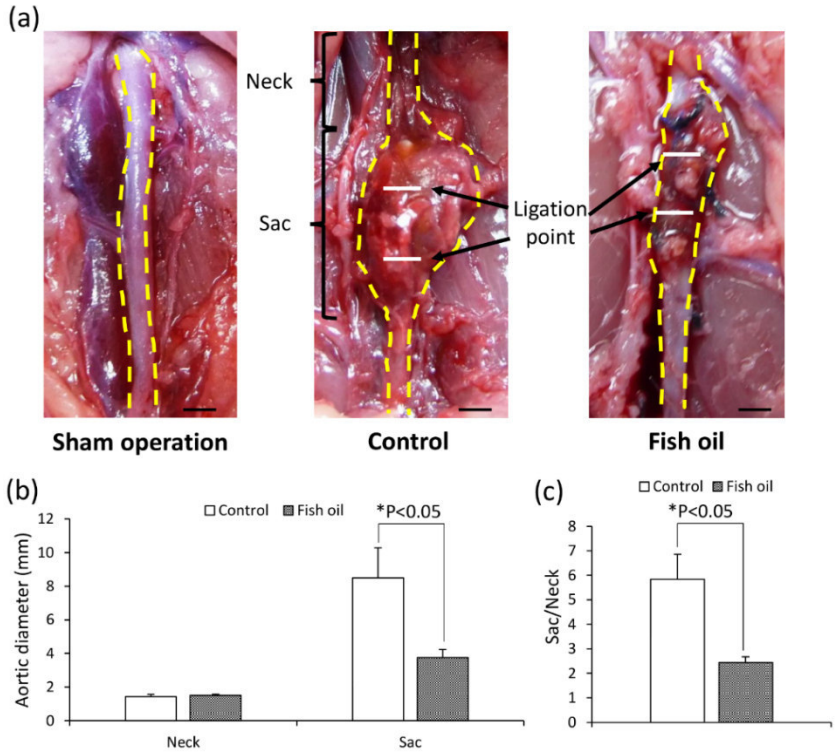

Figure 21 Aortic diameter. (**a**) Representative images of the abdominal aorta in non - treated, control, and fish oil groups. (scale bar = 1.5 mm) (**b**) Quantitative analysis of the aortic diameter. (**c**) Dilation rate (sac/neck). Data are represented as mean ± S.E.M. Control group (n = 5), fish oil group (n = 9). **P* < 0.05 versus the control group. Reproduced from a figure previously published in *Biosci. Biotechnol. Biochem.*[44)]

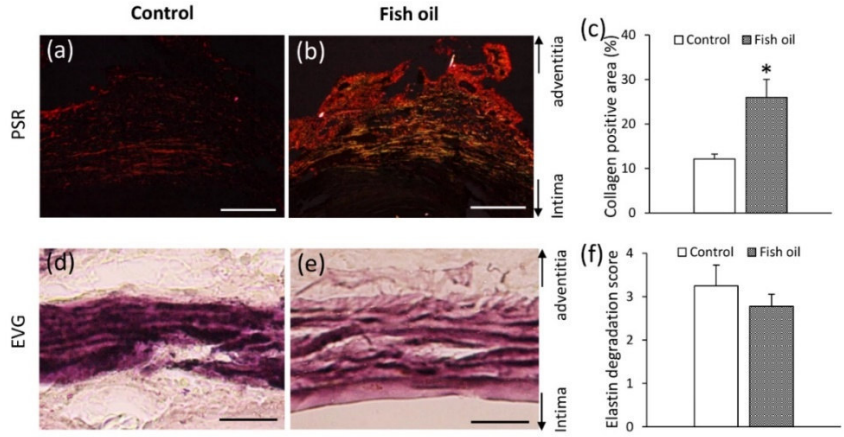

Figure 22 Observation of collagen and elastic fibers. (**a, b**) PSR staining (scale bar = 200 μm). (**c**) Collagen positive area. (**d, e**) EVG staining (scale bar = 25 μm). (**f**) Elastin degradation score. Data are represented as mean ± S.E.M. **P* < 0.05 versus the control group. Reproduced from a figure previously published in *Biosci. Biotechnol. Biochem.*[44)]

4.3.2 Suppressive effect of fish oil administration before the induction of hypoperfusion on the degradation of collagen fibers, MMPs expression, and oxidative stress in vascular wall

Collagen positive areas in the adventitial wall were significantly larger in the fish oil group than those in the control group (**Fig. 22a-c**). The elastin degradation score was not significantly different between groups (**Fig. 22d-f**). Because the degradation of collagen fibers was suppressed in the fish oil group, immunohistochemical examination for MMP-2 (**Fig. 23a-d**) and MMP-9 (**Fig. 23f-i**) was performed. Positive areas for MMP-2 and MMP-9 were significantly decreased in the fish oil group compared with those in the control group (**Fig. 23e, j**). Positive areas for MCP-1 did not differ significantly between the groups (**Fig. 23k-o**). Positive areas for malondialdehyde (MDA), the oxidative marker, were significantly decreased in the fish oil group compared with those in the control group (**Fig. 23p-t**).

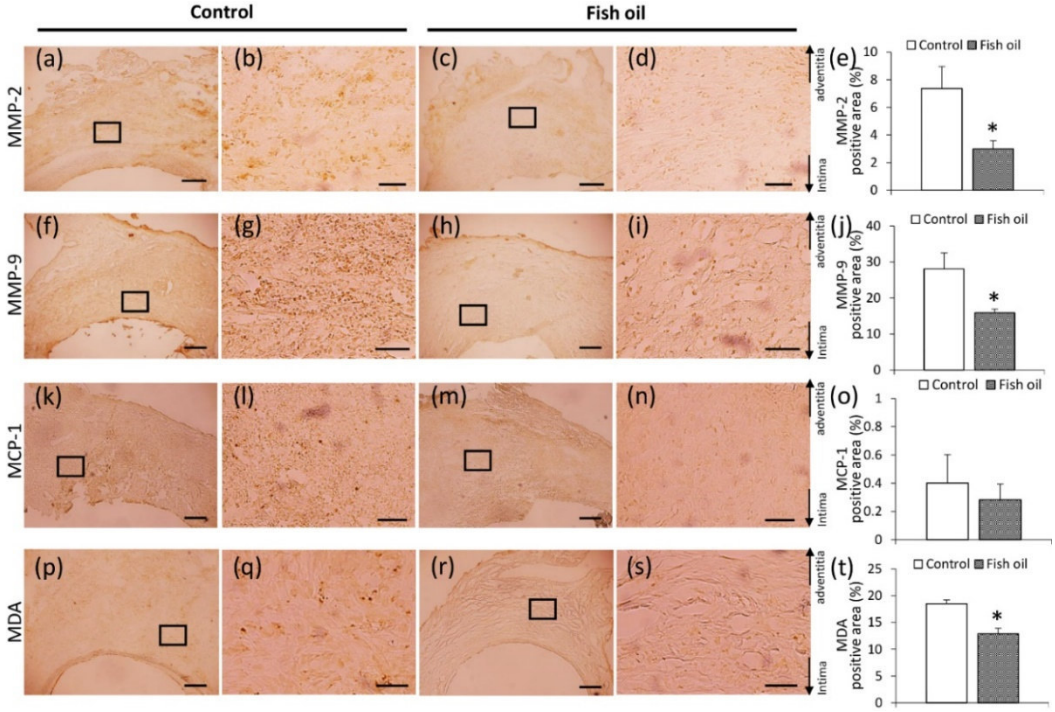

Figure 23 Immunohistochemical staining for MMP-2, MMP-9, MCP-1, and MDA. (**a–d**) Immunostaining for MMP-2. (**e**) MMP-2 positive areas. (**f–i**) Immunostaining for MMP-9. (**j**) MMP-9 positive areas. (**k–n**) Immunostaining for MCP-1. (**o**) MCP-1 positive areas. (**p–s**) Immunostaining for MDA. (**t**) MDA positive areas. (a, c, f, h, k, m, p, r: scale bar = 200 μm; b, d, g, i, l, n, q, s: scale bar = 50 μm). The squared area in the left-side panels is magnified in the right-side panels as a representative image. Data are represented as mean ± S.E.M. *$P < 0.05$ versus the control group. Reproduced from a figure previously published in *Biosci. Biotechnol. Biochem.*[44]

4.3.3 Suppressive effect of fish oil administration after the induction of hypoperfusion on the AAA rupture risk

Oral administration of fish oil before the induction of hypoperfusion showed suppressive effects on the aortic dilation (**Fig. 21**). These results showed the preventive effects when fish oil was taken before hypoperfusion of vascular wall. Since AAA is silent disease, it is not often noticed even if hypoperfusion of the vascular wall which triggers AAA occurs. Next, the effects of oral administration of fish oil after the induction of hypoperfusion on the development of AAA were evaluated.

The average final body weight (g) of the rats was not significantly different between the three groups (343.9 ± 44.0 g in the control group, 341.6 ± 29.0 g in the triolein group, and 373.7 ± 20.4 g in the fish oil group). Serum TG levels (mg/dL) in the fish oil group were significantly decreased compared with the triolein group (112.4 ± 52.0 mg/dL in the control group, 134.5 ± 44.2 mg/dL in the triolein group, 67.3 ± 23.7 mg/dL in the fish oil group). Serum total cholesterol levels (mg/dL) were not significantly different between the three groups (85.0 ± 27.7 mg/dL in the control group, 71.5 ± 12.5 mg/dL in the triolein group, 79.4 ± 16.0 mg/dL in the fish oil group).

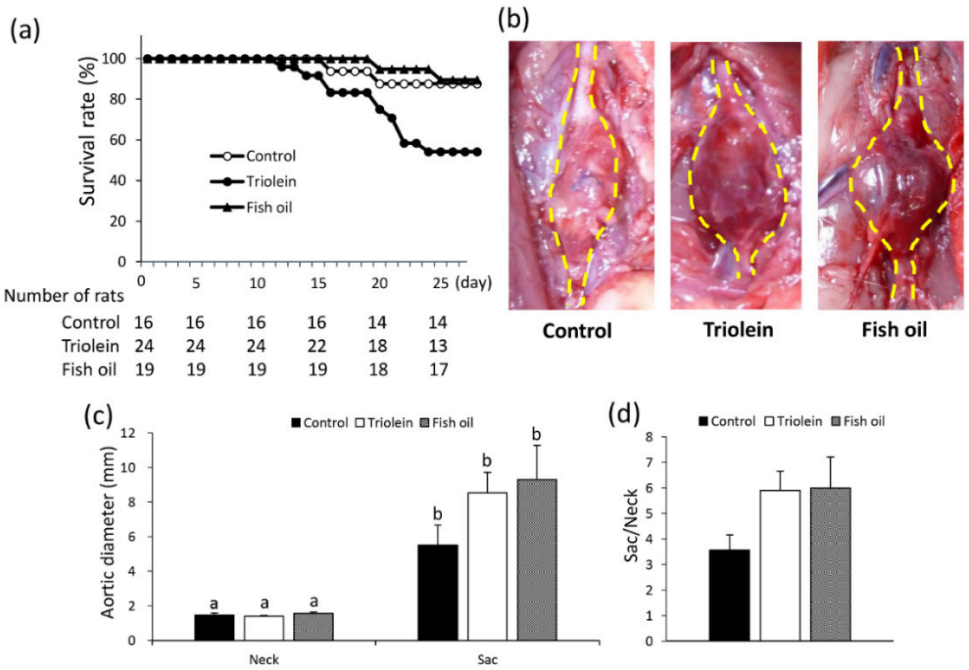

Figure 24 Suppressive effects of fish oil administration on AAA rupture. (**a**) Kaplan-Meier curves for AAA rupture. (**b**) Representative images of abdominal aorta. (**c**) The aortic diameter. (**d**) Dilation ratio. Data are the mean ± S.E.M. Control group (n = 16), triolein group (n = 24), fish oil group (n = 19). Reproduced from a figure previously published in *Sci. Rep.*[19]

The Kaplan–Meier curves for AAA rupture are shown in **Figure 24a**, and the rupture risk in the fish oil group significantly decreased compared to triolein group (P= 0.0348). The AAA rupture risk in the control group was not significantly different from either the triolein group (p = 0.0734) or the fish oil group (P = 0.821). Aneurysm formation was observed for all groups (**Fig. 24b**). The aortic diameter in the AAA sac wall and the dilation ratio were not significantly different between the groups (**Fig. 24c, d**).

4.3.4 Suppressive effect of fish oil administration after the induction of hypoperfusion on the accumulation of adipocytes in vascular wall

The ectopic adipocytes were observed in the AAA sac wall for all groups (**Fig. 25a-f**). The number (/section) and size (μm²/cell) of adipocytes were significantly decreased in the fish oil group compared to the triolein group (**Fig. 25g, h**). The number and size of adipocytes in the fish oil group were not significantly different from those in the control group (**Fig. 25g, h**).

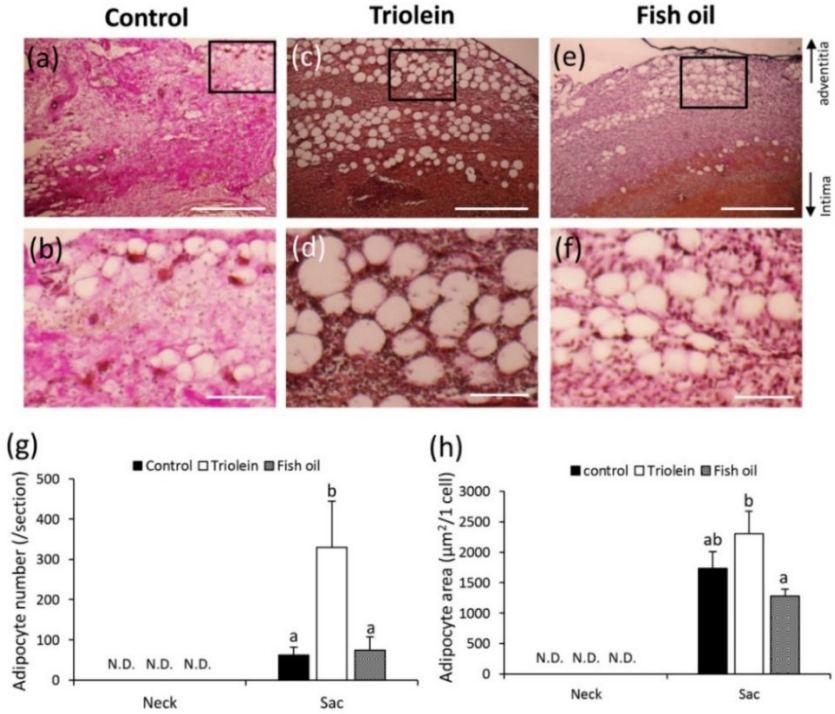

Figure 25 Quantification of adipocytes. (**a-f**) The vascular wall where adipocytes were observed (**a, c, e**: scale bar = 500 μm; **b, d, f**: scale bar = 100μm). The square area in the upper panels is magnified in the bottom panels as a representative image. (**g**) Quantification of the number of adipocytes, and (**h**) the size of adipocytes. Data are the mean ± S.E.M. Control group (n = 14), triolein group (n = 15), fish oil group (n = 14). Values with different letters are significantly different (P < 0.05). N.D. = not detected. Reproduced from a figure previously published in *Sci. Rep.*[19]

Next, for histological analyses, the AAA sac wall were divided into two groups: area with adipocytes and area without adipocytes. The vascular wall thickness was not significantly different between the control, triolein and fish oil groups (**Fig. 26**).

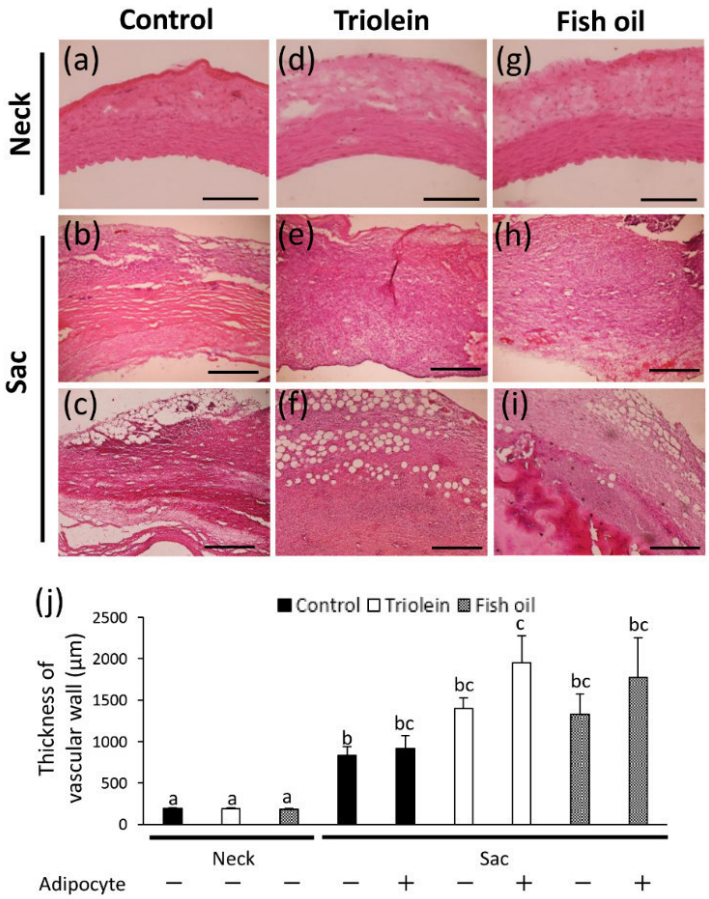

Figure 26 Thickness of vascular wall. AAA sac areas from the three experimental groups were divided into two groups: those without adipocytes (-) (**b, e** and **h**) and those with adipocytes (+) (**c, f** and **i**). (**a-i**) Representative images of HE staining. (**a, b, d, e, g, h**: scale bar = 100 μm; **c, f, i**: scale bar = 400 μm). (**j**) Quantitative analysis of vascular wall thickness. Data are the mean ± S.E.M. Control group (n=9), triolein group (n = 10), fish oil group (n = 8). Values with different letters are significantly different ($P < 0.05$). Reproduced from a figure previously published in *Sci. Rep.*[19]

The elastin degradation score was also not significantly different between the three groups (**Fig. 27a-j**). Collagen positive areas in the triolein group were significantly decreased in the AAA sac walls with adipocytes compared to those without adipocytes (**Fig. 27k-t**). On the contrary, collagen positive areas in the fish oil group were not significantly different in the AAA sac walls with adipocytes compared to those without adipocytes (**Fig. 27k-t**).

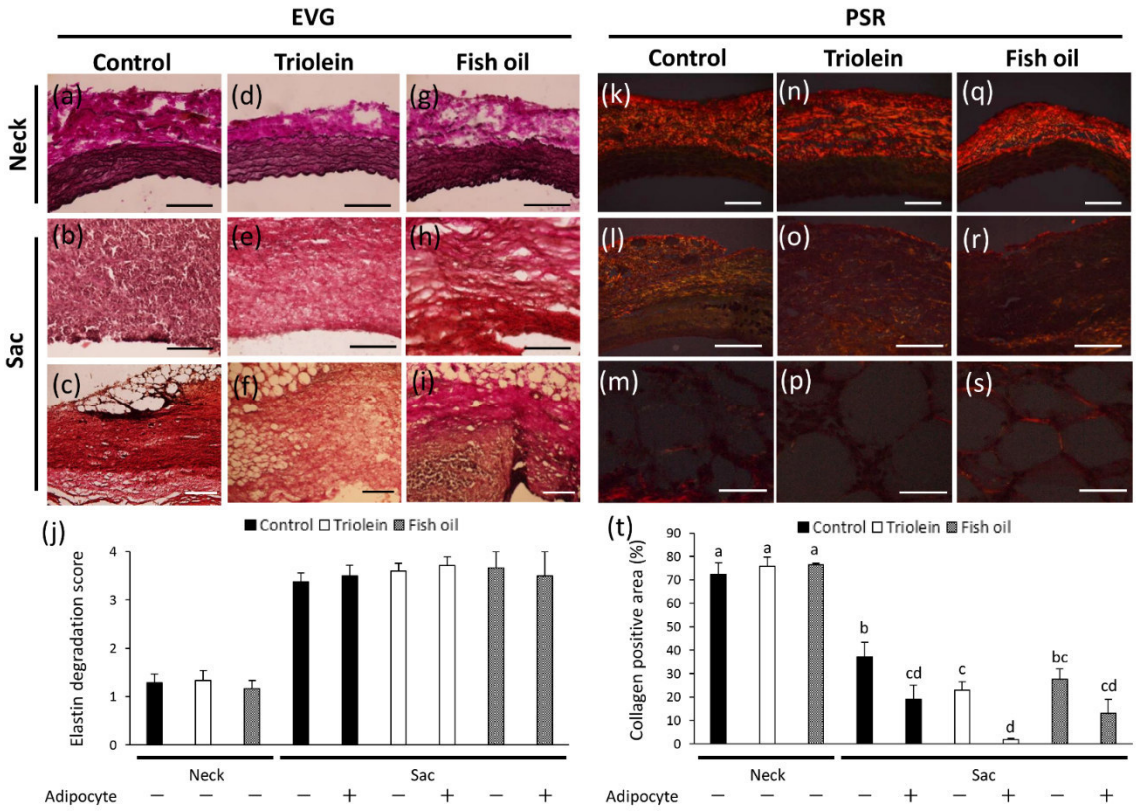

Figure 27 Elastin degradation score and collagen positive area. AAA sac areas from the three experimental groups were divided into two groups: those without adipocytes (-) (**b, e, h, l, o** and **r**) and those with adipocytes (+) (**c, f, j, i, m, p** and **s**). (**a-i**) Representative images of EVG staining (**a, b, d, e, g, h**: scale bar = 100 μm; **c, f, i**: scale bar = 200μm). (**j**) Elastin degradation scores. (**k-s**) Representative images of PSR staining (**k, n, q**: Scale bar = 100 μm, **l, o, r**: scale bar = 400 μm, **m, p, s**: scale bar = 50 μm). (**t**) Collagen-positive areas. Data are the mean ± S.E.M. Control group (n=9), triolein group (n = 10), fish oil group (n = 8). Values with different letters are significantly different ($P < 0.05$). Reproduced from a figure previously published in *Sci. Rep.*[19)]

The α-smooth muscle actin positive areas and the medial wall thickness in the AAA neck and sac walls were not significantly different between the three groups (**Fig. 28**). Areas positive for MMP-2 and MMP-9 in the AAA sac wall without adipocytes were significantly decreased in the fish oil group compared to the triolein group (**Fig. 29**). Areas positive for MMP-2 and MMP-9 in the AAA sac wall with adipocytes were significantly decreased in the fish oil group compared to the triolein group (**Fig. 29**). Areas positive for MMP-2 and MMP-9 in the AAA sac wall with adipocytes were not significantly different between the control and fish oil groups (**Fig. 29**). Areas positive for MCP-1 in the AAA sac wall with adipocytes were significantly decreased in the fish oil group compared to the triolein group (**Fig. 30a-j**). Areas positive for Mac387$^+$ monocytes/macrophages in the AAA sac wall with adipocytes were also significantly decreased in the fish oil group compared to the triolein group (**Fig. 30k-t**). Areas positive for MCP-1 and MAC387$^+$ monocytes/macrophages in the AAA sac wall with adipocytes were not significantly different between the control and fish oil groups (**Fig. 30j, t**).

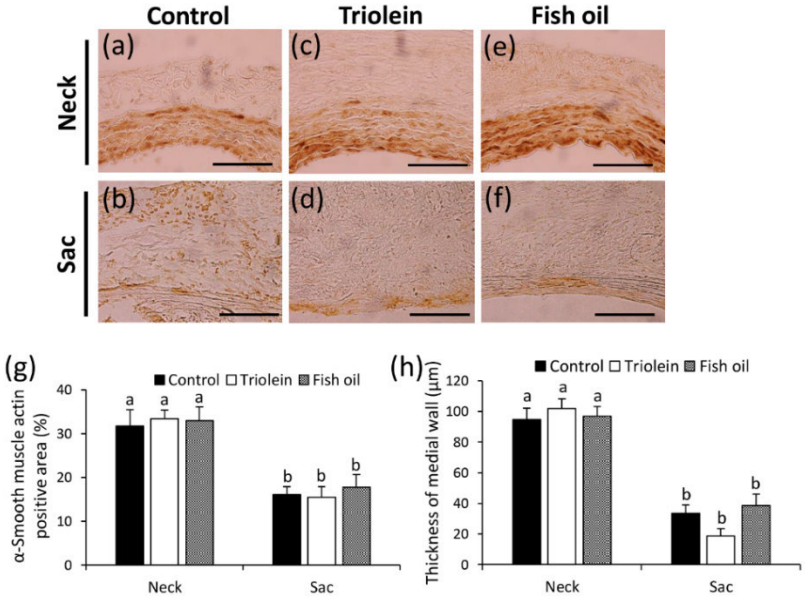

Figure 28 Thickness of medial wall. (**a-f**) Representative images of immunostaining for α-smooth muscle actin (scale bar = 100 μm). (**g**) Quantification of α-smooth muscle actin-positive areas, and (**h**) the medial wall thickness. Data are the mean ± S.E.M. Values with different letters are significantly different ($P < 0.05$). Reproduced from a figure previously published in *Sci. Rep.*[19]

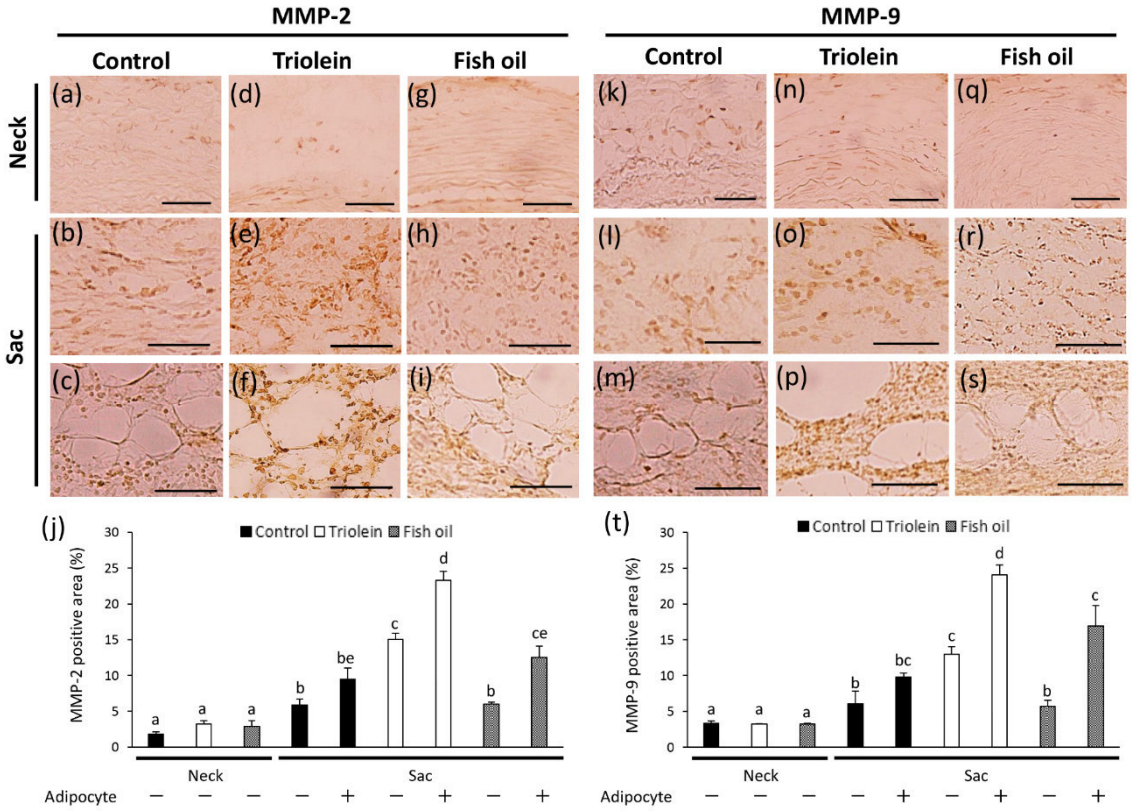

Figure 29 Immunohistochemical staining for MMP-2 and MMP-9. AAA sac areas from the three experimental groups were divided into two groups: those without adipocytes (-) (**b, e, h, l, o** and **r**) and those with adipocytes (+) (**c, f, i, m, p** and **s**). (**a-i**) Immunostaining for MMP-2 (scale bar = 50 μm). (**j**) MMP-2 positive areas. (**k-s**) Immunostaining for MMP9 (scale bar = 50 μm). (**t**) MMP-9 positive areas. Data are the mean ± S.E.M. Control group (n=9), triolein group (n = 10), fish oil group (n = 8). Values with different letters are significantly different ($P < 0.05$). Reproduced from a figure previously published in *Sci. Rep.*[19]

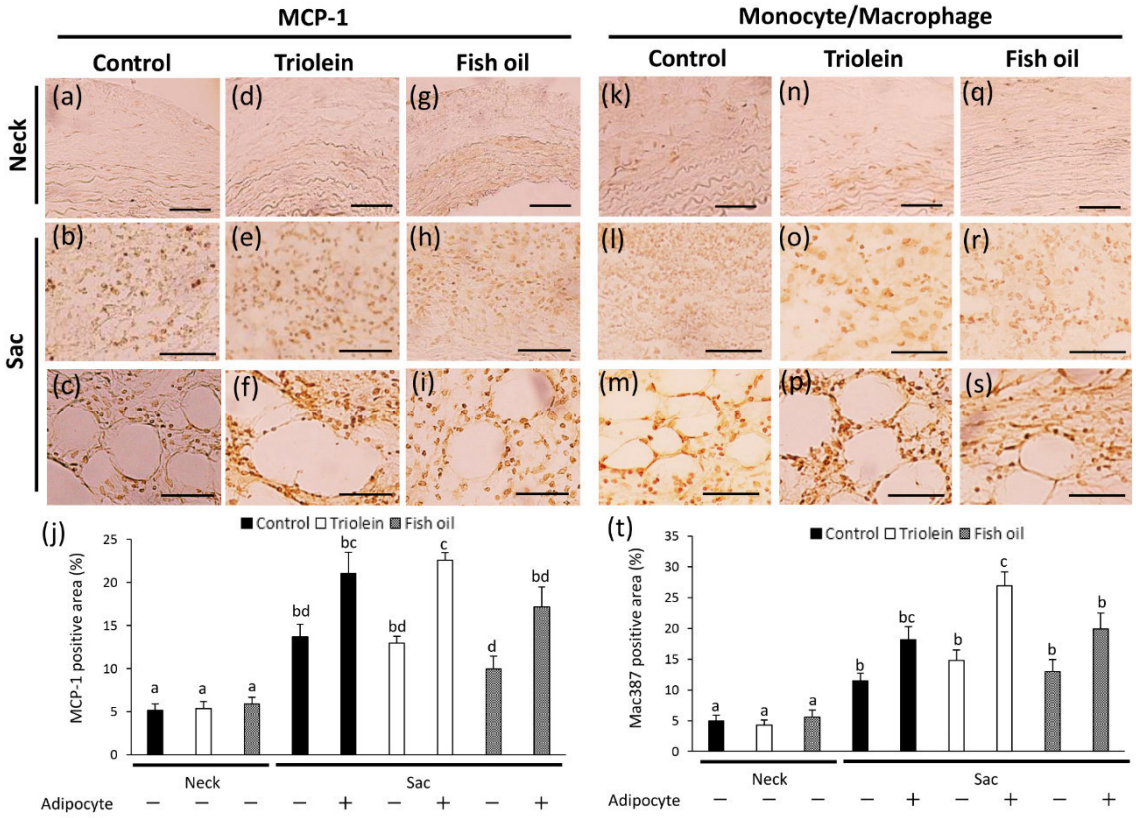

Figure 30 Immunohistochemical staining for MCP-1 and Mac387⁺ monocytes/macrophages. AAA sac areas from the three experimental groups were divided into two groups: those without adipocytes (-) (**b, e, h, l, o** and **r**) and those with adipocytes (+) (**c, f, j, i, m, p** and **s**). (**a-i**) Immunostaining for MCP-1 (scale bar = 50 μm). (**j**) MCP-1 positive areas. (**k-s**) Immunostaining for Mac387⁺ monocytes/macrophages (scale bar = 50 μm). (**t**) Mac387⁺ monocytes/macrophage positive areas. Data are the mean ± S.E.M. Control group (n=9), triolein group (n = 10), fish oil group (n = 8). Values with different letters are significantly different ($P < 0.05$). Reproduced from a figure previously published in *Sci. Rep.*[19]

4.4 Discussion

EPA-rich fish oil showed the suppressive effects on AAA progression both before and after the occurrence of hypoperfusion in the vascular wall which risks AAA. It is speculated that ingesting fish oil can be more effective before the vascular wall becomes pathologic because vascular dilation was suppressed by administration of fish oil before the induction of hypoperfusion. Since the effect of fish oil on rupture was demonstrated after the induction of hypoperfusion, the ingesting fish oil can be effective after the vascular wall becomes pathologic.

Fish oil administration before the induction of hypoperfusion significantly suppressed the aortic dilation compared with triolein group (**Fig. 21**). This result suggests that fish oil administration before the induction of hypoperfusion can suppress the AAA progression by the suppression of ECM degradation in the vascular wall (**Fig. 22, 23**).

The preventive effects of fish oil on AAA development can be attributed to the anti-inflammatory effect of EPA and DHA in fish oil. Fish oil used in this study contains 30.8% EPA and 15.7% DHA. These n-3PUFAs are incorporated into cell membrane phospholipids, and lipid mediators produced in a substrate for cyclooxygenase-2 acts competitively in response to inflammatory lipid mediators derived from n-6 PUFAs, such as arachidonic acid (AA).[45] N-3PUFAs exhibit anti-inflammatory activity by suppressing the activity of nuclear factor-kappa B (NFκB), which is mediated by G protein-linked receptor 120 on the cell membrane.[46] NFκB is known to be involved in the upregulation of MMP-9.[47] NFκB activation is suppressed by EPA.[48] Previous report demonstrated that EPA suppressed the NFκB activation induced by various stimuli.[49] The decrease in MMP-9 protein levels in this study may be mediated by NFκB pathway through EPA in fish oil. In addition, EPA and DHA produce anti-inflammatory metabolites, such as resolvin and protectin.[36] These metabolites may also contribute the suppression of vascular inflammation in fish oil-administered wall.

Previous report showed that n-3PUFAs rich diet can suppress the oxidative stress in the vascular wall in angiotensin II-infused *Apoe-/-* mice.[50] Oxidative stress in the vascular wall is reportedly associated with increased MMP-2 expression.[17] MDA, oxidative stress marker, was decreased in fish oil group in this study (**Fig. 23**). The decrease in MMP-2 protein levels observed in fish oil-administered hypoperfusion-induced model was due to the suppression of oxidative stress in the aortic wall.

Fish oil administration after the induction of hypoperfusion significantly decreased the rupture risk compared with the triolein group (**Fig. 24**). Interestingly, fish oil group suppressed the AAA rupture risk although the aortic diameter in fish oil group

was not difference from triolein group (**Fig. 24**). It is speculated that fish oil-administered wall could continue to dilate without rupture even if aortic wall reached aortic diameter which may rupture in the case of triolein group. In other words, with the same vascular wall, the triolein group may have a higher risk of rupture, and the fish oil group may have a lower risk of rupture due to dilation. In histological analyses, the fish oil group significantly decreased the size of adipocytes compared with the triolein group (**Fig. 25**). Positive areas for collagen fibers in the areas with adipocytes in the AAA sac wall were significantly decreased compared with the areas without adipocytes in the triolein group (**Fig. 27**). On the contrary, positive areas for collagen fibers in the areas with adipocytes in the AAA sac wall were not significantly different compared with the areas without adipocytes in the fish oil group (**Fig. 27**). Positive areas for MMP-2, MMP-9, MCP-1 and macrophages in the areas with adipocytes in the fish oil group was significantly decreased compared with those in the triolein group (**Fig. 29**). It has been reported that adipocytes hypertrophy can cause chronic inflammation in tissues.[25] Here, fish oil reportedly suppresses adipocytes hypertrophy in tissues.[37] This suppressive effect in fish oil may lead to the inhibition of inflammation in the aortic wall. These results suggest that the appropriate control of vascular adipocytes may prevent AAA rupture. Because the vascular tissue around adipocytes may be remarkably degraded, the rupture risk may increase as the number of adipocytes in vascular wall. N-3PUFAs suppress de novo TG synthesis via inhibition of the sterol regulatory element-binding protein 1c expression because they are antagonists of liver X receptor α.[51] Therefore, n-3PUFAs may be contributed to the suppressive effect on adipocytes hypertrophy in this study. In addition, the anti-inflammatory effect in n-3 PUFAs may contribute to the suppression of adipocytes-induced vascular inflammation.

This study was compared the effects of two different TGs (triolein and fish oil), and showed the relationship among vascular inflammation, the ectopic appearance of adipocytes and AAA progression. This study demonstrated that fish oil administration could reduce the risk of AAA progression and rupture by attenuating the vascular inflammation and the hypertrophy of adipocytes in hypoperfusion-induced AAA. Fish oil or n-3PUFA-containing drugs or foods may therefore be effective for the prevention of AAA progression and rupture. The molecular mechanisms underlying suppressive effects of n-3PUFAs on AAA under hypoperfused condition is not fully understood. Further studies are necessary to elucidate the detailed mechanisms.

Chapter 5 - Effects of functional food factors on the degradation of fibers in vascular wall due to nicotine

5.1 Introduction

Cigarette smoking is a major risk factor for AAA formation and rupture.[52, 53] Indeed, many patients with AAA have a history of smoking, and smoking contributes to the enlargement of aortic diameter and increasing the risk of vascular rupture.[16] Recently, it has been reported that nicotine, a primary component of cigarette smoke, is strongly associated with the development and rupture of AAA.[54] Wang et al. reported that the infusion of nicotine in apolipoprotein E (*Apoe*-/-) mice induced AAA formation.[17] In this report, the infusion of nicotine in *Apoe*-/- mice causes phosphorylation of activator protein (AP) -2α by activating AMP activated protein kinase (AMPK) -α2 in vascular SMCs, and this expression induces abnormal expression of MMP-2 and ECM degradation, and induces AAA.[17] In addition, Maegdefessel et al. reported that microRNA-21 could be associated with AAA formation by nicotine.[55] Previous study demonstrated that the chronic nicotine exposure in rats and mice induced the medial elastin fragmentation and adventitial collagen degradation caused by enhanced MMPs expression in the abdominal aortic wall.[18, 56] Jacob-Ferreira et al. reported that both the acute administration of nicotine by intravenous injection and the chronic administration of nicotine by oral administration in rats increased gelatinolytic activity in aortic tissues.[57]

Avoiding nicotine intake by smoking is one of the most important method in AAA treatment, but it is difficult to quit smoking immediately due to dependency on nicotine. Therefore, it is considered to be revolutionary that there are methods to prevent the weakening of vascular wall due to nicotine by dietary food or functional food factors. However, there is little information on the effect of functional food factors on vascular damage due to nicotine. Here, this study focused on fish oil and sesame extract. Fish oil contains rich n-3PUFAs, which have anti-inflammatory and anti-oxidative effects. Chapter 4 showed that administration of EPA-rich fish oil suppressed the aortic dilation and AAA rupture risk under hypoperfused condition. Also, sesamin and sesamolin are functional food factors that are fat-soluble lignans found in *Sesamum indicum* seeds. Sesamin and sesamolin have various functions such as anti-oxidative,[58, 59] anti-inflammatory,[60] and serum lipid-lowering effects.[61] In this study, administration of EPA-rich fish oil or sesamin and sesamolin-rich sesame extract was performed in nicotine administered mice to evaluate the effects of these functional food factors on vascular damage due to nicotine.

5.2 Materials and Methods

Materials and methods in this chapter were previously described in *Food Funct.* and *J. Oleo Sci.* with slight modifications.[62, 63]

5.2.1 Animals

All animal experiments were approved by the Kindai University Animal Care and Use Committee and were performed according to the Kindai University Animal Experimentation Regulations (Approval number; KAAG-25-002). Three-week-old male C57BL/6J mice (Japan SLC, Inc., Shizuoka, Japan) were maintained on a standard 12-hour light/dark cycle at 25 ± 1°C.

5.2.2 Effects of EPA-rich fish oil on nicotine-administered vascular wall

After habituation for 5 days, the mice were divided into four groups: control diet and distilled water (C), fish oil diet and distilled water (F), control diet and nicotine solution (CN), and fish oil diet and nicotine solution (FN) groups. The mice received distilled water in the C (n = 6) and F (n = 6) groups or 0.5 mg/mL nicotine solution (nicotine: Wako Pure Chemical industries, Osaka, Japan) in the CN (n = 6) and FN (n = 6) groups. In addition, mice were administered either control diet in the C and CN groups or fish oil diet in the F and FN groups. All the mice were sacrificed after 14 days. The diet composition is shown in **Table 5a** and the fatty acid compositions of the olive oil and fish oil are shown in **Table 5b**.

Table 5 Diet composition

(a)

	Control diet (%)	Fish oil diet (%)
Choline chloride	0.25	0.25
Cystine	0.3	0.3
AIN-93 vitamin mix	1.0	1.0
AIN-93G mineral mix	3.5	3.5
Cellulose	5.0	5.0
Sucrose	10.0	10.0
Casein	20.0	20.0
Cornstarch	52.95	52.95
Olive oil	7.0	-
Fish oil	-	7.0

(b)

Fatty acid	Olive oil (%)	Fish oil (%)
8 : 0	-	-
10 : 0	-	-
12 : 0	-	-
14 : 0	-	5.2
16 : 0	10.8	6.6
16 : 1	1.0	9.3
16 : 2	-	1.7
16 : 3	-	2.8
16 : 4	-	4.8
18 : 0	2.7	0.5
18 : 1	77.1	9.6
18 : 2 n-6	7.8	1.4
18 : 3 n-3	0.6	0.9
18 : 4 n-3	-	5.1
20 : 4 n-6	-	1.3
20 : 4 n-3	-	1.1
20 : 5 n-3	-	30.8
22 : 5 n-6	-	0.3
22 : 5 n-3	-	2.9
22 : 6 n-3	-	15.7

5.2.3 Effects of sesamin and sesamolin-rich sesame extract on nicotine-administered vascular wall

After habituation for three days, the mice were divided into four groups: control diet and distilled water (C), sesame extract diet and distilled water (S), control diet and nicotine solution (CN), and sesame extract diet and nicotine solution (SN). The mice received either distilled water in the C (n = 6) and S (n = 6) groups or a 0.5 mg/mL nicotine solution (nicotine: Wako Pure Chemical industries, Osaka, Japan) in the CN (n = 6) and SN (n = 7) groups. In addition, the mice were administered either a control diet in the C and CN groups or a sesame extract diet in the S and SN groups. All the mice were sacrificed after 16 days. The diet composition is shown in **Table 6**. Sesame extract contained 42.07% (w/w) sesamin and 41.23% (w/w) sesamolin.

Table 6 Diet composition

	Control diet (g)	Sesame extract diet (g)
Choline chloride	0.25	0.25
Cystine	0.3	0.3
AIN-93 vitamin mix	1.0	1.0
AIN-93G mineral mix	3.5	3.5
Cellulose	5.0	5.0
Sucrose	10.0	10.0
Casein	20.0	20.0
Cornstarch	52.95	52.95
Olive oil	7.0	7.0
Sesame extract	-	1.0
Total (g)	100.0	101.0

5.2.4 Sample collection

The abdominal aorta and thoracic aorta were isolated. The isolated tissue was fixed in 4% PFA (Nacalai Tesque, Kyoto, Japan), soaked in sucrose solution (10%, 15%, or 20%), and then embedded in O.C.T. compound (Sakura Finetek Japan, Tokyo, Japan).

5.2.5 Histological staining

The isolated aorta cross-sections (5-μm-thick) were prepared using a cryostat (CM1850, Leica Microsystems, Wetzlar, Germany). The aortic walls were stained with histological stainings. The quantitative analyses of the histologically stained sections were performed using ImageJ software (National Institutes of Health, Bethesda, Maryland, USA), and the destruction rate of the wavy configuration of the elastic lamina was calculated by dividing the area of destruction (indicated by flattening and fragmentation of the elastic lamina) by the entire area of elastic lamina.

The histological results from the aortic wall were assessed after staining using the following antibodies: rabbit anti-MMP-2 (1:50; Thermo Scientific, San Jose, CA, USA), goat anti-MMP-9 (1:50; Santa Cruz Biotechnology, Dallas, TX, USA), rabbit anti-MMP-12 (1:100; Bioss Antibodies, Woburn, MA, USA), mouse anti-malondialdehyde (MDA) (1:100; Abcam, Tokyo, Japan), rabbit anti-monocyte chemotactic protein-1 (MCP-1) (1:50; Bioss Antibodies, Woburn, MA, USA), and rabbit anti-CD68 (1:50; Bioss Antibodies, Woburn, MA, USA).

5.2.6 *In situ* gelatin zymography

Dye-quenched gelation (DQG; Invitrogen, Carlsbad, CA) 1 mg/mL was dissolved in distilled water, and then diluted 1 : 10 in the reaction buffer (50 mM Tris-HCl, pH 7.6, 150 mM NaCl, 0.2 mM NaN_3). The reaction buffer with DQ-gelatin was then applied to the tissue sections. The sections were maintained at room temperature for 1 hour to allow incubation of tissue gelatinases with the DQG substrate. After the sections were rinsed in PBS and fixed in 4% PFA for 15 min, they were covered with Fluoromount™ (Diagnostic BioSystems, Pleasanton, CA). Gelatinolytic activity in the vascular wall was quantified using ImageJ software.

5.2.7 Statistical analysis

Values were expressed as mean ± standard error of mean (S.E.M.). Statistical differences were determined by the Tukey–Kramer test. The P-value <0.05 was considered a statistically significant difference. Statistical analyses were performed using Stat View 5.0 software (SAS Institute, Cary, USA).

5.3 Results

5.3.1 Suppressive effect of fish oil administration on elastic fiber destruction due to nicotine

The final average body weight (g) was not significantly different between the four groups (22.8 ± 0.7 g in the C group, 22.2 ± 0.8 g in the F group, 22.6 ± 0.9 g in the CN group, and 22.3 ± 1.0 g in the FN group). The food intake (g/day) was not significantly different between the four groups (5.7 ± 0.2 g/day in the C group, 5.6 ± 0.2 g/day in the F group, 5.6 ± 0.2 g/day in the CN group, and 5.7 ± 0.1 g in the FN group).

The aortic wall thickness was not significantly different between the four groups (**Fig. 31a-e**). Collagen positive areas were also not significantly different between the four groups (**Fig. 31f-j**). On the contrary, the destruction areas of elastic fibers were

significantly increased in the CN group compared to the C and F groups (**Fig. 31k-o**). In addition, the destruction areas of elastic fibers were significantly suppressed in the FN group compared to the CN group (**Fig. 31k-o**).

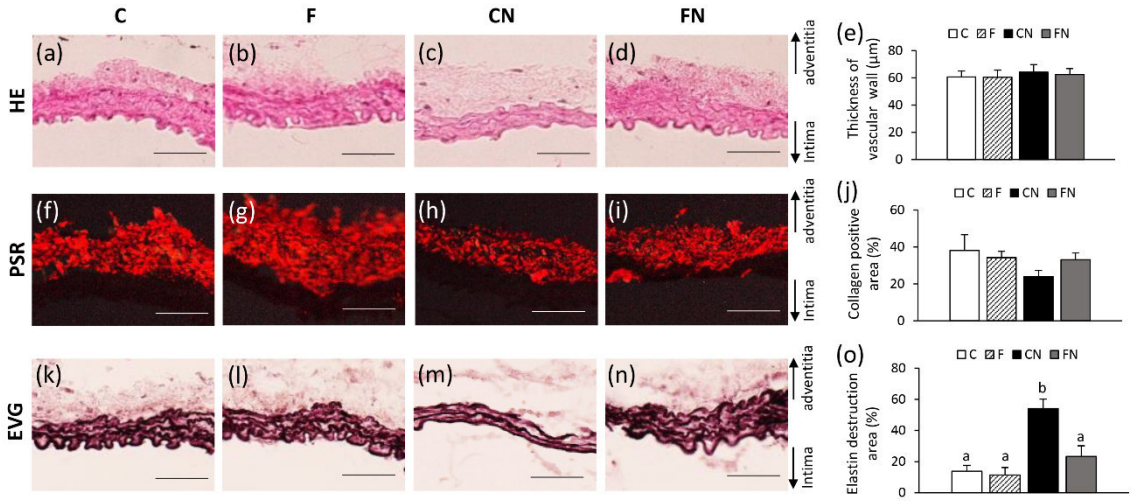

Figure 31 Evaluation of the thickness of the vascular wall, and the degradation of collagen and elastin fibers. (**a-d**) Representative images of HE staining. (**e**) Vascular wall thickness. (**f-i**) Representative images of PSR staining. (**j**) Collagen positive areas. (**k-n**) Representative images of EVG staining. (**o**) Destruction rate of the elastic lamina waveform. Scale bar=50 μm. Data are expressed as the mean ± S.E.M. C group (n=6), F group (n=6), CN group (n=6), and FN group (n=6). Values with different letters are significantly different (P<0.05). Reproduced from a figure previously published in *J. Oleo Sci.*[62]

5.3.2 Suppressive effect of fish oil administration on the expression of MMP-12, oxidative stress, and gelatinolytic activity due to nicotine

MMP-2 positive areas in the intima-media and adventitia of the vascular wall were significantly increased in the CN group compared to the C and F groups (**Fig. 32a-e**). MMP-2 positive areas in the intima-media of the aortic wall tended to decrease in the FN group compared to the CN group (**Fig. 32a-e**). MMP-9 positive areas in the vascular wall were not significantly different between the four groups (**Fig. 32f-j**). MMP-12 positive areas in the intima-media and adventitia of the vascular wall were significantly increased in the CN group compared to the C and F groups (**Fig. 32k-o**). Interestingly, MMP-12 positive areas in the intima-media of the vascular wall were significantly suppressed in FN group compared to the CN group (**Fig. 3k-o**).

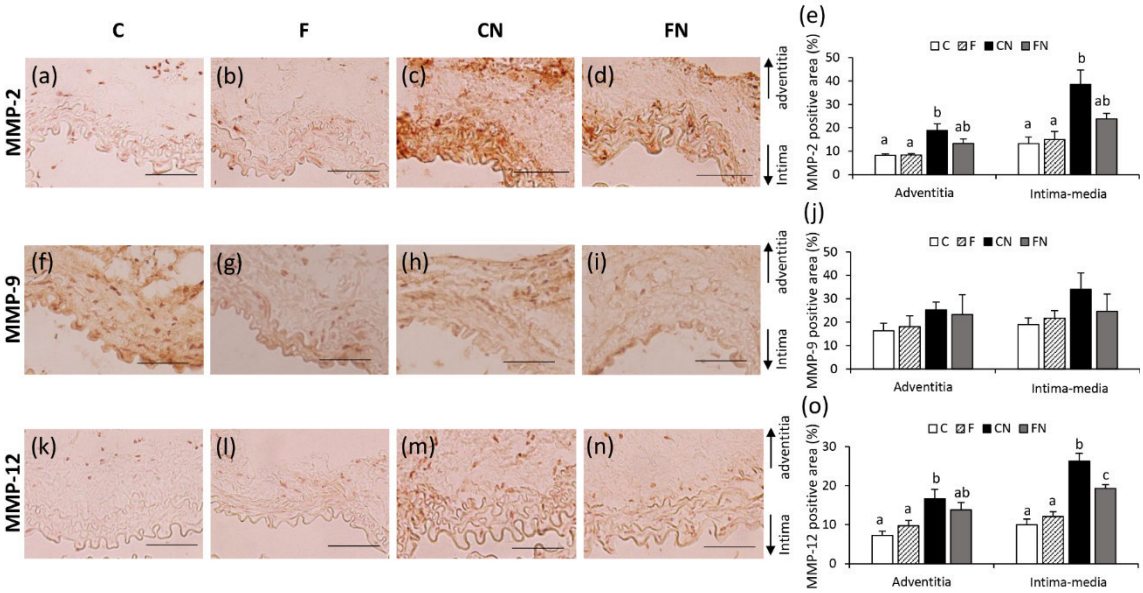

Figure 32 Immunohistochemical examination for MMP-2, MMP-9, and MMP-12. (**a-d**) Representative images of immunohistochemical staining for MMP-2. (**e**) MMP-2 positive area in intima-media and adventitia. (**f-i**) Representative images of immunohistochemical staining for MMP-9 (**j**) MMP-9 positive area in intima-media and adventitia. (**k-n**) Representative images of immunohistochemical staining for MMP-12 (**o**) MMP-12 positive area in intima-media and adventitia. Scale bar=50 μm. Data are expressed as the mean ± S.E.M. C group (n=6), F group (n=6), CN group (n=6), and FN group (n=6). Values with different letters are significantly different (P<0.05). Reproduced from a figure previously published in *J. Oleo Sci.*[62]

MCP-1 positive areas in the vascular wall were not significantly different between the four groups (**Fig. 33a-e**). $CD68^+$ monocytes/macrophages positive areas in the intima-media of the aortic wall were significantly increased in the CN group compared to the C and F groups (**Fig. 33f-j**). $CD68^+$ monocytes/macrophages positive areas in the intima-media of the aortic wall were significantly decreased in the FN group compared to the CN group (**Fig. 33f-j**). MDA positive areas, the oxidative stress marker, in the intima-media and adventitia of the vascular wall were significantly increased in the CN group compared to the C and F groups (**Fig. 33k-o**). In addition, positive areas for MDA in the intima-media of the vascular wall were significantly suppressed in FN group compared to the CN group (**Fig. 3k-o**).

Medial wall thickness was observed by immunohistochemical staining for α-smooth muscle actin (**Fig. 34a-d**). The areas of SMCs and the medial wall thickness were not significantly different between the four groups (**Fig. 34e, f**).

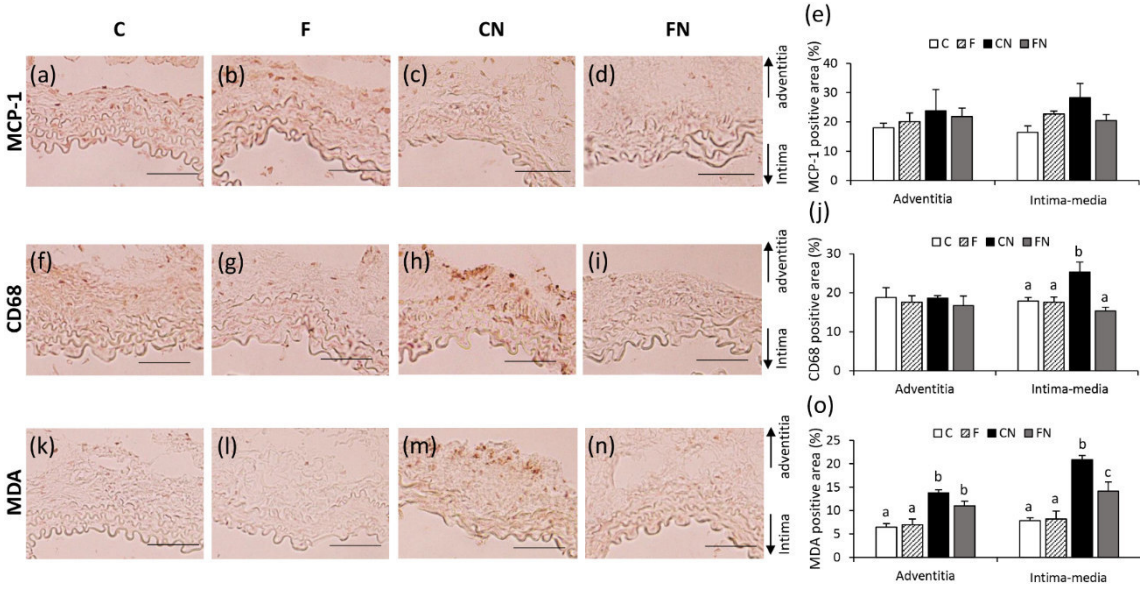

Figure 33 Immunohistochemical examination for MCP-1, CD68+ monocytes/macrophages, and MDA. (**a-d**) Representative images of immunohistochemical staining for MCP-1. (**e**) MCP-1 positive area in intima-media and adventitia. (**f-i**) Representative images of immunohistochemical staining for CD68 (**j**) CD68 positive area in intima-media and adventitia. (**k-n**) Representative images of immunohistochemical staining for MDA (**o**) MDA positive area in intima-media and adventitia. Scale bar=50 μm. Data are expressed as the mean ± S.E.M. C group (n=6), F group (n=6), CN group (n=6), and FN group (n=6). Values with different letters are significantly different (P<0.05). Reproduced from a figure previously published in *J. Oleo Sci.*[62]

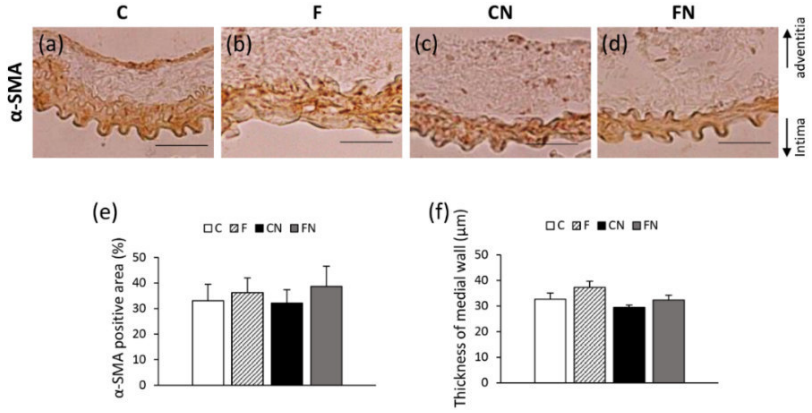

Figure 34 Thickness of medial walls. (**a-d**) Representative images of immunostaining for α-smooth muscle actin. (**e**) The α-smooth muscle actin-positive areas, and (**f**) the medial wall thickness. Scale bar=50 μm. Data are expressed as the mean ± S.E.M. Reproduced from a figure previously published in *J. Oleo Sci.*[62]

Next, the gelatinolytic activity in the vascular wall was evaluated using *in situ* zymography (**Fig. 35a-d**). The gelatinolytic activities in the intima-media and adventitia of the aortic wall were significantly increased in the CN group compared with the C and F groups (**Fig. 35e**). Interestingly, the gelatinolytic activities in the intima-media and adventitia of the aortic wall were significantly decreased in the FN group compared with the CN group (**Fig. 35e**).

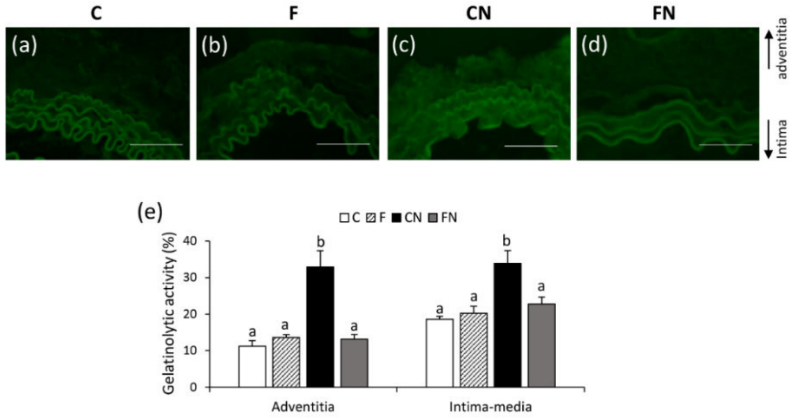

Figure 35 ***In situ*** **gelatin zymography.** (**a-d**) Representative images of *in situ* zymography. (**e**) Quantification of gelatinolytic activity. Scale bar=50 μm. Data are expressed as the mean ± S.E.M. C group (n=6), F group (n=6), CN group (n=6), and FN group (n=6). Values with different letters are significantly different (P<0.05). Reproduced from a figure previously published in *J. Oleo Sci.*[62]

5.3.3 Suppressive effect of sesame extract administration on collagen and elastic fibers destruction due to nicotine

The final average body weight (g) in the S and SN groups was significantly decreased compared to the C and CN groups (21.2 ± 1.6 g in the C group, 18.4 ± 0.6 g in the S group, 21.0 ± 0.8 g in the CN group, and 18.0 ± 0.8 g in the SN group). The food intake (g/day) was not significantly different between the four groups (5.7 ± 0.2 g/day in the C group, 5.6 ± 0.2 g/day in the S group, 5.6 ± 0.2 g/day in the CN group, and 5.8 ± 0.6 g in the SN group).

The thickness of the vascular wall was not significantly different between the four groups (**Fig. 36a-e**). Collagen positive areas of the aortic wall in the CN group were significantly decreased compared with the C and S groups (**Fig. 36f-j**). Interestingly, collagen positive areas of the aortic wall in the SN group were significantly increased compared with the CN group (**Fig. 36f-j**). The destruction areas of elastin fibers of the

aortic wall in the CN group were significantly greater than those in the C and S groups (**Fig. 36k-o**). In addition, the destruction areas of elastin fibers of the aortic wall in the SN group were significantly suppressed compared with the CN group (**Fig. 36k-o**).

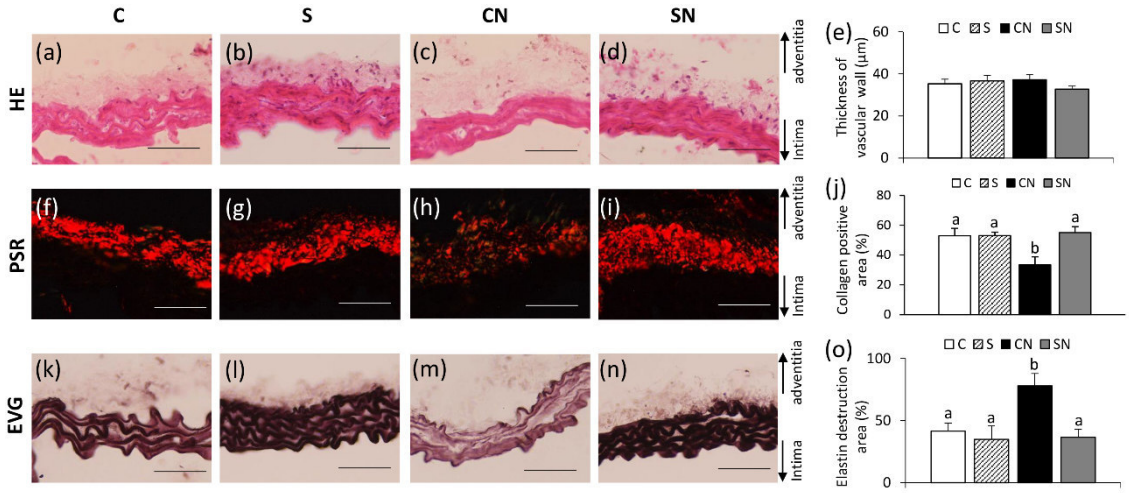

Figure 36 Evaluation of the thickness of the vascular wall, and the degradation of collagen and elastin fibers. (**a-d**) Representative images of HE staining. (**e**) Vascular wall thickness. (**f-i**) Representative images of PSR staining. (**j**) Collagen positive area. (**k-n**) Representative images of EVG staining. (**o**) Destruction rate of the elastic lamina waveform. Scale bar = 50 μm. Data are expressed as the mean ± S.E.M. C group (n = 6), S group (n = 6), CN group (n = 6), and SN group (n = 7). Values with different letters are significantly different (P<0.05). Reproduced from a figure previously published in *J. Oleo Sci.*[63]

5.3.4 Suppressive effect of sesame extract administration on the expression of MMP-12 and oxidative stress due to nicotine

MMP-2 positive areas in the intima-media and adventitia of the aortic wall were significantly increased in the CN group compared with the C group (**Fig. 37a-e**). MMP-2 positive areas in the intima-media of the aortic wall tended to decrease in the SN group compared to the CN group (**Fig. 37a-e**). MMP-9 positive areas in the vascular wall were not significantly different between the four groups (**Fig. 37f-j**). MMP-12 positive areas in the intima-media of the aortic wall were significantly increased in the CN group compared with the C and S groups (**Fig. 37k-o**). In addition, MMP-12 positive areas in the intima-media of the aortic wall were significantly decreased in the SN group compared with the CN group (**Fig. 37k-o**).

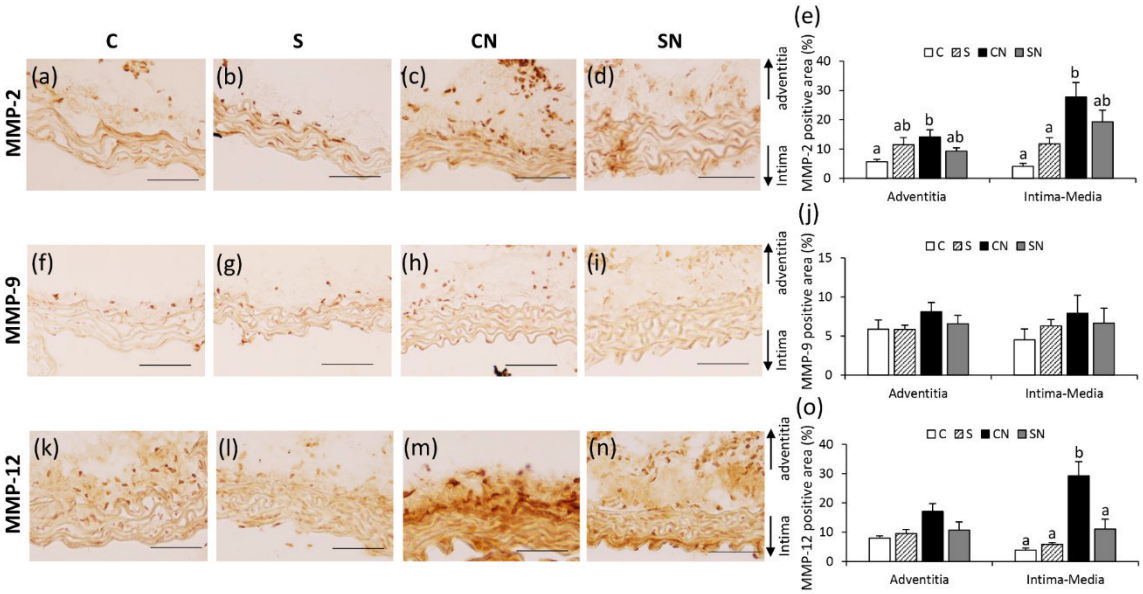

Figure 37 Immunohistochemical examination for MMP-2, MMP-9, and MMP-12. (**a-d**) Representative images of immunohistochemical staining for MMP-2. (**e**) MMP-2 positive area in intima-media and adventitia. (**f-i**) Representative images of immunohistochemical staining for MMP-9 (**j**) MMP-9 positive area in intima-media and adventitia. (**k-n**) Representative images of immunohistochemical staining for MMP-12 (**o**) MMP-12 positive area in intima-media and adventitia. Scale bar = 50 μm. Data are expressed as the mean ± S.E.M. C group (n = 6), S group (n = 6), CN group (n = 6), and SN group (n = 7). Values with different letters are significantly different (P<0.05). Reproduced from a figure previously published in *J. Oleo Sci.*[63]

MCP-1 and CD68 positive areas in the vascular wall were not significantly different between the four groups (**Fig. 38a-j**). Positive areas for MDA in the intima-media of the aortic wall were significantly greater in the CN group than those in the C and S groups (**Fig. 38k-o**). In addition, MDA positive areas in the intima-media of the aortic wall were significantly suppressed in the SN group compared with the CN group (**Fig. 38k-o**).

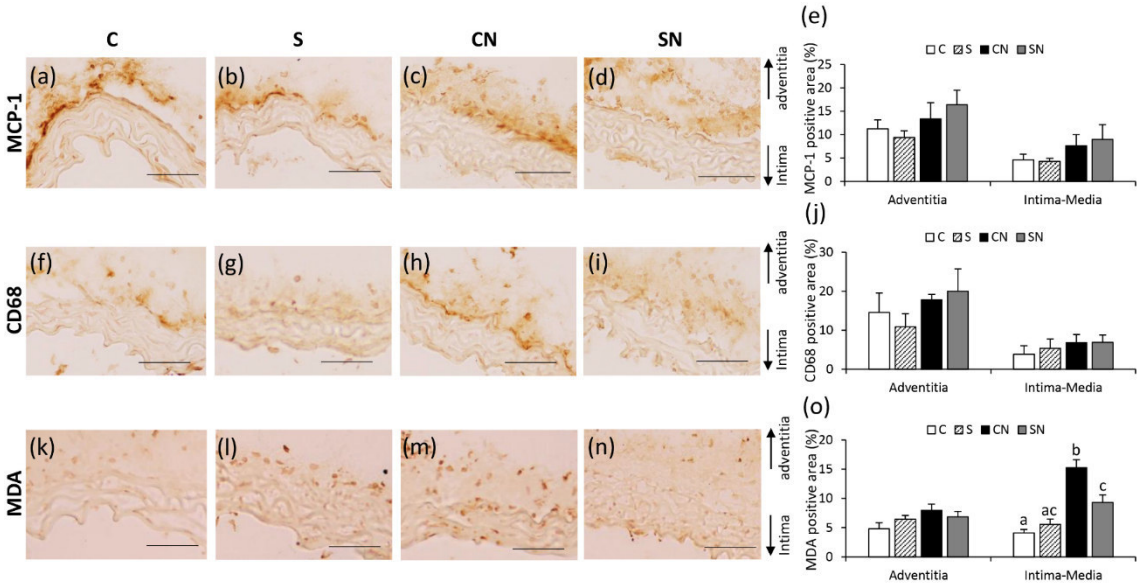

Figure 38 Immunohistochemical examination for MCP-1, CD68+ monocytes/macrophages, and MDA. (**a-d**) Representative images of immunohistochemical staining for MCP-1. (**e**) MCP-1 positive area in intima-media and adventitia. (**f-i**) Representative images of immunohistochemical staining for CD68 (**j**) CD68 positive area in intima-media and adventitia. (**k-n**) Representative images of immunohistochemical staining for MDA (**o**) MDA positive area in intima-media and adventitia. Scale bar = 50 μm. Data are expressed as the mean ± S.E.M. C group (n = 6), S group (n = 6), CN group (n = 6), and SN group (n = 7). Values with different letters are significantly different (P <0.05). Reproduced from a figure previously published in *J. Oleo Sci.*[63]

5.4 Discussion

EPA-rich fish oil suppressed the expression of MMP-12, the gelatinolytic activity, and the degradation of collagen fibers due to nicotine. Sesamin and sesamolin-rich sesame extract also suppressed the expression of MMP-12 and the degradation of collagen and elastin fibers.

This study suggested that nicotine administration could induce the MMP-12 upregulation in the aortic wall (**Fig. 32, 37**). Curci et al. previously reported that the MMP-12 expression and activation were increased in human AAA wall, and MMP-12 was localized to residual elastin fragments within the medial wall.[64] MMP-12 expression is induced from various stimuli, such as activator protein-1 (AP-1),[65] NFκB,[66] Wnt-7a,[67] and heterogeneous-nuclear ribonucleoprotein K,[68] and inhibited by Y-box binding protein-1[69] and PPARα agonist.[70] Nicotine activates p38 mitogen-activated protein

kinase (MAPK) and protein kinase C (PKC), which activate AP-1 and NFκB.[71] p38 MAPK activates both AP-1 and NFκB, and PKC activates only AP-1.[71] Nicotine may increase the MMP-12 expression through AP-1 and NFκB pathways in the vascular wall. MMP-12 upregulation due to nicotine was significantly suppressed in both EPA-rich fish oil and sesamin and sesamolin-rich sesame extract (**Fig. 32, 37**). EPA suppresses the activation of NFκB.[48, 49] In addition, sesamin suppresses the activation of p38 MAPK and NFκB.[72] Therefore, MMP-12 expression suppressed by fish oil and sesame extract in this study may be via the p38 MAPK and NFκB pathways.

Wang et al. previously reported that the increase of oxidative stress in vascular SMCs due to reactive oxygen species (ROS) accumulation by nicotine could induce the MMP-2 expression and AAA formation.[17] In this study, MDA, the oxidative stress marker, was significantly decreased in nicotine-administered mice by both EPA-rich fish oil and sesamin and sesamolin-rich sesame extract (**Fig. 33, 38**). Suppression of oxidative stress by fish oil in this study is consistent with previous report that n-3 PUFAs suppressed the oxidative stress in angiotensin Ⅱ-infused *Apoe-/-* mice.[50] In this study, administration of fish oil or sesame extract did not significantly differ in positive areas for MMP-2 in both administration of fish oil and sesame extract in nicotine-administered mice (**Fig. 32, 37**). It is speculated that anti-oxidative effect of fish oil or sesame extract might inhibit the effect of nicotine.

Previous studies have shown that nicotine can increase the risk of developing AAA by the weakening the vascular wall.[17, 56] This study showed that dietary fish oil or sesame extract suppresses fibers destruction due to nicotine by inhibiting MMP-12 expression and increase in oxidative stress. Fish oil contains rich n-3PUFAs, and sesame extract contains rich sesamin and sesamolin. The preventive effects of fish oil and sesame extract on the inhibition of the effects by nicotine can be attributed to the anti-inflammatory and anti-oxidative effects of these functional food factors. N-3PUFAs or sesamin and sesamolin-containing drugs or foods may be effective for the prevention of AAA progression and rupture by inhibiting the effects of nicotine. Currently, nicotine gum is used as a smoking cessation aid, which includes nicotine. Therefore, even if AAA patients quit smoking, nicotine by taking nicotine gum for smoking cessation may affect the risk of AAA development. The function of sesame extract on nicotine may be used to provide the novel preventing method for those who cannot quit smoking.

Chapter 6 - General Discussion

Hypoperfusion in the aortic wall observed in AAA lesions is an important pathology of AAA development and progression.[8] Previous study succeeded in creating AAA model rats induced by artificial vascular hypoperfusion.[10] In this paper, the mechanisms underlying AAA rupture and the preventive methods for AAA progression were studied using the hypoperfusion-induced AAA model.

In Chapter 2, to elucidate the mechanisms underlying AAA rupture, pathological analyses of ruptured vascular wall in AAA model were performed. The number of adipocytes was significantly increased in ruptured adventitial wall. The degradation of collagen fiber and the expressions of MMP-2 and MMP-9 were significantly increased in the areas with adipocytes. In addition, the recruitment of macrophages was promoted in the areas with adipocytes. These findings suggest that the ectopic appearance of adipocytes in the vascular wall may cause AAA rupture. It is speculated that adipocytes accumulation in the vascular wall may exacerbate the inflammation of the areas around adipocytes and enhance the vascular wall weakness (**Fig. 39**).

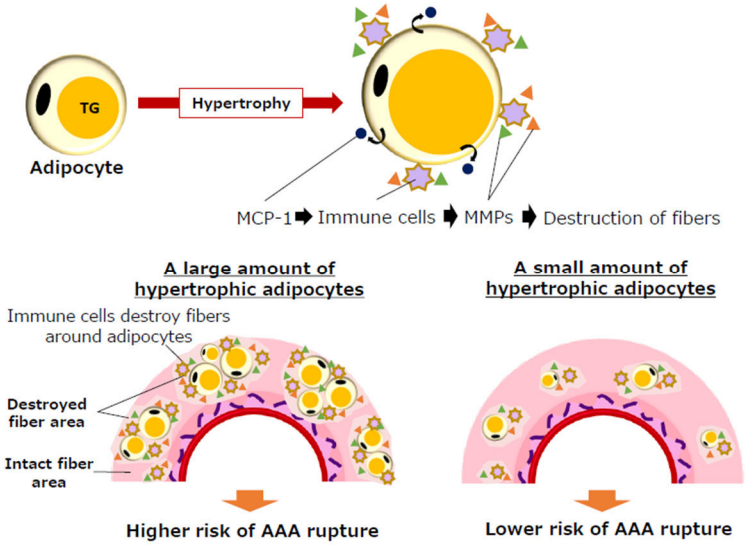

Figure 39 Potential mechanism underlying AAA rupture induced by uninvited vascular adipocytes. Hypertrophic adipocytes due to TG accumulation induce the secretion of MCP-1, and these adipocytokines recruit immune cells increase MMPs levels and the consequent destruction of collagen fibers surrounding the adipocytes. Replacement of collagen fibers with adipocytes causes vascular wall weakness. The vulnerable circle induced around adipocytes can increase the risk of AAA rupture.

In Chapter 3, to evaluate the difference in the effect on ectopic adipocytes appearance depending on the type of aneurysm, the pathological analyses of human TAA wall were performed. In human TAA tissue, the area of adipocytes was significantly increased compared with normal aortic tissue. Therefore, the appearance of adipocytes may be involved not only in AAA but also in TAA.

Vascular hypoperfusion can be involved in AAA development and rupture through the inflammation and fatty degeneration in the aortic wall. In Chapter 4, the preventive effects of food factors on AAA development and rupture induced by vascular hypoperfusion were investigated. Fish oil, which has anti-inflammatory and anti-oxidative effects, and inhibitory effects on de novo TG synthesis and the growth of adipocytes, was focused. Triolein administration (1145 mg/kg body weight/day) and fish oil administration (1145 mg/kg body weight/day; purified TG extracted from sardines) were performed, and the effects of the difference in TG species on AAA development and rupture were evaluated. The fish oil administration before the induction of hypoperfusion which could trigger AAA significantly suppressed the aortic dilation through the suppression of oxidative stress, MMPs expression, and collagen fibers destruction. Anti-inflammatory and anti-oxidative effects of n-3 PUFAs might suppress the weakening of the vascular wall and the aortic dilation by the inhibition of NFκB activation and ROS production (**Fig. 40**). On the contrary, the fish oil administration after the induction of hypoperfusion did not showed the suppressive effect on the aortic dilation. Nevertheless, fish oil group significantly decreased the AAA rupture risk compared with triolein group. Pathological analyses showed that the number and size of ectopic adipocytes in the vascular wall was significantly decreased in fish oil group compared with triolein group. Degradation of fibers in the areas with adipocytes in fish oil group was also suppressed. N-3 PUFAs inhibit de novo TG synthesis in tissues by suppressing the expression of fatty acid synthesis-related factors.[51] Fish oil administration could suppress the AAA rupture risk by the suppression of adipocytes increase and hypertrophy and the degradation of fibers induced by adipocytes (**Fig. 41**). These results suggest that the appropriate control of vascular adipocytes may treat or prevent AAA rupture. N-3PUFAs such as EPA and DHA may be expected to be applied to AAA treatment as a medicine.

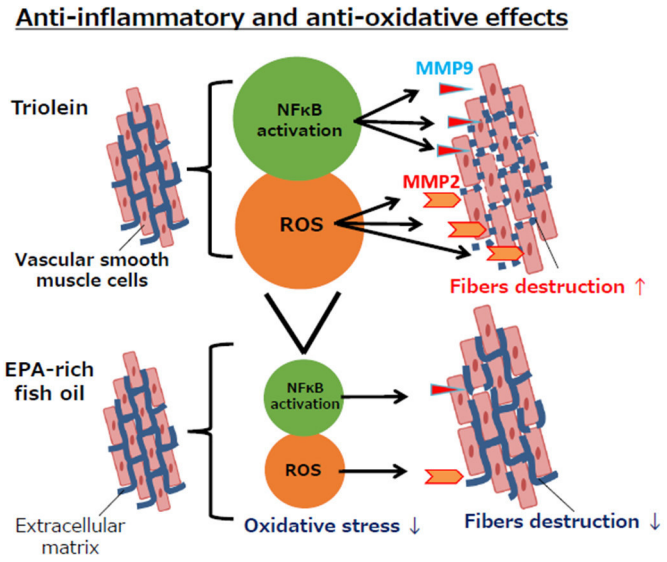

Figure 40 Suppressive effect of fish oil on fibers degradation and aortic dilation. EPA-rich fish oil might suppress the vascular wall weakness and aortic dilation by the inhibition of NFκB activation and ROS production.

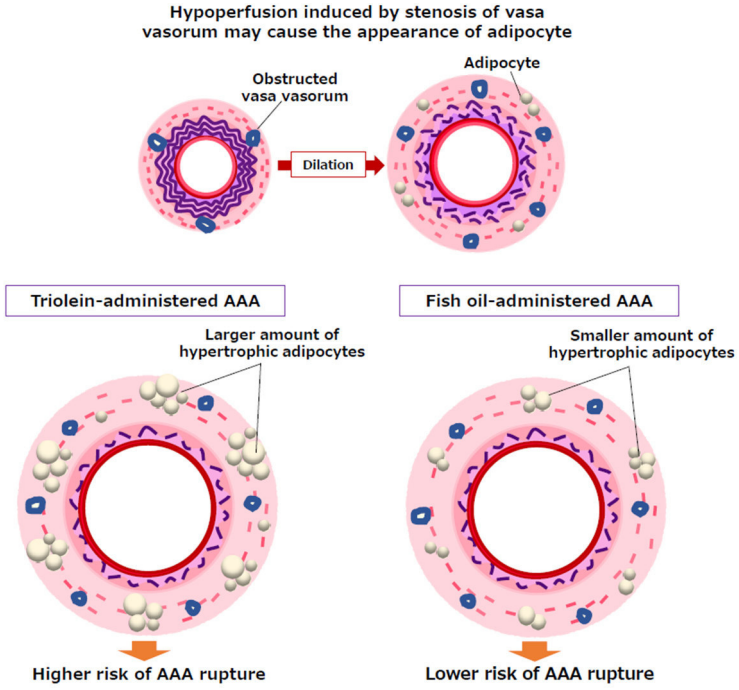

Figure 41 Suppressive effect of fish oil on AAA rupture. Stenosis of VV occurs vascular hypoperfusion and triggers the appearance of adipocytes. Fish oil administration could suppress the risk of AAA rupture by suppression of adipocytes increase and hypertrophy.

These studies are the first report to show the possibility that the increase and hypertrophy of adipocytes in the vascular wall may lead to AAA rupture. The appropriate control of vascular adipocytes may treat or prevent AAA rupture.

In other previous experiments investigating the relation between hypoperfusion-induced AAA rupture and dietary habit, the administration of high fat diet which contains many saturated fatty acids (31.5% lard) significantly increased the number and size of adipocytes in the vascular wall and the AAA rupture risk compared to control diet (1.9% lard) in hypoperfusion-induced model.[24] These reports suggest that excessive fat intake may promote AAA rupture. High sucrose diet also causes TG metabolism abnormality. Interestingly, adipocytes accumulation in the vascular wall and the AAA rupture risk were not significantly different between high sucrose diet-administered group (66% sucrose) and control group (0% sucrose), although TG metabolism abnormality was observed by high sucrose diet.[73] The average intake calorie of high fat diet and high sucrose diet was the same. Therefore, it is speculated that the content of diet is more important than the calorie intake for adipocytes accumulation in the vascular wall.

Here, adipocyte differentiation from mesenchymal stem cells (MSCs) could be promoted in association with HIF-1α and CCAAT / enhancer-binding proteins under hypoxic condition.[74] MSCs have the property of accumulating in damaged tissues involving stromal cell-derived factor 1α / CXC type chemokine ligand 4 axis under hypoxic conditions,[75] and MSCs transfer to damaged tissues in response to highly mobility group box 1 derived from necrosis cells.[76] $CD44^{+}CD90^{+}$ MSCs are present in human AAA wall,[77] and isolated $CD44^{+}CD90^{+}$ MSCs in human AAA tissues have the ability to differentiate into various cells including adipocyte.[78] MSCs within the aortic wall normally differentiate into vascular SMCs, and contribute to the stability of the vascular wall.[79, 80] The appearance of adipocytes might come as a result of unintended differentiation from MSCs in the aortic wall under vascular hypoperfusion. However, the detailed mechanisms underlying adipocytes appearance remain unknown.

Several previous studies reported the involvement of perivascular adipose tissue (PVAT) in aneurysm formation.[81-85] Because PVAT is adjacent to the vascular wall, there is the possibility of being associated with AAA pathology. However, the details of the interaction between PVAT and AAA wall, and the effects on hypoperfusion and adipocytes appearance are in the black box. Future research on the relationship between PVAT and AAA is interesting.

In Chapter 5, the effects of functional food factors on nicotine-induced vascular damage were evaluated because nicotine, one of the main ingredients of cigarette smoke, reportedly increases the risk of AAA development and rupture. In this study, EPA-rich fish oil and sesamin and sesamolin-rich sesame extract which have anti-inflammatory and anti-oxidative effects as functional foods were focused. This study suggested that both EPA-rich fish oil and sesamin and sesamolin-rich sesame extract could suppress the MMP-12 expression and the degradation of fibers in the vascular wall induced by nicotine. Therefore, n-3PUFAs or sesamin and sesamolin containing drugs or foods may therefore be effective for the prevention of AAA progression and rupture by inhibiting the effects of nicotine. In other experiments, DNA-rich salmon milt extracts suppressed the elastin fibers degradation induced by nicotine.[86] These functional food factors may be effective for the prevention of AAA by inhibiting the effects of nicotine.

Advancement of further researches may lead to the establishment of preventive methods and treatments with foods and drugs to inhibit the AAA progression and rupture.

References

1) Aggarwal S, Qamar A, Sharma V and Sharma A: Abdominal aortic aneurysm: A comprehensive review. Exp Clin Cardiol, 2011; 16:11-15

2) Longo GM, Xiong W, Greiner TC, Zhao Y, Fiotti N and Baxter BT: Matrix metalloproteinases 2 and 9 work in concert to produce aortic aneurysms. J Clin Invest, 2002; 110:625-632

3) Lindsay ME and Dietz HC: Lessons on the pathogenesis of aneurysm from heritable conditions. Nature, 2011; 473:308-316

4) Abdul-Hussien H, Hanemaaijer R, Kleemann R, Verhaaren BF, van Bockel JH and Lindeman JH: The pathophysiology of abdominal aortic aneurysm growth: corresponding and discordant inflammatory and proteolytic processes in abdominal aortic and popliteal artery aneurysms. J Vasc Surg, 2010; 51:1479-1487

5) Lindeman JH, Abdul-Hussien H, Schaapherder AF, Van Bockel JH, Von der Thusen JH, Roelen DL and Kleemann R: Enhanced expression and activation of pro-inflammatory transcription factors distinguish aneurysmal from atherosclerotic aorta: IL-6- and IL-8-dominated inflammatory responses prevail in the human aneurysm. Clin Sci (Lond), 2008; 114:687-697

6) Sakalihasan N, Delvenne P, Nusgens BV, Limet R and Lapiere CM: Activated forms of MMP2 and MMP9 in abdominal aortic aneurysms. J Vasc Surg, 1996; 24:127-133

7) Sakalihasan N, Limet R and Defawe OD: Abdominal aortic aneurysm. Lancet, 2005; 365:1577-1589

8) Tanaka H, Zaima N, Sasaki T, Hayasaka T, Goto-Inoue N, Onoue K, Ikegami K, Morita Y, Yamamoto N, Mano Y, Sano M, Saito T, Sato K, Konno H, Setou M and Unno N: Adventitial vasa vasorum arteriosclerosis in abdominal aortic aneurysm. PLoS One, 2013; 8:e57398

9) Wolinsky H and Glagov S: Comparison of abdominal and thoracic aortic medial structure in mammals. Deviation of man from the usual pattern. Circ Res, 1969; 25:677-686

10) Tanaka H, Zaima N, Sasaki T, Sano M, Yamamoto N, Saito T, Inuzuka K, Hayasaka T, Goto-Inoue N, Sugiura Y, Sato K, Kugo H, Moriyama T, Konno H, Setou M and Unno N: Hypoperfusion of the Adventitial Vasa Vasorum Develops an Abdominal Aortic Aneurysm. PLoS One, 2015; 10:e0134386

11) Rius J, Guma M, Schachtrup C, Akassoglou K, Zinkernagel AS, Nizet V, Johnson RS, Haddad GG and Karin M: NF-kappaB links innate immunity to the hypoxic response through transcriptional regulation of HIF-1alpha. Nature, 2008; 453:807-811

12) Eltzschig HK and Carmeliet P: Hypoxia and inflammation. N Engl J Med, 2011; 364:656-665

13) Erdozain OJ, Pegrum S, Winrow VR, Horrocks M and Stevens CR: Hypoxia in abdominal aortic aneurysm supports a role for HIF-1alpha and Ets-1 as drivers of matrix metalloproteinase upregulation in human aortic smooth muscle cells. J Vasc Res, 2011; 48:163-170

14) Wan R, Mo Y, Chien S, Li Y, Tollerud DJ and Zhang Q: The role of hypoxia inducible factor-1alpha in the increased MMP-2 and MMP-9 production by human monocytes exposed to nickel nanoparticles. Nanotoxicology, 2011; 5:568-582

15) Gabel G, Northoff BH, Weinzierl I, Ludwig S, Hinterseher I, Wilfert W, Teupser D, Doderer SA, Bergert H, Schonleben F, Lindeman JHN and Holdt LM: Molecular Fingerprint for Terminal Abdominal Aortic Aneurysm Disease. J Am Heart Assoc, 2017; 6:e006798

16) Lederle FA, Nelson DB and Joseph AM: Smokers' relative risk for aortic aneurysm compared with other smoking-related diseases: a systematic review. J Vasc Surg, 2003; 38:329-334

17) Wang S, Zhang C, Zhang M, Liang B, Zhu H, Lee J, Viollet B, Xia L, Zhang Y and Zou MH: Activation of AMP-activated protein kinase alpha2 by nicotine instigates formation of abdominal aortic aneurysms in mice in vivo. Nat Med, 2012; 18:902-910

18) Kugo H, Zaima N, Tanaka H, Urano T, Unno N and Moriyama T: The effects of nicotine administration on the pathophysiology of rat aortic wall. Biotech Histochem, 2017; 92:141-148

19) Kugo H, Zaima N, Tanaka H, Mouri Y, Yanagimoto K, Hayamizu K, Hashimoto K, Sasaki T, Sano M, Yata T, Urano T, Setou M, Unno N and Moriyama T: Adipocyte in vascular wall can induce the rupture of abdominal aortic aneurysm. Sci Rep, 2016; 6:31268

20) Tanaka H, Unno N, Yata T, Kugo H, Zaima N, Sasaki T and Urano T: Creation of a Rodent Model of Abdominal Aortic Aneurysm by Blocking Adventitial Vasa Vasorum Perfusion. J Vis Exp, 2017; 129:e55763

21) Kanda Y: Investigation of the freely available easy-to-use software 'EZR' for medical statistics. Bone Marrow Transplant, 2013; 48:452-458

22) Kugo H, Zaima N, Tanaka H, Hashimoto K, Miyamoto C, Sawaragi A, Urano T, Unno N and Moriyama T: Pathological Analysis of the Ruptured Vascular Wall of Hypoperfusion-induced Abdominal Aortic Aneurysm Animal Model. J Oleo Sci, 2017; 66:499-506

23) Tanaka H, Zaima N, Sasaki T, Yamamoto N, Inuzuka K, Sano M, Saito T, Hayasaka

T, Goto-Inoue N, Sato K, Kugo H, Moriyama T, Konno H, Setou M and Unno N: Imaging Mass Spectrometry Reveals a Unique Distribution of Triglycerides in the Abdominal Aortic Aneurysmal Wall. J Vasc Res, 2015; 52:127-135

24) Hashimoto K, Kugo H, Tanaka H, Iwamoto K, Miyamoto C, Urano T, Unno N, Hayamizu K, Zaima N and Moriyama T: The Effect of a High-Fat Diet on the Development of Abdominal Aortic Aneurysm in a Vascular Hypoperfusion-Induced Animal Model. J Vasc Res, 2018; 55:63-74

25) Zhang L, Sugiyama T, Murabayashi N, Umekawa T, Ma N, Kamimoto Y, Ogawa Y and Sagawa N: The inflammatory changes of adipose tissue in late pregnant mice. J Mol Endocrinol, 2011; 47:157-165

26) Wellen KE and Hotamisligil GS: Obesity-induced inflammatory changes in adipose tissue. J Clin Invest, 2003; 112:1785-1788

27) Bouloumie A, Sengenes C, Portolan G, Galitzky J and Lafontan M: Adipocyte produces matrix metalloproteinases 2 and 9: involvement in adipose differentiation. Diabetes, 2001; 50:2080-2086

28) Watt HC, Law MR, Wald NJ, Craig WY, Ledue TB and Haddow JE: Serum triglyceride: a possible risk factor for ruptured abdominal aortic aneurysm. Int J Epidemiol, 1998; 27:949-952

29) Norrgard O, Angquist KA and Johnson O: Familial aortic aneurysms: serum concentrations of triglyceride, cholesterol, HDL-cholesterol and (VLDL + LDL)-cholesterol. Br J Surg, 1985; 72:113-116

30) Doderer SA, Gabel G, Kokje VBC, Northoff BH, Holdt LM, Hamming JF and Lindeman JHN: Adventitial adipogenic degeneration is an unidentified contributor to aortic wall weakening in the abdominal aortic aneurysm. J Vasc Surg, 2017; 67:1891-1900

31) Krueger F, Kappert K, Foryst-Ludwig A, Kramer F, Clemenz M, Grzesiak A, Sommerfeld M, Paul Frese J, Greiner A, Kintscher U, Unger T and Kaschina E: AT1-receptor blockade attenuates outward aortic remodeling associated with diet-induced obesity in mice. Clin Sci (Lond), 2017; 131:1989-2005

32) Goldfinger JZ, Halperin JL, Marin ML, Stewart AS, Eagle KA and Fuster V: Thoracic aortic aneurysm and dissection. J Am Coll Cardiol, 2014; 64:1725-1739

33) Kugo H, Ikeda Y, Moriyama T and Zaima N: Appearance of adipocytes in thoracic aortic aneurysm. J Oleo Sci, 2018; 67:1543-1549

34) Brown NK, Zhou Z, Zhang J, Zeng R, Wu J, Eitzman DT, Chen YE and Chang L: Perivascular adipose tissue in vascular function and disease: a review of current research and animal models. Arterioscler Thromb Vasc Biol, 2014; 34:1621-1630

35) Canga A, Kocaman SA, Cetin M, Erdogan T, Durakoglugil ME, Cicek Y, Ugurlu Y and Satiroglu O: Increased epicardial adipose tissue thickness is correlated with ascending aortic diameter. Tohoku J Exp Med, 2012; 226:183-190

36) Schwab JM, Chiang N, Arita M and Serhan CN: Resolvin E1 and protectin D1 activate inflammation-resolution programmes. Nature, 2007; 447:869-874

37) Bargut TC, Mandarim-de-Lacerda CA and Aguila MB: A high-fish-oil diet prevents adiposity and modulates white adipose tissue inflammation pathways in mice. J Nutr Biochem, 2015; 26:960-969

38) Wang JH, Eguchi K, Matsumoto S, Fujiu K, Komuro I, Nagai R and Manabe I: The omega-3 polyunsaturated fatty acid, eicosapentaenoic acid, attenuates abdominal aortic aneurysm development via suppression of tissue remodeling. PLoS One, 2014; 9:e96286

39) Yoshihara T, Shimada K, Fukao K, Sai E, Sato-Okabayashi Y, Matsumori R, Shiozawa T, Alshahi H, Miyazaki T, Tada N and Daida H: Omega 3 Polyunsaturated Fatty Acids Suppress the Development of Aortic Aneurysms Through the Inhibition of Macrophage-Mediated Inflammation. Circ J, 2015; 79:1470-1478

40) Meital LT, Sandow SL, Calder PC and Russell FD: Abdominal aortic aneurysm and omega-3 polyunsaturated fatty acids: Mechanisms, animal models, and potential treatment. Prostaglandins Leukot Essent Fatty Acids, 2017; 118:1-9

41) Kamata R, Bumdelger B, Kokubo H, Fujii M, Yoshimura K, Ishida T, Ishida M and Yoshizumi M: EPA Prevents the Development of Abdominal Aortic Aneurysms through Gpr-120/Ffar-4. PLoS One, 2016; 11:e0165132

42) Pope NH, Salmon M, Davis JP, Chatterjee A, Su G, Conte MS, Ailawadi G and Upchurch GR, Jr.: D-series resolvins inhibit murine abdominal aortic aneurysm formation and increase M2 macrophage polarization. FASEB J, 2016; 30:4192-4201

43) Aikawa T, Miyazaki T, Shimada K, Sugita Y, Shimizu M, Ouchi S, Kadoguchi T, Yokoyama Y, Shiozawa T, Hiki M, Takahashi S, Al Shahi H, Dohi S, Amano A and Daida H: Low Serum Levels of EPA are Associated with the Size and Growth Rate of Abdominal Aortic Aneurysm. J Atheroscler Thromb, 2017; 24:912-920

44) Kugo H, Zaima N, Mouri Y, Tanaka H, Yanagimoto K, Urano T, Unno N and Moriyama T: The preventive effect of fish oil on abdominal aortic aneurysm development. Biosci Biotechnol Biochem, 2016; 80:1186-1191

45) Adkins Y and Kelley DS: Mechanisms underlying the cardioprotective effects of omega-3 polyunsaturated fatty acids. J Nutr Biochem, 2010; 21:781-792

46) Oh DY, Talukdar S, Bae EJ, Imamura T, Morinaga H, Fan W, Li P, Lu WJ, Watkins SM and Olefsky JM: GPR120 is an omega-3 fatty acid receptor mediating potent anti-

inflammatory and insulin-sensitizing effects. Cell, 2010; 142:687-698

47) Takeshita H, Yoshizaki T, Miller WE, Sato H, Furukawa M, Pagano JS and Raab-Traub N: Matrix metalloproteinase 9 expression is induced by Epstein-Barr virus latent membrane protein 1 C-terminal activation regions 1 and 2. J Virol, 1999; 73:5548-5555

48) Camandola S, Leonarduzzi G, Musso T, Varesio L, Carini R, Scavazza A, Chiarpotto E, Baeuerle PA and Poli G: Nuclear factor kB is activated by arachidonic acid but not by eicosapentaenoic acid. Biochem Biophys Res Commun, 1996; 229:643-647

49) Mishra A, Chaudhary A and Sethi S: Oxidized omega-3 fatty acids inhibit NF-kappaB activation via a PPARalpha-dependent pathway. Arterioscler Thromb Vasc Biol, 2004; 24:1621-1627

50) Wales KM, Kavazos K, Nataatmadja M, Brooks PR, Williams C and Russell FD: N-3 PUFAs protect against aortic inflammation and oxidative stress in angiotensin II-infused apolipoprotein E-/- mice. PLoS One, 2014; 9:e112816

51) Yoshikawa T, Shimano H, Yahagi N, Ide T, Amemiya-Kudo M, Matsuzaka T, Nakakuki M, Tomita S, Okazaki H, Tamura Y, Iizuka Y, Ohashi K, Takahashi A, Sone H, Osuga Ji J, Gotoda T, Ishibashi S and Yamada N: Polyunsaturated fatty acids suppress sterol regulatory element-binding protein 1c promoter activity by inhibition of liver X receptor (LXR) binding to LXR response elements. J Biol Chem, 2002; 277:1705-1711

52) Li ZZ and Dai QY: Pathogenesis of abdominal aortic aneurysms: role of nicotine and nicotinic acetylcholine receptors. Mediators Inflamm, 2012; 2012:103120

53) Aune D, Schlesinger S, Norat T and Riboli E: Tobacco smoking and the risk of abdominal aortic aneurysm: a systematic review and meta-analysis of prospective studies. Sci Rep, 2018; 8:14786

54) Sugamura K and Keaney JF, Jr.: Nicotine: linking smoking to abdominal aneurysms. Nat Med, 2012; 18:856-858

55) Maegdefessel L, Azuma J, Toh R, Deng A, Merk DR, Raiesdana A, Leeper NJ, Raaz U, Schoelmerich AM, McConnell MV, Dalman RL, Spin JM and Tsao PS: MicroRNA-21 blocks abdominal aortic aneurysm development and nicotine-augmented expansion. Sci Transl Med, 2012; 4:122ra122

56) Wagenhauser MU, Schellinger IN, Yoshino T, Toyama K, Kayama Y, Deng A, Guenther SP, Petzold A, Mulorz J, Mulorz P, Hasenfuss G, Ibing W, Elvers M, Schuster A, Ramasubramanian AK, Adam M, Schelzig H, Spin JM, Raaz U and Tsao PS: Chronic Nicotine Exposure Induces Murine Aortic Remodeling and Stiffness Segmentation-Implications for Abdominal Aortic Aneurysm Susceptibility. Front

Physiol, 2018; 9:1459

57) Jacob-Ferreira AL, Palei AC, Cau SB, Moreno H, Jr., Martinez ML, Izidoro-Toledo TC, Gerlach RF and Tanus-Santos JE: Evidence for the involvement of matrix metalloproteinases in the cardiovascular effects produced by nicotine. Eur J Pharmacol, 2010; 627:216-222

58) Nakano D, Itoh C, Ishii F, Kawanishi H, Takaoka M, Kiso Y, Tsuruoka N, Tanaka T and Matsumura Y: Effects of sesamin on aortic oxidative stress and endothelial dysfunction in deoxycorticosterone acetate-salt hypertensive rats. Biol Pharm Bull, 2003; 26:1701-1705

59) Kang MH, Naito M, Tsujihara N and Osawa T: Sesamolin inhibits lipid peroxidation in rat liver and kidney. J Nutr, 1998; 128:1018-1022

60) Majdalawieh AF, Massri M and Nasrallah GK: A comprehensive review on the anti-cancer properties and mechanisms of action of sesamin, a lignan in sesame seeds (Sesamum indicum). Eur J Pharmacol, 2017; 815:512-521

61) Ide T, Lim JS, Odbayar TO and Nakashima Y: Comparative study of sesame lignans (sesamin, episesamin and sesamolin) affecting gene expression profile and fatty acid oxidation in rat liver. J Nutr Sci Vitaminol (Tokyo), 2009; 55:31-43

62) Kugo H, Zaima N, Onozato M, Miyamoto C, Hashimoto K, Yanagimoto K and Moriyama T: Suppressive effects of dietary EPA-rich fish oil on the degradation of elastin fibers in the aortic wall in nicotine-administered mice. Food Funct, 2017; 8:2829-2835

63) Kugo H, Miyamoto C, Sawaragi A, Hoshino K, Hamatani Y, Matsumura S, Yoshioka Y, Moriyama T and Zaima N: Sesame extract attenuates the degradation of collagen and elastin fibers in the vascular walls of nicotine-administered mice. J Oleo Sci, 2019;68:79-85

64) Curci JA, Liao S, Huffman MD, Shapiro SD and Thompson RW: Expression and localization of macrophage elastase (matrix metalloproteinase-12) in abdominal aortic aneurysms. J Clin Invest, 1998; 102:1900-1910

65) Wu L, Tanimoto A, Murata Y, Fan J, Sasaguri Y and Watanabe T: Induction of human matrix metalloproteinase-12 gene transcriptional activity by GM-CSF requires the AP-1 binding site in human U937 monocytic cells. Biochem Biophys Res Commun, 2001; 285:300-307

66) Yu Y, Chiba Y, Sakai H and Misawa M: Possible involvements of nuclear factor-kappa B and activator protein-1 in the tumor necrosis factor-alpha-induced upregulation of matrix metalloproteinase-12 in human alveolar epithelial A549 cell line. J Pharmacol Sci, 2010; 112:83-88

67) Lyu J and Joo CK: Wnt-7a up-regulates matrix metalloproteinase-12 expression and promotes cell proliferation in corneal epithelial cells during wound healing. J Biol Chem, 2005; 280:21653-21660

68) Chung IC, Chen LC, Chung AK, Chao M, Huang HY, Hsueh C, Tsang NM, Chang KP, Liang Y, Li HP and Chang YS: Matrix metalloproteinase 12 is induced by heterogeneous nuclear ribonucleoprotein K and promotes migration and invasion in nasopharyngeal carcinoma. BMC Cancer, 2014; 14:348

69) Samuel S, Twizere JC and Bernstein LR: YB-1 represses AP1-dependent gene transactivation and interacts with an AP-1 DNA sequence. Biochem J, 2005; 388:921-928

70) Souissi IJ, Billiet L, Cuaz-Perolin C, Slimane MN and Rouis M: Matrix metalloproteinase-12 gene regulation by a PPAR alpha agonist in human monocyte-derived macrophages. Exp Cell Res, 2008; 314:3405-3414

71) Ueno H, Pradhan S, Schlessel D, Hirasawa H and Sumpio BE: Nicotine enhances human vascular endothelial cell expression of ICAM-1 and VCAM-1 via protein kinase C, p38 mitogen-activated protein kinase, NF-kappaB, and AP-1. Cardiovasc Toxicol, 2006; 6:39-50

72) Hsieh CC, Kuo CH, Kuo HF, Chen YS, Wang SL, Chao D, Lee MS and Hung CH: Sesamin suppresses macrophage-derived chemokine expression in human monocytes via epigenetic regulation. Food Funct, 2014; 5:2494-2500

73) Miyamoto C, Kugo H, Hashimoto K, Sawaragi A, Zaima N and Moriyama T: Effect of a High-sucrose Diet on Abdominal Aortic Aneurysm Development in a Hypoperfusion-induced Animal Model. J Oleo Sci, 2018; 67:589-597

74) Jiang C, Sun J, Dai Y, Cao P, Zhang L, Peng S, Zhou Y, Li G, Tang J and Xiang J: HIF-1A and C/EBPs transcriptionally regulate adipogenic differentiation of bone marrow-derived MSCs in hypoxia. Stem Cell Res Ther, 2015; 6:21

75) Iinuma S, Aikawa E, Tamai K, Fujita R, Kikuchi Y, Chino T, Kikuta J, McGrath JA, Uitto J, Ishii M, Iizuka H and Kaneda Y: Transplanted bone marrow-derived circulating PDGFRalpha+ cells restore type VII collagen in recessive dystrophic epidermolysis bullosa mouse skin graft. J Immunol, 2015; 194:1996-2003

76) Palumbo R, Galvez BG, Pusterla T, De Marchis F, Cossu G, Marcu KB and Bianchi ME: Cells migrating to sites of tissue damage in response to the danger signal HMGB1 require NF-kappaB activation. J Cell Biol, 2007; 179:33-40

77) Ciavarella C, Alviano F, Gallitto E, Ricci F, Buzzi M, Velati C, Stella A, Freyrie A and Pasquinelli G: Human Vascular Wall Mesenchymal Stromal Cells Contribute to Abdominal Aortic Aneurysm Pathogenesis Through an Impaired Immunomodulatory

Activity and Increased Levels of Matrix Metalloproteinase-9. Circ J, 2015; 79:1460-1469

78) Ciavarella C, Gallitto E, Ricci F, Buzzi M, Stella A and Pasquinelli G: The crosstalk between vascular MSCs and inflammatory mediators determines the pro-calcific remodelling of human atherosclerotic aneurysm. Stem Cell Res Ther, 2017; 8:99

79) Klein D, Weisshardt P, Kleff V, Jastrow H, Jakob HG and Ergun S: Vascular wall-resident CD44+ multipotent stem cells give rise to pericytes and smooth muscle cells and contribute to new vessel maturation. PLoS One, 2011; 6:e20540

80) Klein D: Vascular Wall-Resident Multipotent Stem Cells of Mesenchymal Nature within the Process of Vascular Remodeling: Cellular Basis, Clinical Relevance, and Implications for Stem Cell Therapy. Stem Cells Int, 2016; 2016:1905846

81) Police SB, Thatcher SE, Charnigo R, Daugherty A and Cassis LA: Obesity promotes inflammation in periaortic adipose tissue and angiotensin II-induced abdominal aortic aneurysm formation. Arterioscler Thromb Vasc Biol, 2009; 29:1458-1464

82) Kurobe H, Hirata Y, Matsuoka Y, Sugasawa N, Higashida M, Nakayama T, Maxfield MW, Yoshida Y, Shimabukuro M, Kitagawa T and Sata M: Protective effects of selective mineralocorticoid receptor antagonist against aortic aneurysm progression in a novel murine model. J Surg Res, 2013; 185:455-462

83) Li MW, Mian MO, Barhoumi T, Rehman A, Mann K, Paradis P and Schiffrin EL: Endothelin-1 overexpression exacerbates atherosclerosis and induces aortic aneurysms in apolipoprotein E knockout mice. Arterioscler Thromb Vasc Biol, 2013; 33:2306-2315

84) Blomkalns AL, Gavrila D, Thomas M, Neltner BS, Blanco VM, Benjamin SB, McCormick ML, Stoll LL, Denning GM, Collins SP, Qin Z, Daugherty A, Cassis LA, Thompson RW, Weiss RM, Lindower PD, Pinney SM, Chatterjee T and Weintraub NL: CD14 directs adventitial macrophage precursor recruitment: role in early abdominal aortic aneurysm formation. J Am Heart Assoc, 2013; 2:e000065

85) Sakaue T, Suzuki J, Hamaguchi M, Suehiro C, Tanino A, Nagao T, Uetani T, Aono J, Nakaoka H, Kurata M, Okura T, Yasugi T, Izutani H, Higaki J and Ikeda S: Perivascular Adipose Tissue Angiotensin II Type 1 Receptor Promotes Vascular Inflammation and Aneurysm Formation. Hypertension, 2017; 70:780-789

86) Hashimoto K, Zaima N, Sekiguchi H, Kugo H, Miyamoto C, Hoshino K, Kawasaki N, Sutoh K, Usumi K and Moriyama T: Dietary DNA Attenuates the Degradation of Elastin Fibers in the Aortic Wall in Nicotine-Administrated Mice. J Nutr Sci Vitaminol (Tokyo), 2018; 64:271-276

Acknowledgements

The author would like to give heartful thanks to Dr. Nobuhiro Zaima, Department of Applied Biological Chemistry, Gradual School of Kindai University, whose kind suggestions and warm encouragements were innumerably valuable throughout the course of this study. The author owes a very important debt to Prof. Tatsuya Moriyama who gave invaluable comments. The author is greatly indebted to Dr. Hiroki Tanaka, Takeshi Sasaki, and Naoki Unno, Hamamatsu University School of Medicine, for their invaluable comments. The author also would like to offer special thanks to Mr. Youhei Mouri, Gradual School of Kindai University, for his kind guidance.

Finally, the author would like to express her appreciation to all her colleagues of the Laboratory of Applied Cell Biology for their constant guidance, comments and concern. Their valuable assistance and comments ensured the successfulness of this doctoral thesis.

List of Publications

Main publications

1. **Kugo, H.**, Miyamoto, C., Sawaragi, A., Hoshino, K., Hamatani, Y., Matsumura, S., Yoshioka, Y., Moriyama, T., Zaima, N: Sesame extract attenuates the degradation of collagen and elastin fibers in the vascular walls of nicotine-administered mice. *J. Oleo Sci.* 68, 79-85, 2019
2. **Kugo, H.**, Ikeda, Y., Moriyama, T., Zaima, N: Appearance of adipocytes in thoracic aortic aneurysm. *J. Oleo Sci.* 67, 1543-1549, 2018
3. **Kugo, H.**, Zaima, N., Onozato, M., Miyamoto, C., Hashimoto, K., Yanagimoto, K., Moriyama, T: Suppressive effects of dietary EPA-rich fish oil on the degradation of elastin fibers in the aortic wall in nicotine-administered mice. *Food. Funct.* 8, 2829-2835, 2017
4. **Kugo, H.**, Zaima, N., Tanaka, H., Hashimoto, K., Miyamoto, C., Sawaragi, A., Urano, T., Unno, N., Moriyama, T: Pathological analysis of the ruptured vascular wall of hypoperfusion-induced abdominal aortic aneurysm animal model. *J. Oleo Sci.* 66, 499-506, 2017
5. *__Kugo, H.__, *Zaima, N., *Tanaka, H., Mouri, Y, Yanagimoto, K., Hayamizu, K., Hashimoto, K., Sasaki, T., Sano, M., Yata, T., Urano, T., Setou, M., Unno, N., Moriyama, T: Adipocyte in vascular wall can induce the rupture of abdominal aortic aneurysm. *Sci. Rep.* 6, 31268, 2016 *Equal contribution
6. **Kugo, H.**, Zaima, N., Mouri, Y., Tanaka, H., Yanagimoto, K., Urano, T., Unno, N., Moriyama, T: The preventive effect of fish oil on abdominal aortic aneurysm development. *Biosci. Biotechnol. Biochem.* 80, 1186-1191, 2016

Related publications

1. Hashimoto, K., Zaima, N., Sekiguchi, H., **Kugo, H.**, Miyamoto, C., Hoshino, K., Kawasaki, N., Sutoh, K., Usumi, K., Moriyama, T: Dietary DNA attenuates the degradation of elastin fibers in the aortic wall in nicotine-administrated mice. *J. Nutr. Sci. Vitaminol.* 64, 271-276, 2018
2. **Kugo, H.**, Tanaka, H., Moriyama, T., Zaima, N: Pathological implication of adipocytes for AAA development and the rupture. *Ann. Vasc. Dis.* 11, 159-168, 2018

3. **Kugo, H.**, Moriyama, T., Zaima, N: Adipocytes and abdominal aortic aneurysm: Putative potential role of adipocytes in the process of AAA development. *Curr. Drug Targets.* 19, 1228-1232, 2018
4. Hashimoto, K., **Kugo, H.**, Tanaka, H., Iwamoto, K., Miyamoto, C., Urano, T., Unno, N., Zaima, N., Moriyama, T: The effect of high fat diet on development of abdominal aortic aneurysm in vascular hypoperfusion-induced animal model. *J. Vasc. Res.* 55, 63-74, 2018
5. Miyamoto, C., **Kugo, H.**, Hashimoto, K., Sawaragi, A., Zaima, N., Moriyama, T: The effect of high sucrose diet on development of abdominal aortic aneurysm in hypoperfusion-induced animal model. *J. Oleo Sci.* 67, 589-597, 2018
6. Tanaka, H., Unno, N., Yata, T., **Kugo, H.**, Zaima, N., Sasaki, T., Urano, T: Creation of a Rodent Model of Abdominal Aortic Aneurysm by Blocking Adventitial Vasa Vasorum Perfusion. *J. Vis. Exp.* 129, e55763, 2017
7. **Kugo, H.**, Zaima, N., Tanaka, H., Urano, T., Unno, N., Moriyama, T: The effect of nicotine administration on pathophysiology of rat vascular wall. *Biotech. Histochem.* 92, 141-148, 2017
8. *Tanaka, H., *Zaima, N., Sasaki, T., Yamamoto, N., Inuzuka, K., Sano, M., Saito, T., Hayasaka, T., Goto-Inoue, N., Sato, K., **Kugo, H.**, Moriyama, T., Konno, H., Setou, M., Unno, N: Imaging mass spectrometry reveals a unique distribution of triglycerides in abdominal aortic aneurysmal wall. *J. Vasc. Res.* 52,127-135, 2015 *Equal contribution
9. *Tanaka, H., *Zaima, N., Sasaki, T., Sano, M., Yamamoto, N., Saito, T., Inuzuka, K., Hayasaka, T., Goto-Inoue, N., Sugiura, Y., Sato, K., **Kugo, H.**, Moriyama, T., Konno, H., Setou, M., Unno, N: Hypoperfusion of the adventitial vasa vasorum develops an abdominal aortic aneurysm. *PLoS One.* 10, e0134386, 2015 *Equal contribution